The Coalescence Phenomena and Droplets Motion in Spinodal Decomposition of Low-Viscosity Partially Miscible Solvent Mixtures

By
Filomena Califano

A dissertation submitted to the Graduate Center Faculty in Engineering in partial fulfillment of the requirements for the degree of Doctor of Philosophy,
The City University of New York.

2005

This manuscript has been read and accepted for the Graduate Faculty in Engineering in satisfaction of the dissertation requirements for the degree of Doctor of Philosophy.

01-27-05
Date

Chair of Examining Committee

1-31-2005
Date

Executive Officer

Prof. Alexander Couzis

Prof. Morton Denn

Prof. Irven Rinard

Supervisory Committee

THE CITY UNIVERSITY OF NEW YORK

Abstract

THE COALESCENCE PHENOMENA AND DROPLETS MOTION IN SPINODAL DECOMPOSITION OF LOW-VISCOSITY PARTIALLY MISCIBLE SOLVENT MIXTURES

By
Filomena Califano

Adviser: Professor Reuel Shinnar

Spinodal decomposition of deeply quenched, low-viscosity liquid mixtures has been studied. Observing the phase separation of these liquid mixtures in a small cell, it has been inferred that the process is driven by the convection due to capillary forces, and not by molecular diffusion neither by gravity, heat or surface effects. After quenching a partially miscible critical mixture to a temperature deeply below its critical point of miscibility, the formation of rapidly coalescing droplets of the minority phase, moving in random directions at speeds exceeding *100μm/s*, has been observed. This behavior was observed for both density-segregated and density-matched systems, irrespectively whether they were kept in horizontal or vertical cells. Phase separation was very rapid, even in the presence of coalescence retardants.

Spinodal decomposition of an isopycnic system (i.e., a system with a very small density difference between the two phases) has been studied; rapid flows up to *6cm/s* in a horizontal direction of a *20cm*-long condenser tube have been observed. After droplets formed, they started moving horizontally to a forming interface. After *10 seconds* phase separation is complete, resulting in a vertical interface. Depending on which phase was the dispersed, the droplets moved either to the colder or hotter section of the temperature gradient, created unintentionally during the quenching. The results described in this work,

show that this horizontal motion is not due to conventional thermo-capillary migration but it is driven by chemical potential gradients.

These results could open up new possibilities for studying flows in a microgravity environment and opportunities for practical applications in separation processes.

CONTENTS

List of Tables

List of Figures

Chapter 1

Introduction

Despite the extensive application of liquid extraction over the past years, and the extensive amount of research that has been done, liquid extraction is nevertheless a relatively immature unit operation. The large number of variables, which apparently influence the rate of mass transfer, makes it necessary to have a special treatment for each different case. One common case in most of the liquid-liquid extraction processes is the formation of emulsions and slow coalescence due to impurities. In many cases, to break these emulsions, centrifuges are used. However, this requires intense agitation, which may be detrimental for the product. To ameliorate this problem, a novel separation technique, the Phase Transition Extraction (PTE) process, was proposed (*Ullmann et al.*, 1997, 1995; *Ullmann,* 1993; *Ludmer et al.*, 1990). The process consists of two steps: extraction is performed in the homogeneous region by heating two partially miscible solvents above their critical temperature, and thus eliminating the need for intense agitation, and separation is performed by rapidly cooling at a temperature below the coexistence curve. During this research, it was found that under certain circumstances, phase separation is extremely rapid, even in the presence of emulsifiers and impurities that tend to slow down the coalescence. We also discovered rapid flows of large droplets with velocities up to *6cm/s* along the axial direction over large distances (*20cm*). Changing the mole fraction of the two solvents, resulting in a phase transition, could reverse the direction of the flow. Rapid flows were also observed on a smaller scale when the mixture had intentional non-equilibrium concentration gradients before the cooling.

In the present work we explain these unexpected results and present a deep understanding of these phenomena that could have not only scientific but also many practical applications in separation processes.

Essential content of the work.

In Chapter 2 we summarize the basic principles of the liquid-liquid extraction (LLE) process, discussing the extraction operation, properties of dispersions, and the stability of the emulsions. Some common problems with LLE process are also identified, and the prevailing methods to handle them are discussed. Since our whole work is related to partially miscible solvents, we explain their miscibility behavior and the phase-equilibrium thermodynamics. Then, after explaining the characteristics of the two modes of phase separation, nucleation and spinodal decomposition, we discuss the earlier work done on the dynamics of phase separation.

In Chapter 3 we explain the Phase Transition Extraction (PTE) process, in which changing either the composition or the temperature of the mixture induces the phase transition of partially miscible mixtures. Here, we investigate this process macroscopically, and analyze the difference between the PTE phase separation process and the usual LLE process.

Chapter 4 is devoted to the visualization of low-viscosity liquid mixtures morphology during the phase separation. Here, after describing the physical properties of both density-segregated system and density-matched system that were used in our experiments and the experimental setup, we present by direct visual observations the phase separation of these mixtures, following a deep temperature quench into the unstable region of

mutual miscibility. Two experimental procedures were considered: the homogeneous case and the gradient case. Finally we intend to compare the results obtained in the gradient case with those obtained when the liquid mixtures are initially uniform, showing that, in both cases, phase separation is driven by the convection induced by a non-equilibrium capillary force, as predicted by the model H.

In Chapter 5 we continue our study on spinodal decomposition of low-viscosity partially miscible liquids, and we describe rapid flows up to *6cm/sec* in a horizontal direction. Most of previous work in Chapter 4 was carried out in a small glass cell suitable for microscopic observation where due to the large surface to volume ratio of the device, interfacial capillary forces on the glass liquid interfaces could not be disregarded. As we were interested to obtain results that could be applied on industrial scale, we used a condenser tube, *20cm* long and *1cm* diameter, to eliminate the impact of capillary effects. We investigated the spinodal decomposition of a mixture of hexadecane and acetone rapidly cooled to a temperature of *20°C* below the critical point using the horizontally placed condenser tube. The results described in this chapter show that these flows are not due to conventional thermo-capillary motion but they are driven by chemical potential gradients.

In Chapter 6 we intend to study the limitations of the results obtained. In fact, we expected that coalescence could be eventually retarded increasing the amount of surfactants and thickeners, thereby increasing the viscosity of the mixtures, or when we quench the mixture in its metastable region. Therefore we determined the thresholds of the surfactant concentration and of the mixture viscosity and composition beyond which surfactants start to slow down significantly the separation process, just as they do in the

absence of phase transition. From a practical viewpoint, one of the most interesting features of spinodal decomposition in the convective range is that emulsion-promoting compounds have almost no effects on the phase separation rate. In this work we investigated whether the presence of stronger and more concentrated emulsifiers has an impact on the phase separation rate. We also studied the effect of emulsifiers when the mixture was quenched into its metastable region, where convection and diffusion are comparable. As some of these emulsion stabilizers produce non-transparent systems, we had limit ourselves to observing only the time needed to complete the separation.

Finally, in the last Chapter 7 we summarize our work and suggest some advantages of our results.

Chapter 2

Background

In this chapter after a brief introduction of the basic principles of the conventional liquid-liquid extraction (LLE) process and describe some of the most widespread LLE equipments in order to show their advantages and limitations. Some specific applications of the LLE process are also listed identifying difficulties in the use of present LLE methods in various commercial applications.

Emulsion formation is a common problem in industrial LLE process particularly in the biotechnology and pharmaceutical industries. Some of the basic mechanisms of emulsion stabilization are summarized in Section 2.2.

As the whole approach of the PTE process is based on using solvent mixtures with critical point of miscibility, we review their properties in Section 2.3.

Then in Section 2.4, we present a dimensional analysis based on the diffuse interface model, predicting the presence of large attractive forces among phase separating liquid droplets. These forces are responsible for the rapid coalescence among single-phase domains, hence for the fast phase segregation process that is observed experimentally.

2.1 Liquid-liquid Extraction.

Liquid-liquid extraction (LLE) has important uses in many industries and has been extensively studied (Harland, 1963, Treybal, 1963, Hanson, 1971, Lo *et al.*, 1983, Akel and King, 1984 and Alegert, 1988). Such processes are used both for the extraction of one compound as well as for the separation between two or more compounds (fractional

extraction). In one sense there is a strong similarity between the distillation and the LLE processes. In both cases the operations generally rely upon the unequal equilibrium distribution of substances to be separated between two phases. However, while in the distillation operation the two phases are generated from the original solution by addition of heat, and the components of the original solution then distribute unequally between the liquid and vapor phases, in the LLE process, the second phase is created by addition of extraction solvent, and the solutes are distributed between two liquid phases.

In general, LLE will be preferred either where distillation fails or where, despite some disadvantages, it provides a less expensive overall process than the distillation process. The following list indicates some typical examples where LLE has demonstrated its unique abilities as a separation method.

1. As a substitute for distillation process where LLE is less expensive.

- Separation of close-boiling liquids. An example is the separation of butadiene (b.p. - 4.75°C) from Butylenes (b.p. - 6°C).
- Separation of liquids of poor relative volatility. An example is the separation of acetic acid and water, which, despite their relatively large difference in boiling point, have poor relative volatility.
- For mixtures with very high boiling point where high vacuum is essential for the distillation process, like long-chain fatty acids and vitamins.

2. As separation means where distillation fails.

- Separation of heat-sensitive substances such as antibiotics.
- Separation of solvents that form azeotropes.

- Separation according to chemical type, where boiling points overlap. An example is the separation of aromatic hydrocarbons from paraffin hydrocarbons.

The LLE process procedure is simple in concept and usually requires contacting of feed containing the solute to be extracted with a solvent, this solvent/feed mixture is usually immiscible but may be partially miscible in some cases. After forward extraction, the solute remains in the solvent phase and depleted feed becomes the raffinate (see Figure 2. 1). In fractional extraction the extract is scrubbed with an immiscible phase (usually involving the same phase type as the original feed) in order to improve the purity of final product. After scrubbing, the solvent is stripped of its solute and the regenerated solvent returned as solvent feed to the process. Often the returned solvent is washed to remove breakdown products. The strip solution provides a product stream.

It is important at this stage to recognize certain features of the process that the present work will seek to change. The extraction and the stripping involve liquid-liquid contacting in which the droplets of one phase are dispersed in a second phase and mass-transfer has to take place across liquid-liquid boundary. There are several types of contact-equipment in industrial use; basically there are two types of units. Those in which each individual stage is a separate unit and those in which several stages are integrated into one column. Multistage-columns can be simple spray or packed columns or can have stages equipped with various types of mixing devices separated by coalescence sections. The stage efficiency and the throughput of such devices are a strong function of the mass-transfer and the coalescence rate.

Another important point worth mentioning is the fact that high intensity mixing is required in order to form small drops and good contact between the phases in slow mass-

transfer systems. However, the shear stress induced by such a mixing can, in many cases, damage high molecular weight molecules (Hsien-Wen, 1980). In addition, the intense mixing forms fine dispersions which reduces the coalescence rate, or in the presence of surface active impurities, may even cause a "stable emulsion", one of the operating hazards of solvent extraction equipment. In the presence of surface-active impurities, this intense mixing may even cause emulsion formation, which is a common problem in the pharmaceutical industry, where the desired products are frequently extracted from fermentation broths containing surface-active impurities. Furthermore, the active compounds to be extracted from the fermentation broths are often "imprisoned" in cell debris, which makes the penetration of solvents even more difficult to achieve.

It would be a novel approach with significant advantages to have contacting equipment and solvent systems that will operate with minimal or without any mechanical agitation and in which there will be no stable boundaries to slow down the mass-transfer and the coalescence rates.

2.1.1 Some Applications of Solvent Extraction.

There are many applications of LLE a most of them are summarized in various reviews (Lo, 1983, Ritcey and Ashbrook, 1979, Schweiter, 1979, Alegret, 1988, Blumberg, 1988). Some specific applications are listed below in order to point out the range of importance of the LLE process and to identify difficulties in the use of the present methods of solvent extraction in various commercial applications.

Organic Solutes.

The applications of the LLE in chemical industry can be grouped as follows:

- Petroleum and petrochemical industry.
- Coal tar industry.
- Pharmaceutical and food industry.

a) Petroleum and petrochemical industry. The need to separate mixtures of aliphatic and aromatic hydrocarbons provided the first large-scale applications for LLE. The advantage of solvent extraction was that it represented a physical means for separating groups of components of similar chemical type, so energy intensive processes such as distillation are avoided. Thus a solvent, which preferentially dis solved aromatic c omponent from mixtures of hydrocarbons, could be used to remove aromatics from kerosene and lubricating oils. LLE is now used for the production of high-purity aromatic extracts.

b) Coal tar industry. In the coal tar industry LLE is used to separate tar acids from basic or natural compounds. These processes use the principles of fractional extraction. An example of fractional extraction is the separation of tar acids from crude tar distillate using aqueous methanol and hexane (Newworth *et al.*1951).

c) Pharmaceutical and food industry. The most important use of solvent extraction in the pharmaceutical industry is the manufacture of penicillin. It is produced by fermentation process and extracted by organic solvent such as butyl or amyl acetate, chloroform, or methyl isobutyl ketone. In order to increase the solvent to aqueous distribution coefficient of the penicillin, the pH of the broth is typically reduced to about 2-2.5 with sulfuric acid. However, the low pH causes a rapid decomposition of the penicillin so a fast extraction is needed. The need for rapid extraction favors the use of centrifugal contactors, where the residence time is typically of the order of seconds. Emulsion formation is a common problem in extraction of penicillin from the fermentation liquor. Current practice to

overcome this is to add a precise quantity of demulsifying agent to the aqueous stream just prior the extraction. An example for such a treatment is given by Stroud and Ransley (1956). The traditional process for the manufacture of penicillin requires that the broth be filtered to remove mycelium prior to solvent extraction. Direct extraction of unfiltered fermentation broth has the potential of increasing the extraction efficiency by up to 10% since penicillin adsorbed into the mycelial solid can also be extracted. In addition, there are the advantages that filter aid is not required and the broth is not diluted with wash water from the filtration stage. Anderson and Lau (1955) reported extraction processes of unfiltered broth.

The application of LLE in food industry long predates modern technology. In the eighth century the use of aqueous alcohol as an extraction solvent was known in the Arabic world and before then extraction with water was used to recover aroma-bearing extracts. Presently, some of the applications are extraction of lipids, the removal of caffeine from coffee and the extraction of flavors and aromas (Randall et al., 1971).

Inorganic Solutes.

Solvent extraction may be usefully applied to salt-acid reactions. This permits the production of salt and acids from primary raw materials (Baniel and Blumberg, 1957) as the solvent dissolves both acids completely but dissolves the salts only sparingly. In this way the reaction products may be separated. These methods are well adapted for up-grading the alkali chlorides KCl and NaCl. For example, nitrates and sulphates of sodium, potassium and ammonium cations may be prepared from their chlorides; phosphoric acid can be produced by direct attack of hydrochloric acid on phosphate rock.

Other areas where LLE is successfully used include production boric acid and hydrogen peroxide (Brown and Sanderson, 1977).

Metal Solutes.

The field of extractive metallurgy has been one of the most rapidly growing areas in the use of LLE. The solvent extraction of metals, on a large scale, originated in the uranium industry because it was required to produce ultra pure uranium for primary fuel for the reactors and to separate the uranium and plutonium fission products after burn up of the fuel in the reactor. The atomic energy industry has been the largest user of LLE for metal separation and recovery, and many of the extractant solvents first used in that industry have been later adopted for the recovery of other metals. These solvents include the polyethers, ketones, organ phosphorus compounds and long chains amines.

The extraction of irradiated compounds introduces special requirements for the contact equipments. The need for remote routine operation and the difficulties of maintenance in case of breakdown mean that equipment should be as simple as is compatible with other requirements, with as few moving components as possible in contact with radioactive materials.

During the study of LLE for the nuclear industry it was soon realized that the extractants had wider use and that other valuable cationic metals could be extracted. The value of the metals led to the development of LLE processes for rear earth metals such as vanadium, zirconium, tantalum and hafnium (Sekine and Hasegawa, 1977). Recent developments include the extraction of metals such as aluminum (Muhl et *al.*, 1980), boron, gallium (Schepper, 1979), germanium (Cote and Bauer, 1980) and lithium (Epstein et al., 1981).

Another use of LLE is the removal of metals from liquid effluent streams to environmentally acceptable levels. The type of metals removed and recovered includes zinc, copper, nickel, chromium and mercury (Anderson and Reinhart, 1983).

2.1.2 Extraction Equipment.

Extraction equipment may be operated batch wise or continuously. A quantity of feed liquid may be mixed with a quantity of solvent in an agitated vessel, after which the layers are settled and separated. The extract is the layer of solvent plus extracted solute and the raffinate is the layer from which solute has bee removed. The extract may be lighter or heavier than the raffinate and so the extract may be shown coming from the top of the equipment in some cases and from the bottom in others. The operation may be repeated if more than one contact is required, but when the quantities are large and several contacts are needed, continuous flow becomes economical. Most extraction equipment is continuous with either successive s tage contacts or differential contacts. Representative types are mixed-settlers, vertical towers of various kinds, which operate by gravity flow, agitated, tower extractors and centrifugal extractors and are discussed in detail in most of the Separation Processes text.

2.2 Stability of Dispersion and Emulsion Formation.

Phase dispersion and coalescence phenomena are important in LLE with either stage-wise or differential contact. Agitation or mixing of two liquid phases that are not or only slightly mutually soluble results in the formation of emulsion or dispersion of one phase

in the continuum of the other. Dispersions are generally considered to be unstable or temporary emulsions and stable dispersions or emulsions are those that remain unchanged for considerable time after preparation.

From the point of view of LLE processes the stability or permanence of the dispersion is its most important property, since it is necessary to separate the phases at each extraction stage. For all practical purposes, the breakup time or the coalescence rate will determine the workable throughput of the extraction equipment. In countercurrent column-type contactors, steady operation is possible when the rate of droplets arrival does not exceed the coalescence rate at the main interface, otherwise the dispersed band will extend over the entire column leading to flooding. In mixer-settler contactors, the dimensions of the settler are designed according to the coalescence rate and increasing the throughput above the coalescence rate will result in flooding of the settler. It is clear therefore that conventional extractors cannot operate systems with emulsification tendency. Commonly such systems are handled in centrifugal extractors.

Emulsion formation is a common problem in the pharmaceutical industry where the desired products are extracted from the fermentation broth by organic solvents, but virtually it is also common in many other extraction processes where mechanical agitation is used to increase the mass transfer rates. The problem of emulsion formation is more severe for industrial systems than it is in the laboratory because in industry there is a greater opportunity for system contamination, such as by dirt or rust, which later constitute emulsion stabilizer. Over the last 40 years there has been a growing interest in understanding the factors controlling dispersions stability and breakdown (good reviews are given by Bencher, 1983).

Stability represents the resistance offered by the dispersion to ultimate coalescence of the dispersed phase droplets. In order for dispersion to separate into its phases, the droplets have to undergo the following steps: a) collision, b) flocculation or agglomeration, c) coalescence (Treybal, 1963).

Collision. For very fine droplets their Brownian movement dominates the rate of collision. For larger droplets, external force fields, usually gravitational, centrifugal or electrostatic are acting on the system and causing settling or sedimentation, thus bringing the droplets into contact with each other to form a closed-packed array.

Flocculation. In this case, aggregates of droplets are formed within the dispersion. This process results from the existence of attractive forces between the droplets.

Coalescence. Flocculated droplets in an aggregate in the bulk of the dispersion, or droplets within a closed-packed array resulting from sedimentation, coalesce to form larger droplets. The limiting case considered here is the complete separation of the dispersion into two bulk liquids. The coalescence process is the combination of two different steps: first, drainage of the continuous phase film trapped between the drops and, second, ruptures of the lamellar film.

Not every collision of droplets is resulted with coalescence and if the collisions in the dispersion are completely ineffective, the dispersion is said to be stable. Two pure liquids rarely form stable emulsion and a third substance nearly always must be present. The additional substances are commonly impurities, surface-active agents (surfactants) or finely divided solids, which are absorbed at the liquid-liquid interface. These substances (emulsifiers) stabilize the dispersions against breakdown by preventing either the flocculation or the coalescence of the droplets.

The emulsions can be stabilized by one or more different mechanism. Basically there are three of these to consider: charge stabilization, steric stabilization and stabilization by adsorbed solid particles at the liquid-liquid interface.

Charge stabilization is caused by the adsorption of ionic stabilizer, e.g., an ionic surfactant or a polyelectrolyte at the droplets interface. The increase in the coalescence time is caused by the formation of electrical double layers on the surface of droplets. The electrical double layers tend to retard the flow or the draining of the liquid film due to the attraction force of the opposite charges at the interface and the flowing film (electro viscous effect). Furthermore, the repulsion of the equally charged droplets prevents the flocculation of the droplets (Tadros and Vincent, 1983).

In the presence of non-ionic emulsifiers, especially polymers, the steric mechanism of stabilization dominates. Polymer molecules adsorb on the liquid-liquid interface and form a protective layer (Shinnar 1961). The protective layer comprised of loops and tails extending into the solution phase. These protective layers generate a repulsive force between the droplets and prevent the flocculation (Heller, 1954). Moreover, the macromolecular film formed at the interface, in view of its viscoelastic properties, can provide a mechanical barrier to coalescence. This is particularly the case with many adsorbed protein molecules, which denature on adsorption and hence collapse at the interface, forming rigid film (Bikerman, 1958).

The mechanism of emulsion stabilization by the presence of finely divided solids at the liquid-liquid interface is far from being understood at present. Presumably, the presence of solid particles at the liquid-liquid interface plays an important role in preventing this thinning of the liquid film between the droplets. For the solid particles to be effective,

they should form a continuous monoparticulate film on the droplet interface, thus making the coalescence more difficult, essentially by keeping the droplets from coming into close contact (Tadros and Vincent, 1983). If the particles are relatively large compared to the droplets, and they are preferentially wetted by droplet phase, they can act as connecting links across the draining film causing film rapture almost instantaneously and promoting the coalescence (Charles and Mason, 1960).

As in the case of solid particles, an effective stabilization of dispersions by any of the above mentioned stabilizing substances requires a full coverage of the droplet interface by the adsorbed molecules. If this is not the case, bare patches on the two surfaces may come into direct contact leading to coagulation or even coalescence.

The adsorption of the emulsifier molecules on the interface is a dynamic process that includes the diffusion of the molecules from the bulk liquid to the interface and adsorption on the interface. The adsorption rate is highly affected by the properties of the dispersed and the continuous liquids and the adsorbed molecules, as well as the fluid-dynamic conditions (laminar or turbulent flow). In some cases the adsorption rate is very low. For example, the adsorption of macromolecule at liquid-liquid interface is a very slow process and equilibrium is only reached after a long time (hours or days), depending strongly on molar mass distribution of the adsorbed molecules.

2.3 Properties of Solvent System with Critical Point of Miscibility.

As our whole approach, in the present work, is based on using partially miscible liquid solvents, a short review of their properties is in the following.

2.3.1 Introduction-Partially Miscible Solvent Systems.

Two-component liquid system may be classified according to whether the components are completely or only partially miscible. From practical viewpoint, it may be sometimes considered that complete immiscibility occurs, but it should be realized that actually all liquids dissolve in each other if only to a limited extent.

Consider two liquids A and B, exhibiting only partial miscibility. While complete miscibility is obtained whenever a small amount of A is added to B, as more A is added to the solution, eventually the limit of solubility of A in B at the current temperature is reached. Then, further addition of A will result in appearance of two liquid phases that are saturated solutions of A in B and B in A. finally, sufficient addition of A will bring the system to a condition of one liquid phase. Thus, for a range of the system composition at a given temperature, two liquid phases of constant composition, the saturated solutions, will coexist. Variation in composition of these saturated solutions with temperature is conveniently shown graphically in the so-called miscibility curves.

In the case described in Figure 2.2a, which is typified by the system butanol-water, the solubilities of A in B and B in A increase with increase in temperature, so at some elevated temperatures, at point C, the two conjugate solutions become identical and the interface between them disappears. This point is termed as the critical solution temperature (CST) and in Figure 2.2a point C is an upper critical solution temperature (UCST). There are other systems whose mutual solubility increase with decreasing temperature, as the system triethylamine-water and described in Figure 2.2b. In this case the point, in which the compositions of the two phases approach each other, is a lower

critical solutions temperature (LCST). Figure 2.2c describes two-component systems with both UCST and LCST.

2.3.2 The Physical Chemistry of Consolute Systems.

The physical explanation of the critical miscibility phenomena is based upon the interplay of intermolecular forces (Rowlinson, 1969, Domb and Green, 1972).

For example, the existence of UCST can be explained assuming that A-B molecular bond is weaker than individual interaction A-A and B-B, then at high temperatures entropy effects are favored and complete miscibility results. At low temperatures the free energy of interactions is favored and phase separation occurs.

Explanation of LCST (Domb and Green, 1972) revolves around the highly directional short-range interaction of entities A and B as in the hydrogen bonding case. At low temperatures the decrease in free energy of solution due to specific interaction of A with B gives rise to miscibility. However, as temperature rises above the LCST entropy effects take over favoring a more random orientation of the entities. This then destroys the directional bonds resulting in unfavorable free energy of solution and thus phase separation.

2.3.3 Effect of Third Component Dissolution on Critical Mixture.

The addition of even small amount of a third component to a two-component liquid system may alter considerably the CST. Typically, when the third component is much more soluble in one of the binary mixture components, its addition raises the UCST

(Hales *et al.*, 1966). When the third component distributes in roughly equal proportions between the two components, its addition tends to lower the UCST (Synder and Eckert, 1973). Therefore, water for example, raises the UCST of methanol/n-hexane mixture (Rogers, 1969), whereas acetone, as a third component, lowers the UCST of methanol/cyclohexane by 3.5°C per percent of acetone dissolved (Cohn and Jacob, 1984). In similar way, the addition of a third component that is soluble in both liquids raises the LCST and addition of a third component that is mainly soluble in one of the binary solution mixture components lowers the LCST.

Due to the addition of a third component to a two-liquid system and its distribution between the equilibrium phases, the critical composition will be altered as well. However, for a small amount of a third component, the solvents mixture can be regarded as a pseudo two-component system and the changes in critical temperature and critical composition can be considered linear (Tveekrem and Jacobs, 1983, Cohn and Jacobs, 1984).

2.3.4 Phase-Equilibrium Thermodynamics.

Using the classical phase-equilibrium thermodynamics and performing thermodynamic stability analysis can examine the mutual solubility of solvents and the critical solution temperature phenomena.

A state of equilibrium is characterized as having a minimum Gibbs energy at a given temperature, pressure and composition. Thus, a mixture of solvents will split to separated phases whenever the total Gibbs energy of heterogeneous solution is less then that of

homogeneous solution. This can be easily demonstrated for the case of binary solutions. In Figure 2.3 the Gibbs energy G of binary mixtures is plotted as function of composition x. the convex portion a-d-h of the curve represents an unstable region of which the stable Gibbs energy is along the straight-line a-f-h. For any overall mixture composition between a and h the mixture will split into two coexisting phases with equilibrium compositions of points a and h and with an equal chemical potential. Such a curve always has at least one local maximum and two or more minimum and is described as having convex portions. The mathematical condition for convexity and therefore the mixture instability is that

$$\frac{\partial^2 G}{\partial x^2} < 0 \qquad (1)$$

The inflection points at which $\frac{\partial^2 G}{\partial x^2} = 0$ separate the regions of instability and stability and is called spinodal point (see Figure 2.3).

If the range of immiscibility decreases gradually, by reason of temperature change or other factors, eventually it degenerates to a point. This point of incipient immiscibility, or critical solution, is mathematically characterized as having

$$\frac{\partial^2 G}{\partial x^2} = \frac{\partial^3 G}{\partial x^3} = 0 \qquad (2)$$

This behavior of binary mixtures, as well as the generalization to multi-component mixtures, was described by Lupis (1983).

When the relations between composition, temperature and Gibbs free energy of mixture are known, the above considerations can be used to evaluate the CST and the equilibrium compositions of coexisting phases. The former can be determined by using

the conditions of Eq. 2, whereas the equilibrium composition can be evaluated by applying the principle of equality of chemical potentials.

The above thermodynamic analysis can serve as an analytical tool to evaluate the behavior of solvent mixtures, namely to predict the existence of a critical point and to estimate the composition of coexisting liquid phases. It is important for preliminary screening of solvents and when performing feasibility study of a new extraction process.

2.3.5 Nucleation vs. Spinodal Decomposition.

Consider a liquid mixture of liquids A and B cooled off-critically from an initial composition x_1 to some temperature T_1 (Figure 2.4). In order for a nucleus of ultimate composition x_2 to form, a small group of atoms, an embryo, must acquire a higher B content than the surroundings and an interface must appear. It can be shown that when such a group of atoms is small and has not yet raised its B content very much above the average, the presence of interface and the composition change are accompanied by an increase in overall free energy rather than by decrease associated with the final formation of a large particle of composition x_2. Only when the embryo has grown a certain critical size and critical composition is its further growth associated with decrease in free energy. Thus this embryonic nucleus must overcome both a size barrier and a compositional barrier before it can grow stably. This growth behavior in metastable region is known as nucleation-and-growth.

At temperature below the spinodal such as T_2 in Figure 2.4, the bulk free energy change on forming an embryo plus halo region is negative for even the smallest possible difference in composition between the embryo and parent solution. Thus, below the

spinodal the compositional barrier disappears and only the size barrier restrains phase separation. As a result, transformation in solutions quenched to temperatures somewhat below the spinodal is considerably less sluggish than in those quenched to temperatures somewhat above the spinodal. The type of transformation below the spinodal curve is termed as spinodal decomposition, a particular case of first-order phase transition.

The morphology of the transformation product changes also in the spinodal region. Above the spinodal, the large compositional difference necessary for stable growth of the new ensures that there will be a discrete boundary between the phases, i.e., discrete nuclei will form, even in the early stages of decomposition.

2.3.6 Dynamics of Phase Transition.

When an initial single-phase binary mixture is brought across its miscibility curve into the two-phases region at temperature T, it phase separates. This process can occur either by nucleation (both heterogeneous and homogeneous) or by spinodal decomposition (Debenedetti, 1996). The former process describes the relaxation to equilibrium of a metastable system, while the second one is typical of unstable systems. Many theories have been developed to describe the kinetics and dynamics of phase separation. Studies have been carried out on various systems, including polymers (Cumming *et al.*, 1992), and fluid systems (Chou and Goldburg, 1981, Wong and Knoble, 1981, Siggia, 1979, Mauri, Shinnar, 1996). Most of the efforts have gone into describing the growth of domain size R, after the system is brought into two-phase region, by the power law dependence in time, $R(t) = t^n$.

Nucleation is an activated process, where a free energy barrier has to be overcome in order to form embryos of a critical size, beyond which the new phase grows spontaneously; in most practical cases, suspended impurities or imperfectly wetted surfaces provide the interface on which the growth of the new phase is initiated (Frankel, 1946).

Contrary to nucleation, spinodal decomposition occurs spontaneously, without any energy barrier to be overcome and involves the growth of fluctuations of any amplitude that exceed a critical wavelength (Hohenberg and Halperin, 1977; Gunton , Miguel and Sahni, 1983). The theoretical basis of this process is the Cahn and Hilliard theory (1958), later extended by other authors (Gunton, Miguel, 1983) that generalize the previous approach by Van der Waals 1984. In principle, nucleation and spinodal decomposition are fundamentally different from each other, as metastable system relaxes via the activated growth of localized fluctuations of large amplitude, whereas unstable systems do so via spontaneous growth of long-wavelength fluctuations of any amplitude. However, for deeply quenched systems, the distinction between the two regimes becomes murky, as both the critical nucleus size and the critical fluctuation wavelength decrease. In fact, a rigorous treatment of the transition between these two basic mechanisms of phase transition does not exist and neither of the classical theories of nucleation and spinodal decomposition seems to be able to describe the behavior of a deeply quenched system.

Following the temperature quench into the unstable region the system first quickly attains the state given by spinodal curve, and then reaches to the equilibrium state on the coexistence curve. Therefore, the process of phase transition is usually divided in two

time regimes: the early spinodal decomposition stage, consisting of exponential growth of long-wavelength concentration fluctuations, and a late stage given by nucleation and growth of localized microdomains. However, understanding the spinodal decomposition phenomenon has always been a complex problem.

The basis of most of the theoretical work on spinodal decomposition is the linear Cahn-Hilliard theory (1959). Following a linearization of the generalized diffusion equation and using the Landau-Ginsburg form for the free energy, Cahn-Hilliard model leads to prediction of an exponential growth of microdomains during the initial stage of spinodal decomposition. The validity of Cahn-Hilliard theory is limitated for very short times following the quench (Gunton, 1983), and for later times non-linear terms neglected in their work become important. Recently, it was shown in 1D (Mauri, 1996) that the non-linear terms saturate the exponential growth predicted by the linear theory so that the concentration distribution tends to a steady state, periodic profile.

The exponential study of spinodal decomposition in fluids is also a challenging task. The interdiffusion constant D in fluids is normally several orders of magnitude larger than alloys and polymers, and so the time for spinodal decomposition in fluids is very small. However, near the critical point the diffusion rate is very low and spinodal decomposition occurs on an experimentally observable time scale. Therefore, most of the experimental studies on liquid binary mixtures (Chou and Goldburg, 1979, Wong and Knobler, 1982) were done by staying close to the critical temperature ($\varepsilon = /T - Tc//Tc < 10^{-5}$). It was shown that while the initial stage of phase separation is still too rapid to be observed, during nucleation process the domain growth exponent $n = 0.3\text{-}0.4$ in the early diffusive stage, and $n = 1$ in the late stage. Guenoun et al. (1987) also studied the effect

of gravity in the late stages of separation and found that gravity effect was negligible during the whole separation process.

Most of the previous studies on phase separation of liquid mixtures have used light scattering techniques. In the classic experiments by Chou et al. and Wong et al., phase separation process was critically retarded by quenching the system to a temperature T only by few millikelvin below the critical value Tc, i.e. with reduced temperature $\varepsilon = 10^{-5}$. Similar slowing can also be achieved by studying polymer blends (Cumming et al., 1992) with viscosities hundreds of times larger than water's and reduced temperature $\varepsilon \approx 10^{-2}$. The dynamics of phase separation process has been observed directly as well with either very small quenches (Beynsen *et al.,* 1994), or using high viscosity systems (White and Wiltzius, 1995). Most of these experimental studies observed that, right after the temperature of the system has crossed that of the miscibility curve, the solution starts to separate by diffusion and coalescence, leading to the formation of well-defined patches, whose average concentration is near its equilibrium value (Chou and Goldburg, 1981, Wong and Knobler, 1978, Guenoun *et al.*, 1990). The shape of these patches appears to depend strongly on the composition of the system: for critical mixtures, they are dendritic, interconnected domains, while for off-critical systems they appear to be spherical drops. Then, in the so-called late stage of coarsening, these patches grow by diffusion and coalescence, until they become large enough that buoyancy dominates surface tension effects and the mixture separates by gravity. This occurs when the size of the domains exceeds the capillary length, $R_c = O(\sqrt{\sigma/(g\Delta\rho)})$, where σ is the surface tension, g the gravity field, and $\Delta\rho$ the density difference between the two separating phases (Siggia, 1979). In the case of a liquid mixture that would correspond to *Rmax* =

O(1mm). Now, if diffusion was the only driving force of the phase separation process, it is well known, both experimentally (Chou and Goldburg, 1981) and theoretically (Lifshitz and Slyozov, 1961) that the typical size of a nucleating drop grows with time as $R(t) \propto t^{1/3}$; for strongly off-critical mixtures, this same *1/3* exponent law is also the signature of coalescence driven by Brownian motion. Consequently, in this case, we would predict that it takes a very long time for the nucleating drops to become large enough (i.e. to exceed the capillary length) and sediment. Obviously, while similar times are needed to phase segregate polymer melts and alloys, liquid mixtures separate within seconds of the temperature quench, and therefore diffusion and buoyancy alone cannot explain the segregation process.

The other mechanism of growth is convection-driven coalescence, which implies that drops move against each other under the influence of an attractive force. Like all convective mechanisms, this coalescence predicts a linear growth law, $r(t) \propto t$, which agrees with most of the experimental measurements (Chou and Goldburg, 1981, Wong and Knobler, 1978, Guenoun *et al.*, 1990). However, the nature of this convective driving force in phase separating systems is not well known, although it has been explained by the so-called model *H* (Cahn and Hilliard, 1979) as the result of the minimization of the interfacial energy, inducing a (non equilibrium) body force that is proportional to the gradient of the chemical potential. In particular, at the late stages of phase separation, after the system has developed well-defined phase interfaces, this body force reduces to the more conventional surface tension, as shown by Jasnow and Viñals (1996), so that the driving force can be thought of as a non-equilibrium capillary force. Applying the model *H*, Farrell and Valls (1983), Tanaka and Araki (1998) and Vladimirova *et al.* (1998)

showed by numerical simulation that spinodal decomposition of fluid mixtures strongly depends on the relative importance of convection and diffusion, and that the enhanced coarsening rate is due to the strong coupling between concentration and velocity fields. This result was confirmed by the experimental observation of Gupta *et al.* (1999) that the coarsening rate of phase separating liquid mixtures is almost independent of the presence of surface-active compounds, indicating that the convective forces that induce drop coalescence are much larger than any surfactant-driven repulsive interactions.

2.4 Theoretical Model.

2.4.1 Binary mixture at equilibrium.

Consider a homogeneous mixture of two species A and B with molar fractions $x_A = \phi$ and $x_B = 1-\phi$, kept to a temperature T and pressure P. A and B are assumed to have equal viscosity η, density ρ a nd molecular weight M_W, with the composition of the system uniquely determined through the molar fraction ϕ of, say, species A.

The equilibrium state of this system is described by the molar Gibbs energy of mixing:

$$\Delta g^{eq} = g^{eq} - (g_A x_A + g_B x_B), \tag{1}$$

where g^{eq} is the energy of the mixture at equilibrium, while g_A and g_B are the molar free energies of pure species A and B, respectively, at temperature T and pressure P. Δg^{eq} is the sum of an ideal part Δg^{id} and a so-called excess part g^{ex}, with

$$\Delta g^{id} = RT[x_A \log x_A + x_B \log x_B], \tag{2}$$

where R is the gas constant, while the excess molar free energy is typically expressed trough the Margules correlations (*Smith* and *Van Ness*, Chapter 11) and

$$g^{ex} = RT\Psi x_A x_B, \tag{3}$$

where Ψ is a function of T and P and it is well known as Flory parameter.

Let us assume the pressure P is fixed, so that the physical state of the mixture at equilibrium depends only on T and ϕ.

Ψ can be easily determined from the phase diagram of the mixtures. In fact, phase separation process occurs whenever the temperature of the system is lower than the critical temperature. Now, let us call τ the reduced temperature with

$$(T_c - T)/T_c = \tau \approx \Psi - \Psi_c, \text{ where } \Psi_c = 2.$$

Below the critical temperature, $\Psi \geq 2$.

In order to take into account the effects of spatial inhomogeneities, Cahn and Hilliard (1958) introduced the generalized specific free energy g, which is given by the expression

$$g = geq + \tfrac{1}{2}RTa^2(\nabla\phi)^2 \qquad (4)$$

where a is the typical length of spatial inhomogeneties in the composition and it depends on the surface tension σ. At the end of the phase separation process, σ can be measured at the interface and from that, as shown by Van der Waals (1979),

$$\sigma \approx \frac{1}{2}\frac{\rho RT}{M}a^2\int(\nabla\phi)^2 dl \approx \frac{\rho RTa}{M}(\Delta\phi)^2\sqrt{\Psi - 2} \qquad (5)$$

Since the surface tension σ is the energy stored in the unit area of the interface separating two phases at local equilibrium, we have:

$$a \approx \frac{1}{\sqrt{\tau}(\Delta\phi)_{eq}^{\ 2}}\frac{\sigma M_W}{\rho RT} \qquad (6)$$

where $(\Delta\phi)_{eq}$ is the composition difference between the two phases at equilibrium.

For liquid systems the surface tension was measured using a Pendant Bubble Technique, and found that at room temperature $\sigma \approx 1 dyne/cm$. For a typical liquid mixture near its miscibility curve $a \approx 0.1 \mu m$.

Now, it is well known that the molar free energy can be written (*Smith and Van Ness*) as

$$g^{eq}/RT = \mu\phi \tag{7}$$

where $\mu = \mu A - \mu B$ denotes the difference between the chemical potentials of species A and B in solution.

Since

$$g^{eq} = \Delta g^{eq} + (g_A \phi + g_B (1-\phi))$$

$$g^{eq} = (g_A \phi + g_B (1-\phi)) + RT(\phi \ln\phi + (1-\phi)\ln(1-\phi)) + RT\Psi\phi(1-\phi) \tag{8}$$

$$g = (g_A \phi + g_B (1-\phi)) + RT(\phi \ln\phi + (1-\phi)\ln(1-\phi)) + RT\Psi\phi(1-\phi) + \tfrac{1}{2}Rta^2(\nabla\phi)^2 \tag{9}$$

Let us consider $\tilde{\mu}$ as the generalized chemical potential, defined as $\tilde{\mu} = \delta(g/RT)/\delta\phi$, we have

$$\tilde{\mu} = \frac{gA - gB}{RT}\ln\frac{\phi}{1-\phi} + \Psi(1-2\phi) - a^2|\nabla\phi|^2 \tag{10}$$

2.4.2 Equations of Motion.

For an incompressible mixture composed of two species with equal physical properties and if the flow is assumed to be slow enough to neglect the dynamic terms in the *Navier-Stokes* equation, conservation of mass and momentum lead to the following system of equation,

$$\rho\left(\frac{\partial\phi}{\partial t}+\mathbf{v}\cdot\nabla\phi\right)=\nabla\cdot\mathbf{J}, \tag{1}$$

$$\eta\nabla^2\mathbf{v}-\nabla p=\mathbf{F}_\phi;\qquad \nabla\cdot\mathbf{v}=0, \tag{2}$$

where v is the average local fluid velocity, **J** is the diffusion flux (Lifshitz and Pitaevski,1978) and $\boldsymbol{F}_\phi$ is a body force. As shown by Mauri *et al.* (1996), **J** is determined through the relation,

$$\mathbf{J}=\rho\phi(1-\phi)(v_A-v_B)$$

the velocities (v_A-v_B) are the sums of a convective part v and a diffusive part, where D is the composition-independent diffusion coefficient

$$v_A = v - D\nabla\mu_A \qquad\qquad v_B = v - D\nabla\mu_B$$

We have assumed that the diffusive parts are proportional to the gradients of chemical potential (Lifshitz, 1978*)*, so the diffusive flux is

$$\mathbf{J}=-\rho\phi(1-\phi)D\nabla\tilde{\mu}, \tag{3}$$

where D is the molecular diffusivity, and $\tilde{\mu}$ is the generalized chemical potential, defined as $\tilde{\mu}=\delta(g/RT)/\delta\phi$, with g denoting the molar Gibbs free energy, T the temperature and R the gas constant. Plugging the equation 10 in the above, we have:

$$\frac{J}{\rho}=-D\nabla\phi+D\phi(1-\phi)[a^2\nabla\nabla^2\phi+2\Psi\nabla\phi+(2\phi-1)\nabla\Psi] \tag{4}$$

where the term $D\nabla\phi$ is the regular diffusion flux, the term $(2\phi\text{-}1)\nabla\Psi$ is zero for small concentrations of either solvents ($\phi\to 0$ *and* $\phi\to 1$) and for ideal mixtures ($a=0$ *and* $\Psi=0$), the term a^2 is relevant only at small length scales, while Ψ is a function of T and near the critical temperature is proportional to $(T_c - T)$.

The body force in the Eq. (2) equals the gradient of free energy as the following:

$$\mathbf{F}_\phi = \frac{\rho}{M_W}\frac{\delta g}{\delta \mathbf{r}} = -\left(\frac{\rho RT}{M_W}\right)\phi\nabla\tilde{\mu}. \qquad (5)$$

This body force can be thought of as a non-equilibrium capillary force. In fact:

a) Being proportional to $\nabla\tilde{\mu}$, which is identically zero at local equilibrium, $\mathbf{F}_\phi$ is a non-equilibrium force. Therefore, since we observed that micro-domains continue to move rapidly until full segregation is achieved, we conclude that the condition of local equilibrium (where the concentration of the drops and that of the surrounding continuous phase equal their equilibrium values) can be reached only well after sharp interfaces are formed.

b) As it is driven by surface energy, $\mathbf{F}_\phi$ tends to minimize the energy stored at the interface driving, say, A-rich drops towards A-rich regions. The magnitude of the resulting non-equilibrium attractive force $\mathbf{f}_A$ between two isolated drops of radius r separated by a thin film of thickness λ can be easily evaluated as $f_A \approx F_\phi r^2 \lambda \approx \sqrt{\tau} r^2 \sigma / a$, where $F_\phi \approx \sigma / \lambda^2$ can be obtained through Eqs. (5) and (6). Therefore, this attractive force is much stronger than that of any repulsive interaction among drops due to the presence of surface-active compounds, thus explaining why the rate of phase separation in deeply quenched liquid mixtures is almost independent of the presence of surfactants (Gupta, Mauri and Shinnar, 1996).

Vladimirova et al. (1999and 2000) showed that model H in two dimensions reduces to a set of two equations which can easily be integratated numerically and whose predictions can be compared with experiments. In fact, expressing the velocity v in terms of stream function ψ:,

$$v_x = \frac{\partial \psi}{\partial r_y} \qquad v_y = -\frac{\partial \psi}{\partial r_x},$$

the equations of motion become:

$$\begin{aligned} \frac{\partial \phi}{\partial t} &= \nabla \psi \times \nabla \phi + \frac{1}{\rho} \nabla J \\ \eta \nabla^4 \psi &= \nabla \mu \times \nabla \phi \end{aligned} \tag{6}$$

Since the mechanism of mass transport at the beginning of phase separation is diffusion, the length scale of the process is a

$$r^* = \frac{1}{a} r \qquad t^* = \frac{D}{a^2} t \qquad \psi^* = \frac{1}{\alpha D} \psi$$

Plugging everything in the equations 6

$$\begin{aligned} \frac{\partial \phi}{\partial t^*} &= \alpha \nabla^* \psi^* \times \nabla^* \phi + \nabla^* [\nabla^* \phi - \phi(1-\phi)(2\psi + \nabla^{*2}) \nabla \phi] \\ \nabla^{*4} \psi &= -\nabla^* (\nabla^{*2} \phi) \times \nabla^* \phi \end{aligned} \tag{7}$$

The Peclet number, which is the ratio between the convective and diffusive mass fluxes defines, $Pe=vR/D$, where v is a characteristic velocity, which can be estimated through Eqs, provides a quantitative measure of the importance of convection. Finally we obtain,

$$N_{Pe} = \alpha \sqrt{\tau}, \quad \text{where} \quad \alpha = \frac{R^2 \rho RT}{D \eta M_W}. \tag{7}$$

α coincides with the "fluidity" parameter defined by Tanaka and Araki (1998). Diffusion is the dominant mechanism of phase segregation when either α or τ are small, that is when, respectively, either the viscosity of the mixture is very large, or the temperature of

the system is close to its critical value. In the first case, the model describes the diffusion-driven separation process occurring in polymer melts and alloys (Mauri, Shinnar and Triantafyllou, 1996), in the second case, that of near-critical liquid mixtures (Wong and Knobler, 1985, Beysen and Guenoun, 1994). In Gupta *et al.*'s experiments (1996), however, at $T = 20\,°C$: $a \approx 10^{-5}\ cm$ [cf. Eq. (5) with $\sigma = 1\ dyne/cm$] and $D \approx 10^{-5}\ cm^2/s$, so that $\alpha \approx 10^5$. This shows that in our case diffusion is important only at the very beginning of the separation process, when $\tau << 1$. Then, as the concentration field becomes non-uniform, the chemical potential gradients within the system drive the subsequent convection, which therefore becomes the dominant mechanism of mass transport until drops become large enough that gravity takes over. Since the other condition for diffusion-driven separation, i.e. $\tau << 1$, is met only for times of $O(ms)$, it is not surprising that we did not observe any diffusion-driven process.

Our theoretical analysis leads to the following expression for the rate of growth of the mean micro domain size r (see Gupta *et al.*),

$$\frac{dr}{dt} = k_b \frac{\sigma}{\eta}, \tag{8}$$

where $k_b = \sqrt{\Psi}\text{-}2/N_{Pe} \approx 10^{-4}$ is in good agreement with the experimental results. Using a different approach, this equation was obtained by Siggia and San Miguel *et al,* although their prediction $k_b \approx 10^{-2}$ far overestimates our growth rate results, $k_b \approx 10^{-5}$. Note also that the expression $dr^*/dt^* = 0.022$, where $r^* = r/a$ and $t^* = tD/a^2$, which was proposed by

Guenoun *et al* , is in good agreement with our experimental results, despite the fact that they considered very shallow temperature quenches.

Using this theoretical model, Vladimirova, Malagoli, and Mauri (2000) simulated the phase separation of a partially miscible demixed liquid mixture and obtained results that, in the absence of convection (i.e., for very shallow quenches and/or viscous liquid mixtures) are in agreement with the experimental results by Beynsens (1992). When convection is taken into account, however, Vladimirova et al. showed that the morphology of the system is radically different and obtained pictures that are strikingly similar to those obtained in our experimental results. They showed that, at a very early stage, the phase separation of an initially demixed system and that of an initially homogeneous mixture are similar to each other, leading to the formation of small microdomains. At this point, driven by the nonequilibriium capillary force, these domains start moving toward one or the other of the homogeneous regions, where they will be readsorbed, so that larger domains do not have the chance to form during the phase separation process.

Chapter 3

Phase Transition Extraction (PTE)

In this section a new separation process discovered over the past years by Shinnar and Mauri research group is described. In this process, named PTE (Phase Transition Extraction), the system, together with the solute to be separated, is first heated above its critical temperature, where it forms an uniform solution, and then cooled to the thermodynamically unstable region below the miscibility curve, where the solvents separate in two coexisting phases. The important feature of this process is that the resulting separation of solvents into two coexisting phases is very rapid, even in presence of emulsion-forming impurities.

3.1 The PTE Process Using the Temperature-Induced Phase Separation.

All phase transition extraction (PTE) processes capitalizes on the properties of partially miscible solvents with a critical point of solubility. In this process the liquid mixture is first heated to a temperature T_1 above the critical temperature T_{cr} and then rapidly cooled to a temperature T_2 below the critical point (see Figure 3.1). Ullman, Ludmer and Shinnar (1995) described an important application of this process to extract antibiotic from a fermentation broth, finding that the new process had higher yields than its conventional counterpart. In addition, coalescence was very rapid and phase separation was completed within few minutes, despite the fact that the broth was not filtered and that the suspended cells normally form a stable emulsion that need a centrifuge to separate.

Ullmann, Ludmer and Shinnar (1997) described how this process could be used to design and operate a multistage countercurrent extraction column composed of successive heating and cooling units (Figure 3.2). In this new column equipping each mixing section with a heater and each settling section with a cooler modified the process.

Ullman *et al.* studied the rapid coalescence of critical mixtures in detail (1995) using as a model system a dye (crystal violet) dissolved in water. Since the dye acted as an emulsion stabilizer, the timescale of the hindered coalescence during conventional liquid-liquid extraction could be varied from minutes to hours, by simply increasing the dye concentration from *2* to *5 ppm*. Ullmann used acetonitrile as main solvent to which he added *4%* (molar) of toluene to raise the critical temperature of the solution from *0℃* to *40℃*. The water-acetonitrile-toluene system was put in a vial, heated to *50℃*, where it became homogeneous, and then cooled back to ambient temperature, at which point the system phase-separated very quickly. On the other hand, when the system was agitated isothermally, separation occurred very slowly (up to several hours), as crystal violet had caused formation of a stable emulsion.

Ullmann *et al.'s* results had one limitation, namely the cooling was too slow (about one minute) to allow observations at short timescales. This is important because, when PTE is performed, one minute after cooling the main phase separation has already been completed, and the small changes that are observed at later times are due to a secondary nucleation. Therefore, other experiments were repeated using a much thinner glass cell, where cooling could be completed within two seconds. Finally, the resulted phase separation performing LLE was compared with PTE: there was an inherent difference between the two processes. In LLE two interfaces appeared, which moved towards the

center of the cell until they merged; in PTE the interface appeared almost immediately at its final position and the solution cleared up rapidly (see Figure 3.3). These observations are clearly at odds with the explanation of the phenomenon that was put forward by Ullmann *et al.* (1995), who assumed that at beginning of the process very small nuclei are formed, which subsequently grow by both diffusion and coalescence. However, following a temperature quenching, a process, generally referred to as spinodal decomposition, takes place, which can lead to phase separation without nucleation. In fact, the process begins with the appearance of a uniformly dispersed phase that develops into distinct regions of coexisting equilibrium phases.

Gupta, Mauri and Shinnar (1996) studied experimentally phase separation of fluid mixtures by direct visualization. Two experimental procedures were considered: in the first, so-called homogeneous case, the solution was first heated to a temperature above the coexistence curve, then mixed thoroughly and finally cooled down to the initial temperature with a cooling rate $dT/dt = 3\,°C/s$, in the second, so-called gradient case, after being heated, the solution is kept at a high temperature for two hours without mixing and only then it was cooled down (Santonicola, 2001).

In the homogeneous case, Gupta *et al.* found that, as in the case of shallow quenches, interconnected domains and well-separated droplets were formed, depending on whether the system undergoes critical or off-critical quenches, respectively. They found that the typical size of single-phase domains grew linearly in time with a growth rate $dR/dt = 100\,\mu m/s$, which is a few order of magnitude larger than that measured for shallow quenches. The growth rate that was obtained is about three times larger for interconnected domains than for droplets. In addition, since the equilibrium composition

of the system keeps changing as the temperature of the mixture decreases, "double phase separation" was observed, thus confirming Tanaka's observations (1998). The typical velocity of single-phase domains was also measured, obtaining a value of $100\mu m/s$, which is of the same magnitude as the growth rate.

In the gradient case, after the quench, the system remained unchanged for about three seconds, until suddenly a sharp interface appeared. Only then, droplets moved towards the interface, where they coalesced. At later times, analyzing the few scattered drops that were suspended within the mixture, forming what in engineering is called secondary emulsion, their mean radius R grow in time as t^{γ}, where the exponent $\gamma = 0.3 \pm 0.04$. This was in agreement with the theory of Lifshitz and Slyozov (1961).

The behavior of a phase separating mixture is well described by the model H (Hohenberg and Halpering, 1977), which predicts that after an initial diffusion-driven stage leads to a non-uniform concentration field, a concentration-gradient-induced material flux is generated, which is orders of magnitude larger than its diffusive counterpart and drives the successive process of phase separation. Based on this model, Gupta *et al.* (1996) derived an expression estimating the growth rate of single-phase domains, which is in excellent agreement with the experimental results. In addition, the presence of this concentration-gradient-induced driving force explains why in the gradient case we do not observe any drop large enough to be observed using our experimental apparatus.

3.2 Phase Separation in Liquid Mixtures in The Presence of Surfactants.

Gupta, Mauri and Shinnar (1999) compared two different processes involving mixtures of two partially miscible liquids, initially in their two-phase state: in the former, the mixture is agitated isothermally, while in the latter it is heated and cooled across its miscibility curve, inducing phase transition. The most important result of this study was that while, as expected, coalescence rate and settling time in the first case were strongly influenced by the presence of emulsifiers within the mixture, this was no when the mixture undergoes phase transition. In fact, in this case phase separation was rapid. Irrespective of whether surface-active compounds were added.

In this work, Gupta *et al.* offered a clear explanation of this phenomenon. First, they showed by microscopic visualization that the morphology of a liquid mixture in the presence of surfactants after isothermal mixing and that during phase separation were radically different from each other. The emulsions that formed after isothermal mixing were composed of a tightly packed suspension of micron-size drops, which hardly moved and coalesced only at the edge of the emulsion region. This accounts for the slow settling time observed macroscopically, and the fact that the presence of surface-active compounds does stabilize the emulsion. On the other hand, when the mixture was brought across its miscibility curve, it was composed of drops moving rapidly and coalescing, revealing that the process was driven by convection and not by diffusion. This conclusion was confirmed by the fact that at the end of phase separation, the partition coefficient of a solute (i.e. the ratio between its concentration within the two phases) equals its equilibrium value, irrespective of the molecular weight of the solute. In

fact, the extraction times of crystal violet and blue dextran were the same, although these compounds have *407* and *2,000,000* molecular weights, respectively.

These experimental results were explained, at least qualitatively, using the model H, where a body force drives fluid convection, which is proportional to the gradients in the system composition. The model H predicts that after an initial stage, characterized by long-range concentration fluctuations, the system separates into single-phase domains, with sharp interfaces. The body force can be identified with the traditional capillary interaction, which drives motion of the single-phase domains and acts as an attractive interparticle force. As the fluid motion convected surfactant molecules, they rapidly clustered on the droplet interfaces, inducing electrostatic repulsion. A simple dimensional analysis shows that the coalescence-enhancing attractive capillary force is much larger than the repulsive force among drops, which is due to the presence of surfactants, thereby showing why indeed surface active compounds do not appear to influence the settling time of phase separating liquid mixtures.

3.3 Concentration-Induced Phase Separation Process.

In another work Gupta, Mauri and Shinnar (1996) also presented a novel separation method named Concentration Induced Phase Separation or CIPS. The CIPS process is composed of two mixing stages: first, the system to be extracted is mixed with a primary solvent, which is soluble with the native solvent; then, a modifier is added, which is insoluble with either the native or the primary solvent. Immediately after the addition of the modifier, the system separates rapidly into two coexisting phases, even in the presence of emulsion-forming impurities.

CIPS is conceptually similar to the Temperature-Induced Phase Separation, or TIPS, described in Ullmann et al. (1995), where a mixture of native and primary solvents is heated and cooled across its miscibility curve. In fact, when the same solvent system is used, CIPS gives the same result as TIPS, provided that the temperature differential of TIPS is workable. The similarity of the two methods was demonstrated experimentally.

The advantages of CIPS over the conventional Liquid-Liquid Extraction, or LLE, process can be summarized as follows.

- *Improved extraction yield.* When the solute is adsorbed on solid particles, CIPS has a clear advantage over LLE, since, by using primary solvents that are miscible with the native solvent, it does not have the wetting problems that are encountered in LLE, where insoluble or partially miscible solvents are used.
- *Ability to handle emulsion-forming systems.* Unlike LLE, CIPS is almost unaffected by the presence of surface-active agents and no stable emulsions are formed.
- *Equipment savings.* Since we do not need centrifuges to break stable emulsions, as we do when using the traditional LLE process, the equipment required to perform CIPS is only a tank. Even when distillation equipment is required to separate the primary solvents from the modifier, CIPS is still cheaper to perform than LLE.
- *Lower product degradation.* Any possible shear stress damage to large solute molecules is prevented in the CIPS process, where only a mild mixing is required, as opposed to the high centrifugation of traditional LLE. In addition, the fact that in the CIPS process a small mount of the native solvent is contained

in the extract will help preventing the unfolding of large solute molecules, such as proteins.

- *Use of water-soluble solvents*. The CIPS process allows the use of water-soluble solvents, which, despite being in general good solvents of biological materials, cannot be used in conventional extraction processes.

TIPS also share most of these advantages over traditional LLE. Like the CIPS process, TIPS takes place rapidly and is not much affected by the presence of surface-active agents in the native system. In addition, since during the heating stage the native and primary solvents are miscible, the resistance to extraction of the solute through the cell interfaces is greatly reduced; in fact, Gupta et al. found that when they used the same solvents the extraction efficiency of the CIPS and TIPS was the same, and larger than that of traditional LLE. Therefore, it appears that TIPS, like the CIPS process, has many significant advantages over the traditional LLE process, at least for cases in which either stable emulsions are formed or the solute is sensitive to shear.

Chapter 4

Phase Separation of Deeply Cooled Low-viscosity Liquid Mixtures

In this Chapter, we present a visualization of the morphology of low-viscosity liquid mixtures during spinodal decomposition, following a deep temperature quench into the unstable region of mutual miscibility. Unlike previous studies, we consider deep quenches with $\tau = |T - Tc|/Tc \approx 0.1$*, in addition, we studied the phase separation of low-viscosity liquid mixtures that were initially mostly demixed with the exception of a thin, few millimeter-thick layer where a concentration gradient was present. After describing the physical properties of the liquid mixtures that were used in our experiments, we present the visualization of the phase separation of low-viscosity, deeply quenched fluid mixtures.*

4.1 The Experimental Setup.

An experimental setup was designed and built to allow the observation of the phase separation process, both the bulk flows as well as the motion of droplets of *10 μm* and up to *7mm*. It consisted of a temperature regulated, *1 mm* thick, *40 mm* high sample cell (Figure 4.1), an optical microscope (Nikon Optiphot-2) with Xenon illuminator (Nikon XBO Lamp 75W) and a digital camera (Fuji FinePix S1 Pro) with high resolution and high-speed continuous shooting (up to five frames per second). Placing the sample cell into a 8mm thick water jacket, into which temperature-controlled water was circulated, allowing a *3°C/sec*-quenching rate, regulated the temperature. Temperatures were

measured by inserting $350\mu m$ thermocouples, with $0.04\ sec$ response time and connecting them with a data acquisition system.

In our experiments we used two liquid mixtures. The first (System I) is the mixture that was extensively studied in previous works (Ullmann et al., 1995, Gupta et al., 1996), composed of water, acetonitrile and toluene; it has a critical volumetric composition of *38%* water, *58%* acetonitrile, *4%* toluene and it undergoes phase transition at critical temperature of $35°C$ (see phase diagram in Figure 4.2). At ambient temperature, this mixture separates into two phases with a density difference $\Delta\rho_I = 7 \bullet 10^{-2}\ g/cm^3$ and surface tension $\sigma_I = 1.3\ dyne/cm$, so that its capillary length is $Rc_I = 1.3\ mm$. Here, water is the continuous phase.

The second mixture (System II) is a nearly isopycnic system (i.e., a system that separates into two phases having, approximately, the same density) that is composed of *50%* acetone, *50%* hexadecane critical volumetric composition, critical temperature of *27°C*, viscosity $\mu_{II} = 2.3\ cp$ (see phase diagram in figure 4.2). At ambient temperature, this mixture separates into two phases, with a density difference $\Delta\rho_{II} = 6\ 10^{-4}\ g/cm^3$ and surface tension $\sigma_{II} = 1.2\ dyne/cm$, so that its capillary length Rc_{II} is about ten times larger than Rc_I i.e. $Rc_{II} = 1.4\ cm$. In this case, hexadecane is the continuous phase.

In addition, *50 ppm* of Oil 0 Red and *10 ppm* of Crystal Violet were added to System I and System II, respectively, to enhance the visualization of the two phases as they separate. When dissolved in such small percents, these dyes do not change the phase diagrams of the mixtures, or the characteristic of the phase separation process. All the solvents were HPLC grade, while water was double distilled. The analysis of the phase composition was conducted using an HP 5890 Gas Chromatograph.

Two experimental procedures were considered. In the first (to be referred to as homogeneous case), the solution was first heated to a temperature above the critical point, then mixed thoroughly and finally quenched with a cooling rate of about *3°C/sec*. The quenching was achieved by circulating cooling water at *20°C* and *7°C* temperature through the outer chamber of cell, resulting a temperature drop, illustrated in Figure 4.3. In the second case (to be referred to as a gradient case) after being heated, the solution was kept at a temperature above the critical point for two hours without mixing, and only then it was quenched. Mixing the solutions before the quench is extremely important when we want to study the behavior of initially homogeneous mixtures. In fact, when the system is kept at a temperature above the critical point without mixing for hours, the mixture is still mostly demixed, with the exception of a thin, few millimeters thick layer around the phase interface, where there is a sharp concentration gradient.

In Table 1 are summarized our mixtures' physical properties.

	Volumetric Composition	***Critical Temp.***	***Density Difference***	***Viscos.***	***Surface tension***
Syst. I	58%Acetonitrile, 38%Water, 4%Toluene	*35°C*	$7 \bullet 10^{-2}\ g/cm^3$	*1.2 cp*	*1.3 dyne/cm*
Syst.II	50%Acetone, 50%Hexadecane	*27°C*	$6 \bullet 10^{-4}\ g/cm^3$	*2.3 cp*	*1.2 dyne/cm*

Table 1: Physical Properties of Mixtures.

4.2 The Experimental Results.

4.2.1 Homogeneous Case.

The results of the visualization of phase separation of System I (acetonitrile, water, toluene) are shown in Figure 4.4, using a field of view of $300\mu m$, with the time $t=0$ corresponding to the moment when the temperature of the mixture crosses the miscibility curve. At first, we saw the appearance of $10\ \mu m$ isolated micro domains of the dispersed phase (in our case, the solvent-rich phase), which grew mainly by coalescence. In contrast, as shown in Gupta *et al.* (1999), the morphology of a critical liquid mixture is bicontinuous and consists of interconnected domains. This transition from bicontinuous structures to isolated droplets was also observed, among others, by Guenoun *et al.* (1987), Cumming (1992) and Tanaka (1998), although only for very small temperature quenches, and it agrees with the results of numerical simulations (Vladimirova *et al.*, 1999). The time evolution of these fast coarsening structures was determined in terms of their equivalent radius using Matrox Inspector Software (Gupta *et al.*, 1999), showing that the domain size grew rapidly within $1.5\ s$ from 10 to $100\ \mu m$ (see Figure 4.5), with a constant growth rate of $70\ \mu m/s$. Later, when the size of the nucleating drops became comparable to the capillary length $Rc_1 = 1mm$, the two phases separated rapidly by sedimentation. We also monitored the movement of a typical nucleating drop with radius $R<R_{c,\,1}$. As shown in Figure 4.6, we saw that, $0.5\ s$ after crossing the miscibility curve, a drop with radius $R \cong 30\ \mu m$ can move at a speed exceeding $100\ \mu m/s$, showing that strong convection exists within the system even after drops with sharp interfaces have formed and before they have

become large enough to sediment. In addition, the motion of the drops a) appears to have, approximately, random directions and b) does not depend strongly on the drop size. The source of this rapid movement cannot be molecular diffusion, as that would predict drop velocities a few orders of magnitude smaller than those observed experimentally. Such strong convection cannot be gravity-driven either, since in that case the motion would be directed preferentially downward and, in addition, it would be, of smaller magnitude. In fact, *0.5 s* after the quench the temperature of the system is about *33 ℃*, corresponding to a density difference between the two phases $\Delta\rho = 7*10^{-3} g/cm^3$ and therefore the Stokes sedimentation speed $v_{St} = (2/9)r^2 g\Delta\rho/\mu \approx 1 \mu m/s$ is two orders of magnitude smaller than the measured drop velocity. As for the fact that the drop speed does not depend strongly on the drop size and is similar to the velocities of micron-size particles suspended within the system, that seems to indicate the existence of a bulk convection, induced by some type of body force acting on the whole system.

We also studied the influence of the wetting properties of the cell walls by comparing the experimental results obtained using an untreated (i.e. hydrophilic) glass wall with those obtained depositing an OTS layer on the glass wall, making the surface hydrophobic. In both cases we found the morphology of phase separation to be identical, proving that wetting did not affect the phase separation process. Thermal effects were also ruled out, as the temperatures measured at different locations within the cell were found to differ from each other by less than *0.2 ℃*. In addition, when the mixture was replaced with water, with *10μm* size silica particles suspended in it, we saw that silica particles continued to slowly sediment during the temperature quench, with no additional

convection (we only observed a slight decrease in the sedimentation speed, due to a progressive increase of the water density as the temperature decreased).

In another set of experiments, we studied the phase separation process of an isopycnic mixture (System II with 50% acetone and 50% hexadecane) that was quenched in a cell, either horizontal or vertical. Since the capillary length of *System II* (acetone, hexadecane) is about *10* times larger than that of *System I*, i.e. $R_{cII} \approx 1cm$, here we could follow directly the motion of the millimeter-size nucleating drops, without using the microscope. Following the time evolution of the drops for $R < R_{cII}$ we saw that the drop size appears to grow linearly with time, with a growth rate of $400\mu/s$ (see Figure 4.7). However, since in this case, the drops could grow much larger than those of System I, the overall behavior of System II depended on whether the cell was kept horizontal or vertical. In fact, when the cell was kept vertical the process of phase segregation of System II was the same as the one of System I (see Figure 4.8): the nucleating drops grew, without sediment, until they reached millimeter size; at that point, they started to sediment and the mixture phase separated by gravity, forming a horizontal interface. We saw the same morphology for both systems either we used a quench to $20°C$ or to $7°C$.

Figure 4.9 compares initial droplets formation occurring in the two systems within the cell, when it is kept horizontal and the cooling is to $7°C$. We see that, initially, the behavior is similar though droplet growth is faster in the isopycnic system. After *20 seconds* the morphologies of the two systems are quite different. System II shows a vertical, clear interface while System I forms some large droplets. The separation process occurred in two stages. First, small droplets form in the whole cell, which rapidly coalesce into larger droplets, as it was observed in previous experimental works. Then,

acetone-rich droplets moved rapidly to the right along the longitudinal direction and coalesced, until, eventually, the two phases were completed separated by a clear vertical interface, which remained stable even when complete phase equilibrium was achieved. When the flow of the cooling water was inverted, phase segregation took place in the same way, but the acetone-rich phase moved to the left and the hexadecane-rich phase to the right. The most plausible explanation is that in isopycnic system the chemical potential-driven force is much larger than gravity, allowing phase separation to occur in horizontal direction, while in the density segregated system the opposite is true. On the other hand, gravity was never a dominant factor in the phase separation process, since the capillary length Rc_{II} was larger than the cell thickness. Therefore, when the drops were too small to sediment, i.e. at times t<3 s, the morphology of the mixture did not depend on the orientation of the cell, while at later times phase segregation could only occur through the horizontal motion of the drops, due to the fact that the glass walls had a larger wettability towards the minority phase. Eventually, the minority phase was distributed along the walls, whereas the majority phase formed a large domain at the center of the cell.

4.2.2 Gradient Case.

Here we studied the phase separation of low-viscosity liquid mixtures that were initially demixed, with the exception of a thin, few millimeter-thick layer, where a concentration gradient was present. In all of our experimental studies the mixtures were initially in its phase-separated state at a constant temperature of *15 ℃*. Then, they were heated to *40 ℃* and kept at that above-critical temperature for a given, so-called, stalling

time of *30min*, without any mixing. At the end of this time, the mixture was still mostly demixed, with the exception of a thick region around the phase interface where the composition, which was initially discontinuous, changed gradually from one to the other of its equilibrium values. Finally, the mixture was quenched back to a temperature below the critical point, which corresponds to a reduced temperature $\tau = (T - T_c)/T_c \approx 0.1$, at a quenching rate $dT/dt \approx 3\,°C/s$.

When an initially phase-segregated mixture is heated above its miscibility curve, the spontaneous mixing process is governed by diffusion alone, as the solution is gravity stabilized, and therefore it progresses slowly. In our case, the thickness of the mixing layer could be easily estimated observing that the color of the mixture at the interface region changed gradually from the bright red of the upper, solvent-rich phase to the plain white of the lower, water-rich phase for System I. The observed thickness of the mixing layer was about *1.8mm* for both systems, which is in agreement with the measured value $D=3\times10^{-5}\ cm^2/s$ of the solvent diffusivity, obtained using both GC techniques and laser absorption, which coincides with the theoretical prediction of the Wilke-Chang equation. That corresponds to an initial concentration gradient of $0.1\phi_A+T/mm$ for *System I* and $0.3\phi_A/mm$ for *System II*, where ϕ_A+T and ϕ_A are, respectively, the volume fraction of acetonitrile plus toluene and that of acetone.

Two other diffusion times were considered, namely, *10* minutes and *2* hours, corresponding to approximately *1* and *3.5mm* thicknesses of the diffusion layer, respectively. However, the results that were obtained in these cases are not reported here, as they were very similar to those obtained with *30min* of diffusion time and did not add any new element to our understanding of the phenomenon.

The morphologies of Systems I and II as they phase separates is shown in Figures 4.10, 4.11, and 4.12, where the time t=0 denotes the moment when the temperature of the mixture crosses the miscibility curve. As mentioned above, the system was initially demixed, with the exception of a millimeter-thick mixing region, in which the composition varied gradually from that of the lower, water-rich phase (white color) to that of the upper, solvent-rich one (red color). Note that, for System I, the lower, water-rich phase is white, while the upper, acetonitrile-rich phase is red, whereas for System II, the colors are inverted. Focusing the experimental apparatus on the diffusion region, in Figures 4.10 and 4.11 we see that, after the quench, System I remained unchanged for about *6 seconds*, when, first, micron-sized drops appearing and then, within few seconds, a sharp interface suddenly appeared. Only then, we saw drops appearing and moving towards the interface, where they coalesced. A very similar morphology was observed in the isopycnic system, where, however, the process was much faster and the interface formed within a few tenths of a second. This behavior looks remarkably different from that of an initially well-mixed (i.e. uniform) mixture, where single-phase domains appear immediately after the temperature of the system has crossed its critical value and then grow rapidly until they b ecome large enough that they start sediment, so that system rapidly segregates by gravity, indicating that the process is driven by convection.

Figures 4.10 and 4.11 offer clear evidence of the fact that phase separation in low-viscosity liquid mixtures is too rapid to be due to diffusion alone, as a typical solvent molecules takes *1h* to diffuse and form the interface region but only a few seconds to move back during phase separation. In addition, the fact that the morphology of isopycnic system during phase separation changes in the same way as the morphology of density-

segregated system shows that gravity does not play any role in the process. Actually, we can see from the figures, the isopycnic system separates *10 times* faster than the density-segregated one.

The convection field of System I was studied by inserting glass particles into the cell with a syringe; then, after waiting until the particles had reached the diffusion region, we quenched the system and monitored the particle motion. On the other hand, measuring the velocity of the glass particles during the phase transition and then subtracting their constant sedimentation velocity studied the convection field of System II. As it turned out, the particle velocity was mostly horizontal, and therefore, the influence of sedimentation was small.

One of the most important stages of our work was the determination of the most appropriate particles to suspend in the mixtures for direct observation of the bulk flow. These particles had to have a small enough buoyancy to minimize sedimentation and not interfere with the phase separation process. In particular, they could not denature at *50 ℃,* nor could they interact with the solvent mixtures of flocculate. After careful testing, we found that, for System I, the best choice was *S60/10000 3M Scotchlite* glass bubbles, consisting of hollow glass micro-spheres, *5-50μm* in size, with a density of *0.8-0.9 g/cm*^{3}. Of these particles, we selected those whose density lies between the densities of the two separating phases of System I, so that, during the phase transition, they would remain confined in the interface region, while the heavier or lighter particles would either sediment or float out, respectively.

Figures 4.12, 4.13, 4.14 represent more direct evidence of the convection-driven nature of the phase separation process. In Figure 4.12, the convective bulk flow, prior to the

formation of the interface, is visualized by following the trajectory of a glass particle in System I. As shown in Figure 4.13, as soon as the temperature of the mixture decreases below its critical value, the particle suddenly accelerates vertically toward the center of the diffusion region and then starts drifting horizontally with increasing speed until the interface appears; at this point, the particle stops, and the mixture returns to its macroscopically quiescent state. Finally, in Figure 4.14, the average velocity of 100 glass particles is represented, showing that it increases with time up to values of about $350\mu m$. These results show that convective movements occur even during the first $5s$ following the quench, when the system does not display any macroscopic morphological changes (see Figure 4.11). Note that, unlike phase transitions in homogeneous systems, where convective motion is random, in our case, the particle trajectories are deterministic, directed toward the interface within the xy plane of view. In fact, had particles moved along the transversal z direction, they would have become out-of-focus (which never happened), as the depth of field of our camera was about $5\mu m$.

To demonstrate that the bulk flow was not due to thermal gradients within the cell, we suspended heavier silica particles in System I, measuring a horizontal velocity field identical to that obtained with glass particles, while in the vertical direction a steady sedimentation speed was superimposed on the clean phase-transition-induced velocity field of the glass particles. Now, when the System I was replaced with water, we saw that the silica particles continued to sediment during the temperature quenched, with no horizontal movement and only a slight decrease in sedimentation speed, due to a progressive increase of the water density as the temperature decreased. In addition, we studied the influence of the wetting properties of the cell walls by comparing the

experimental results obtained using an untreated (i.e. hydrophilic) glass wall with those obtained depositing an OTS layer on the glass wall, making the surface hydrophobic. In both cases we found the morphology of phase separation to be identical, proving that wetting did not affect the phase separation process.

Chapter 5

Gravity-Free Phase Separation of Liquid Mixtures

During our study on spinodal decomposition of low-viscosity partially miscible liquid , we observed rapid flows up to 6cm/sec in a horizontal direction. Most of our previous work was carried out in a small glass cell suitable for microscopic observation. Due to the large surface to volume ratio of the device, interfacial capillary forces on the glass liquid interfaces could not be disregarded. As we were interested to obtain results that could be applied on industrial scale, we designed a larger device and used a condenser tube, 20 cm long and 1 cm diameter, to eliminate the impact of capillary effects.

We investigated the spinodal decomposition of a mixture of hexadecane and acetone rapidly cooled to a temperature of 20°C below the critical point using a horizontally placed condenser tube. The droplets formed, moved horizontally to the forming interface, resulting in a vertical interface. Depending on which phase was the dispersed, the droplets moved either to the colder or hotter section of the temperature gradient. The results described in this chapter show that this is not conventional thermo-capillary motion but a flow driven by chemical potential gradients. This opens up new possibilities for studying flow in a microgravity environment and opportunities for practical applications in separation processes.

5.1 The Experimental Setup.

To minimize the impact of gravity we used the acetone-hexadecane liquid mixture with a critical temperature of $T_c = 27℃$ that was used in previous studies and whose phase

diagram is represented in Figure 4.2b. At ambient temperature, this mixture separates into two phases, with a density difference $\Delta\rho = 6\ 10^{-4}\ g/cm^3$. This density difference, although very small, is still sufficient to cause a slow separation of droplet dispersion by settling and coalescence. Similar, so called, isopycnic mixtures have been also used by Guenoun *et al.* (1987). In addition, *100 ppm* of crystal violet, a dye that absorbs preferentially in acetone, was added to the mixture to enhance the visualization of the process. When dissolved in such small percents, this dye does not change the phase diagram of the mixture, or the characteristics of the phase separation process.

Two different initial concentrations were used, the former having a *50%* acetone, *50%* hexadecane volumetric critical composition, in which the dispersed phase is acetone-rich, while the second system consisted of a *70%* acetone - *30%* hexadecane mixture, where the dispersed phase is hexadecane-rich.

We also used the mixture composed of acetonitrile, water and toluene with a larger density difference between the phases ($\Delta\rho = 7^*\ 10^{-2}\ g/cm^3$) for comparison whose phase diagram is in Figure 4.2a.

It was pointed out by reviewers that in the small cell used previously (see Chapter 4) interfacial forces between the glass and liquid as well as capillary forces could play a role. Furthermore since we were interested to obtain results that could be applied on industrial scale, we needed to get data in large dimensions. To do so we designed and built a new experimental setup consisting in a condenser tube (see Figure 5.1), which is *20 cm* long and *1 cm* in diameter. This new experimental setup allowed the observation of the motion of individual droplets in a size range of *0.5 mm* of diameter and up.

The condenser tube is closed on both ends and placed horizontally to minimize gravity effects on the total separation. The temperature was controlled by currently heat transfer liquid trough the cooling system of the condenser, using two constant temeparture reservoirs, one hot and one cold, keeping the temperature of each reservoir constant at the desired value and allowing a fast switch between the hot and the cold loops.

In all our experiments, we started with the mixture in its phase-separated state at a constant temperature of *20 ℃*. Then, the solution was first heated to *38 ℃* (i.e. well above its *27 ℃* critical temperature), mixed thoroughly and finally quenched back to *7 ℃*, with a quench rate of about *3 ℃/s* (see Figure 5.2 for the temperature drop in various positions of the condenser tube). This quenching was achieved by circulating cooling water at *7°C* through the outer chamber of the condenser. The mixture reached complete separation before it becomes completely cooled. The time reported in all experiments is measured from the moment the temperature crosses the miscibility curve. As the flow rate in our overall equipment was limited, we observed a small temperature gradient of *0.25 ℃/cm* along the axes, but only a very small gradient across the diameter (see Figure 5.3).

In Figure 5.3 the temperature profile along the axial direction of the condenser is shown, revealing that during the phase separation process there was, at most, a *0.25 ℃/cm* temperature gradient. This is the reason that in the following we will distinguish two separate regions in the condenser: the inlet region, which is the colder region and the outlet region, which is the warmer region.

This new experimental setup allowed the observation of the motion of individual droplets in a size range of diameters *0.5mm* to *6mm* and up. The study of coalescence in spinodal decomposition requires the observation of the simultaneous motion of a number

of individual droplets, each with a potential different direction and velocity. In previous studies we took a sequence of photographs and followed a few droplets. This is inaccurate and hard to do in the large tube. To get better measurements, we developed a special new method. We used a stereo-microscope (Nikon SMZ1500) and a digital camera (SPOT, Model 3.2.1) with high resolution and high speed continuous shooting (up to *10 frames* per second). This camera has unique properties for studying dynamic phenomena and is especially useful for observing the fast motion of droplets. It captures the three basic colors (red, green and blue) separately in succeeding pictures with an adjustable time interval. In our experiments we chose a time interval between these colors of *0.12 seconds*. Therefore this camera allows measuring simultaneously both velocity and direction of a large number of droplets (see Figure 5.4). This greatly enhances our experimental capabilities especially for fast separations. In the figure we can see a green shadow after the droplet, which indicates the position and the direction of this droplet after *0.12s*.

5.2 Experimental Results.

We started first with the isopycnic mixture (i.e. *50%* Hexadecane and *50%* Acetone). In Figure 5.5 we see that the phase separation of this critical mixture in the condenser tube occurred in the much same way as in the cell: acetone-rich droplets formed in the whole tube. But later these droplets started to move along the axial direction, towards the warmer region of the tube. Then, as more droplets moved towards the interface, a vertical interface appeared at the warmer end of the tube. Then, this interface moved towards the middle of the tube, until complete phase segregation was

achieved after *8 seconds*. This was similar as that happened in the vertical small cell where the overall droplet motion was due to gravity. At the end, after *20* seconds, the small gravity difference made the system unstable, resulting in a horizontal interface. When we reversed the temperature gradient by exchanging the inlet and the outlet of the cooling mantle, the flow was reversed. In addition, we observed that, initially, when the drops were small, a strong random motion was superimposed to their net drift, while as the drop size increased, such random motion was no longer observable experimentally.

We also noted another interesting phenomena. The interface was formed before the final temperature was reached. As the separated acetone phase cooled further, secondary phase separation occurred, leading to the formation of droplets of the hexadecane-rich phase, flowing towards the colder region. To confirm this effect, we repeated the experiment using a *70%* Acetone - *30%* Hexadecane mixture, so that the acetone-rich phase became the continuous phase. We saw that (Figure 5.6) the hexadecane-rich dispersed phase moved to the colder region, with similar motion of the droplets and morphology as in Figure 5.5.

We also measured the velocity of the individual droplets by using a macro lens, in the camera described before, observing only a small section of the tube at different locations. Typical results for both cases are given in Figure 5.7 and 5.8 (we took pictures every second, but we only give typical results). After two seconds, droplets sizes were between about *2 mm* and we observed a horizontal velocity in the direction of the interface of approximately *3 mm/s* with no clear dependence on the droplet size. As the droplets size increased, the horizontal velocity increased while random motion decreased. After four seconds, droplet size increased to over *5 mm* and their velocity to *6 cm/sec*. In

addition, droplet velocities became nearly proportional to the droplet size, with no random motion. At this point, we saw a remarkable fact: when the flow of the cooling water was changed so that the longitudinal temperature gradients decreased by a factor four, we did not see any change in the velocities of the drops.

Similar effects are observed in an acetone-rich mixture, but the droplet motion was in the direction of decreasing temperature. To make sure that this effect was not caused by flow instabilities, we took pictures at different cross sections along the tube after *2 seconds*, when droplets were still smaller, and found that all droplets in all the cross sections moved in the same direction, with no reverse flow.

These experiments were repeated cooling only to *20°C*, instead of *7°C*. In this case, gravity dominated and no vertical interface was ever observed. Instead, a horizontal interface was formed within *10* seconds from the temperature quench. Also, we used a mixture with a large density difference between the phases composed of *58%* acetonitrile, *38%* water and *4%* toluene in volume that, at ambient temperature, separates into two phases with a 7×10^{-2} g/cm^3 density difference. In that case, too, heating the mixture above its *35 ℃* critical temperature and then cooling it down to *7 ℃*, vertical interfaces never formed, while a horizontal interface appeared within *5* seconds from the temperature quench (see Figure 5.9). Clearly, in these cases, the force due to chemical potential gradients was too small to overcome the effect of gravity, especially as the vertical distance to the condenser wall is small compared to the length (*0.5mm*). To observe a horizontal motion one could need a setup allowing a motion in both directions.

To study the impact of the temperature gradient, we increased the gradient used in our experiments from *0.25 ℃/cm* to *1 ℃/cm*, there was no effect on droplet velocity, while the

separation time increased by *50%*. This indicates that temperature gradient is not responsible for the force acting on the droplets, but somehow it acts as a switch for the direction of the flow.

5.3 Discussion.

In this part of our research we present an unexpected experimental phenomenon: when a low viscosity and nearly isopycnic binary partially miscible system is quenched deeply and rapidly into its spinodal region, it develops large scale fast and uniform motions of the growing droplets along a direction determined by an imposed small temperature gradient. In fact, thanks to such large-scale flows, complete phase segregation may occur on a *20-centimeter* scale, even in the absence of gravity. Although it was well known that the process of phase separation of such mixtures is driven by convection (see Chapter 4), this is the first time that such motions were observed to occur on such a long scale with such high velocities.

While the magnitude of the phenomenon is surprising and the results are very reproducible, an explanation is much more difficult.

The results were surprising; clearly they were related to spinodal decomposition. In order to observe this phenomenon the solvent mixture had to have special properties: a small density difference between the phases, a low viscosity and furthermore the cooling has to be rapid and deep into the spinodal region. The reason that, despite the large research in spinodal decomposition, the phenomenon was not observed before is that most of the previous experimental investigations were carried out close to the critical point.

If the system were at local equilibrium, we could argue that the movement of the drops was due to thermo-capillary effects, since the surface tension of the drops decreases as temperature increases. In fact, it has long been known that a droplet suspended in a non-isothermal liquid migrates in the direction of the temperature gradient *(∇T)*. This droplet's migration is due to the temperature-induced surface tension gradient at the droplet interface and is denoted thermo-capillary motion. *Young et al.* (1959) found that the droplet velocity is related to the local temperature gradient by the following equation:

$$v = \frac{R}{\eta}\frac{d\sigma}{dT}|\nabla T|$$

where R is the droplet's radius, $d\sigma/dT$ is the rate of change of interfacial tension, ∇T is the temperature gradient imposed in the continuous phase and η is its dynamic viscosity. However, this explanation must be ruled out, as we saw that hexadecane-rich drops moved towards the cooler section of the condenser tube, while acetone-rich drops moved in the opposite direction. Therefore, the observed drop migration is not a thermo-capillary motion, although they are both caused by gradients in chemical potential (Jasnow and Viñals, 1996).

In addition, if we were dealing with thermo-capillary migration, we could never expect the magnitude of the velocity measured experimentally. In fact, for our system at temperature of *20 ℃*, the surface tension σ *=1.2 dyne/cm*, the rate of the surface tension $d\sigma/dT$ = *0.048 dyne/cm ℃*, the temperature gradient ∇T= *0.25 ℃/cm* and η is *1 cp*, therefore, for a droplet of *5mm* in diameter, we expect to have a thermo capillary velocity of *0.6 cm/s* which is *10* times smaller than that measured experimentally (*6cm/s*). Finally,

the explanation that thermo-capillary migration could be responsible of the observed phenomenon is inconsistent with the fact that a decrease of the temperature gradient by a factor of four had no impact on drop velocity.

It should also be stressed that the fact that the velocity of the droplets is independent of the magnitude of the temperature gradient, whereas the direction of the flow depends on that of the temperature gradient seems to indicate some type of instability mechanism. However, it is clearly not flow instability due to a temperature gradient, since the detailed simultaneous velocity measurement of a large number of droplets of different sizes showed that they all flowed is in the same direction. On the other hand, conventional flow instability should show the existence of a reverse flow.

The diffuse interface model, predicting that convection in systems far from equilibrium, such as ours, is driven by chemical potential gradients, instead, provides a possible explanation of this phenomenon. In that case, when acetone-rich and hexadecane-rich phases replace one another, this driving force (and therefore convection as well) reverses its direction. In fact, it has been observed experimentally and confirmed numerically that, in the absence of temperature gradients, drops move in random directions, with an instantaneous velocity that depends on how far the system is from equilibrium and is therefore a function of the composition of the drops (and that of the continuous phase as well). As soon as a small temperature gradient is applied to the mixture, drops start moving coherently either parallel or antiparallel to the temperature gradient. Accordingly, the effect of the temperature gradient is merely that of orienting all the drop speeds along the same direction and that is why its magnitude does not influence the phenomenon, lies with a certain range: it cannot be too small, otherwise it is

not strong enough to orient the drop velocities, but it cannot be too large either, otherwise conventional flow instabilities and thermo capillary effects become relevant. This explanation is consistent with previously obtained results, where we studied the phase separation in a system with a preexisting concentration gradient.

While the existence of flows driven by chemical potentials has been previously observed on a smaller scale, flows of this magnitude have never been reported. This new phenomenon is totally reproducible and controllable, therefore offering a challenging subject for theoretical and experimental investigations of separation processes, as well as for inducing flows in micro-gravity environments.

Chapter 6

The Influence of Surfactants and Viscosity on the Phase Separation Rate of Liquid Mixtures

In this chapter we intend to study the limitations of the results obtained. In fact, we expected that coalescence could be eventually retarded increasing the amount of surfactants and thickeners, thereby increasing the viscosity of the mixtures, or when we quench the mixture in its metastable region. Therefore we determined the thresholds of the surfactant concentration and of the mixture viscosity and composition beyond which surfactants start to slow down significantly the separation process, just as they do in the absence of phase transition. From a practical viewpoint, one of the most interesting features of spinodal decomposition in the convective range is that emulsion-promoting compounds have almost no effects on the phase separation rate. In this work we investigated whether the presence of stronger and more concentrated emulsifiers has an impact on the phase separation rate. We also studied the effect of emulsifiers when the mixture was quenched into its metastable region, where convection and diffusion are comparable. As some of these emulsion stabilizers produce non-transparent systems, we had limit ourselves to observing only the time needed to complete the separation.

6.1 Experimental Setup.

An experimental setup similar to that described in Chapter 4 was designed and built to allow the observation of the phase separation process in these different cases (Figure 6.1). As before, we used a temperature-regulated, *1mm* thick, *40mm* high sample cell and a

20cm long and *1cm* diameter condenser tube. Placing the sample cell into a *8mm* thick water jacket, into which temperature-controlled water circulated, we could regulate the temperature. The condenser tube is a glass double-pipe with an internal *1mm* thick pipe and an external pipe as a jacket and it is *20 cm* long.

Since we were also interested to study the effect of cooling rate on phase separation process, we used two different volumetric pumps: one pump had a flow rate of *43.5cc/s* and the other a flow rate of *9.7cc/s*. Using the pump with the flow rate of *43.5cc/s* we achieved a cooling rate of *3 ℃/s* which is relatively fast and then we called it "*fast cooling*". Using the other pump we obtained a cooling rate of *1.3 ℃/s* so called "*slow cooling*". In Figure 6.2 we can see the temperature drops using both pumps. Temperatures were measured by inserting *350 μm* thermocouples, with *0.04 s* response times, at various locations inside the cell and condenser, and connecting them with a data acquisition system.

The experimental setup has a digital camera (FinePix S1Pro) that was chosen for its high-resolution and high-speed continuous shooting at *1.5 frames/s* (for up to five frames). This digital camera employs *3.4-megapixel*, *23.3x15.6 mm* sized Super CCD image sensor. The combination of the enlarged pixel size through the use of octagonal shaped photodiodes and the larger size of Super CCD captures a great deal of light, resulting in superior image sensing capability and ultrahigh resolution image files with up to *6.13 million pixels* (*3,040x2, 016 pixels*). The digital camera is provided with a resolution monitor with *200,000 pixels* and it can be used to playback and to check images.

The measure of viscosity of our solutions was done by a *TA* instrument viscometer (model AR 1000).

In all of these experiments we used a liquid mixture of water, acetonitrile and toluene, whose thermodynamic properties were described in Chapter 4.

This mixture has a critical volumetric composition of *38%* water, *58%* acetonitrile and *4%* toluene, undergoing phase transition at $Tc = 35\,^{\circ}C$. All solvents were HPLC grade. In addition, *50 ppm* of Oil 0 Red dye were added to our system to enhance the visualization of the separation process, as it dissolves preferentially in the upper, acetonitrile-rich phase. When dissolved in such small percents, this dye does not change the characteristics of the phase separation process. This dye allows us to see, at the end of phase separation, two different phases: the upper organic, acetonitrile-rich phase (lighter) and the aqueous, inorganic phase (heavier).

In previous work of this research, Gupta *et al.* (1999) studied the phase separation of only two liquid mixtures, in which two types of emulsifiers were dissolved at given concentration. We needed to generalize our results to a wider range of emulsifiers; in particular we intended to investigate how the phase separation rate was affected by the concentration of emulsifiers. Typically, surface-active compounds can be of two types, inducing the formation of either electrical double layers (charge stabilization) or protective layers (steric stabilization) on the droplet surface. Ionic surface-active agents belong to the first type of surfactants, inducing charge stabilization through the adsorption of ions or polyelectrolyte at the surface of the droplets. In this case droplets are stabilized because, o n the hand, these electrical double layers tend to prevent the flocculation of equally charged droplets, and, on the other hand, they retard the draining

of the liquid film, due to electro viscous effect (i.e. the electrostatic attraction between droplet interfaces and flowing films). The second type of surfactants are far less efficient, as they simply form a protective layer at the surface of the drop, thus obstructing mass transport across the interfaces, as it happens with nonionic emulsifiers, polymers or finely divide solids. Finding the right emulsifiers was a crucial problem and after trying many of them, we found the right candidate in a surfactant named *IGEPAL CO-730*. The emulsion formed by this surfactant was stable for more than one our.

Our experimental setup was not able to handle polymers, so in order to study phase separation of high-viscosity mixtures we created mixtures similar to polymers. To do that we used CMC (carboxyl-methyl-cellulose) in our mixtures because it is soluble in hot and cold water, increasing its viscosity. We used two types of CMC: one was *CARBOFIX 5A* (Bargazi srl) and the other was carboxyl-methyl-cellulose sodium salt (*Fluka)*. In Appendix A we can see that the solution with *CARBOFIX 5A* in water has a much smaller viscosity than the *Fluka*.

All of the experiments were carried out in similar way: the mixture was initially in its phase-separated state below the miscibility curve, at a constant temperature $T1=25\,℃$, then it was heated to a temperature $Th \approx Tc + 5\,℃$, that in our case is $Th = 40\,℃$, mixed thoroughly and finally it was cooled back to the temperature T_1. Since one of the goals of this work was to study the behavior of phase separation process changing the cooled temperature, we also performed the experiments using a lower temperature of $2\,℃$ (the smallest temperature we can reach with our experimental set up) in order to achieve a bigger ΔT.

6.2 Experimental Results.

In this experimental part we focused on studying: a) influence of coalescence retardant, mixture composition and different cooling rates on phase separation; b) influence of cooling temperature on phase separation; c) influence of viscosity on phase separation.

6.2.1 Influence of Mixture Composition, Coalescence Retardants and Cooling Rate on Phase Separation.

This first set of experiments allowed us to understand how the phase separation rate is affected by using a stronger surfactant concentration, strongly off-critical mixtures and different cooling speeds. We used a mixture of acetonitrile-water-toluene with three different compositions: a mixture with a critical composition and two with an off-critical composition. As shown in Figure 6.3, we had two different points of off-critical composition, first with *90%* of organic phase and *10%* of aqueous phase, second with *90%* of aqueous phase and *10%* of organic phase. We obtained these off-critical solutions starting heating a solution with critical composition to a temperature above the critical point and then we cooled it down to the room temperature: at this point we have two different phases. The lighter phase is the organic one where Oil 0 Red dye dissolves preferentially; the heavier phase is aqueous and it is colorless. We can observe in Figure 6.3 that in off critical case the temperature at which the phase separation occurs is *28 ℃* instead of the *35 ℃* of the critical case.

We used three different surfactant amounts *(0%, 2%, 5%)* and cooled the system from a temperature T_h=*40 ℃* to T_l=*25 ℃*, using, first, a fast cooling of *3 ℃/s* and then a slow cooling of *1 ℃/min*.

The results are summarized in Table 2. The emulsion-promoting compound has almost no effects on the phase separation rate in the mixture with critical composition, in fact, phase separation seems to occur at a rate that is independent of its presence. This result was already obtained by R. Gupta *et al.* (1999), who added two types of solute to the liquid mixture, namely, *50ppm* of crystal violet and *100ppm* of blue dextran. The most important result of that study was that the coalescence rate and the settling time were not strongly influenced by the presence of emulsifiers when the mixture underwent phase transition.

We also studied the effect of emulsifiers when the mixture is quenched into its metastable region, where convection and diffusion are comparable (off-critical case). We can observe that when the mixture is quenched in its metastable region, the phase separation is a little faster (*16sec*) than in mixture with critical composition (*20sec*) in absence of surfactant (Figure 6.4). This happens because in the mixture with critical composition at the end of phase separation, the two phases at equilibrium are in a rate of 1:1, while in the mixture with metastable composition they are in a rate of 1:9 inducing a faster sedimentation of the minor phase.

We also observed that in mixtures with off-critical composition the presence of emulsion-promoting compound slows down the complete separation (see Figure 6.5). In fact, for the mixture with *90%AQ* and *10%ORG* the presence of *2%* of surfactant slows the complete phase separation that occurs after *5min*. In Figure 6.6, we can observe similar behavior for the mixture with the composition of *10%AQ* and *90%ORG*.

We conclude that changing the mixture composition to metastable region in presence of surfactant, convection ceases to be a dominant factor in phase separation process and diffusion becomes dominant.

	No Surfactant	*+2% Surfactant*	*+5% Surfactant*
Critical composition 38%Water, 58% Acetonitrile, 4%Toluene	20s	23s	28s
Off-critical composition 90% AQ, 10% ORG	16s	35s	90s
Off-critical composition 90% ORG, 10% AQ	16s	35s	90s

Table 2: Separation Time in the cell using a Fast Cooling from Th = 40° to Tc = 25 °C.

When we repeated the same experiments but using a slow cooling (see Table 4), we observed that the dynamics of phase separation is the same of that of fast cooling, it is much more slower but does not depend on cooling rate.

	No Surfactant	*+2% Surfactant*	*+5% Surfactant*
Critical composition 38%Water, 58% Acetonitrile, 4%Toluene	**10m**	**10m and 15s**	**10m and 50s**
Off-critical composition 90% AQ, 10% ORG	**3m**	**3m and 10s**	**3m and 30s**
Off-critical composition 90% ORG, 10% AQ	**3m**	**3m and 10s**	**3m and 30s**

Table 3: Separation Time in the Cell using a Slow Cooling from Th = 40° to Tc = 25 ℃.

6.2.2 Influence of Cooled Temperature.

In a second set of experiments we studied the effect of cooled temperature on phase separation of our mixture. We used the same mixtures described above with the same amount of emulsion-promoting compound, using a fast cooling to a temperature of *2 ℃* and *32 ℃*. The results are summarized in Table 5.

	No Surfactant	*+2% Surfactant*	*+5% Surfactant*
Critical composition 38%Water, 58% Acetonitrile, 4%Toluene	**14s**	**21s**	**25s**
Off-critical composition 90% AQ, 10% ORG	**14s**	**31s**	**2m**
Off-critical composition 90% ORG, 10% AQ	**14s**	**31s**	**2m**

Table 4: Separation Time in the cell using a Fast Cooling to T_f=2 ℃.

For mixture with critical composition the cooled temperature influences the separation rate, in fact we can see from the diagram in Figure 6.7 that phase separation is much more faster when the temperature is low. We can observe that using a bigger ΔT (see table 5) phase separation is faster than using a smaller ΔT (see table 6). We can explain this result observing that bigger is the ΔT, bigger is the body force and formed droplets reach their capillary length in less time, so they can sediment (see Figure 6.8) and phase separation is complete.

	No Surfactant	*+2% Surfactant*	*+5% Surfactant*
Critical composition 38%Water, 58% Acetonitrile, 4%Toluene	**21s**	**24s**	**29s**

Table 5: Separation Time in the cell using a Fast Cooling to T_f=32 ℃.

6.2.3 Influence of Viscosity.

In this set of experiments we used three mixtures: *System I* with critical composition, *System II* composed of *60%* Acetonitrile, *30%* Water and *10%* Toluene whose continuous phase is acetonitrile (organic phase), *System III* with *10%* Acetonitrile, *80%* Water, *10%* Toluene whose continuous phase is water (aqueous phase).

We started to study the behavior of *System I* with and without CMC in the cell, placed vertically and horizontally, and in the condenser tube; for this mixture we used *Fluka CMC* that gives a system more viscous (Appendix A) and we compared the results with the same system with no CMC. In the case with no CMC, after cooling, the system remained unchanged for a few seconds and then droplets of acetonitrile-rich phase started forming and moving to a formed interface (Figure 6.9). In Table 7 we can see the time needed to complete phase separation adding CMC in water using a fast cooling from a temperature of *40 ℃* to a temperature of *25 ℃* in a vertical cell. Phase separation of

mixtures with a higher viscosity is much more slower; this happens because viscosity slows down the convective motion between the droplets during phase separation.

In the case with *2%* and *3%* of CMC we saw that the dynamics of phase separation and the final morphology did not change a lot from the previous case. As we can see from Figure 6.9, there is, first, formation of acetonitrile droplets, then formation of interface and then slow motion of droplets toward the interface.

% CMC in water	Separation Time	Viscosity
0.0	*16 s*	*1 cP*
0.3 %	*3 min*	*124 cP*
0.5 %	*5 min*	*207 cP*
1 %	*20 min*	*414 cP*
1.5 %	*1 hr*	*611 cP*
2.5 %	*2 hr*	*1025 cP*

Table 6: Impact of viscosity on phase separation.

With *2%* of CMC complete phase separation occurs after *1 hour*, with *3%* CMC complete separation is very slow, it takes more than four hours. In order to minimize the effects of gravity we repeated the experiments in a horizontal cell. In system with no CMC we can see, first, the appearance of acetonitrile droplets with circular shape and then their motion in the aqueous phase. The motion of these droplets is very fast (*9mm/s*) and the equilibrium is reached after *5 minutes*. Using *2%* CMC we can see that the

droplets motion is really slow and they have a circular-oval shape, while using *3%* CMC the droplets have an oval, non-regular shape, they start to grow at the beginning of phase separation and then they become smaller.

In *System II* and *III* we added Carbofix CMC in different amounts and we obtained the results in Tables 7 and 8:

% CMC	Viscosity aqueous phase (cp)	Separation Time (s) for Sytem II
0	~ 1	29
2	~ 5.5	50
4	~ 21	90
6	~ 70	90

Table 7: Phase Separation for System II with organic continuous phase.

% CMC	Viscosity aqueous phase (cp)	Separation Time (s) for System III
0	~ 1	10 ÷15
2	~ 5.5	45 ÷ 65
4	~ 21	180 ÷ 240
6	~ 70	660 ÷ 780

Table 8: Phase Separation for System III with aqueous continuous phase.

Chapter 7

Conclusions

Phase separation of deeply quenched liquid mixtures in a *1mm* thin cell and *1cm* diameter condenser tube was studied experimentally in the range of *10μm-7mm.*

We started our experimental work with the thin cell where two systems were considered, one density-segregated and the other density matched (the so-called quasi-isopycnic mixture), with capillary length *rc* (i.e., the typical length above which gravity becomes the dominant force) of *O(1mm)* and *O(1cm)*, respectively. In both cases the systems were quenched to a reduced temperature of *0.1* with a quenching rate of *3 ℃/sec.*

Two experimental procedures were used: the homogeneous case and the gradient case. We started our studies considering the homogeneous case. Using this procedure, in the density-segregated case we found that, as in the case of shallow quenches, domain growth was linear with time mainly due to coalescence. Following the motion of *10μm* size nucleating droplets, we showed that they move rapidly and with random directions, with typical speeds exceeding *100μm/s*, which is much larger than the *O(1μm/s)* Stokes sedimentation velocity. Finally, when the typical size of the drops approached the capillary length, the mixture phase separated by gravity. Since the capillary length was of the same magnitude as the cell thickness, at the end of the process the two phases were separated by a horizontal interface, irrespectively whether the cell was kept horizonal or vertical.

In the density-mathed case, initially we observed again that the morphology of the system did not depend on whethet the cell was kept horizontal or vertical. Then, when the size of the nucleating droplets exceeded the cell thickness, the behavior in the two cases

was quite different, since in this case the capillary length was much larger than the cell thickness. In fact, when the cell was vertical, drops kept growing and then started to sediment until, as in the density-segregated mixture, a horizontal interface was formed. On the other hand, when the cell was kept horizontal, phase segregation occureed through the horizontal motion of the acetone-rich drops towards the hydrophobic walls.

In the gradient case, we shoved that, after the quench, both systems remaind macroscopically unchanged for a few seconds, at which point micron-sized drops first appeared, and then, within a few tenths of a second, a sharp interface suddenly formed. Only later larger drops started to appear and move toward the interface, where they coalesced. This behavior is radically different from that of an initially well-mixed system, where single-phase domains appear immediatly after the quench and then grow by convection-driven coalescence until they become large enough to sediment. As it takes one-half hour to diffuese and a few seconds to segregate, our experimental results indicate that the phase separation process is not driven by diffusion. In addition, because no significant differences were observed between density-segregated and density-matched systems, the process is also not driven by gravity.

The large bulk flows predicted by the theory were visualized by adding glass particles to the phase-separating systems. We saw that the typical bulk velocities continues to increase in time, reaching values of about *0.4mm/s* for the density-segregated system and even higher values for the isopycnic system. Eventually, the interface appears, and at this point, the bulk flow vanishes, and the system resumes its quiescent state. This behavior can be explained, albeit qualitaqtively, via model H by considering that the increasing convection within the diffusion layer stems from an increase in the concentration

gradients with time, as the thickness of the diffusion layer steadily decreases. In addition, as the difference in compositions between the two phases at the end of the temperature quench is about theree times larger in System II than it is in System I, this model also predicts taht the corresponding driving force is about 10 times larger, which therefore explains why System II phase separates about 10 times faster than System I.

During our study on spinodal decomposition of partially miscible solvents of low viscosity, we discovered the occurence of rapid, large-scale, unidirectional flows in a horizontal direction over a distance of *20cm*. It was pointed out by reviewers that in the small cell interfacial forces between the glass and liquid as well as capillary forces could play a role. Futhrmore since we were interested to obtain results that could be applied on industrial scale, we needed to get data in large dimensions. To do so we designed an built an inexpensive system consisting in a *1cm* diameter condenser tube, *20cm* long. With this larger device, we unintentionally created a significant temeprature gradient (*0.25 ℃/cm*) along the tube as the flow of the cooling liquid was too slow. We also placed the tube horizontally and used a system (hexadecane and acetone) with a very small density gradient to minimize the gravity effect.

We found that the coalescence was very rapid and observed within ten seconds complete separation into two phases separated by a vertical interface. By our detailed obsevrations we found that large droplets grow by coalescence to much larger sizes and moved with totally unexpected high velocities up to *6cm/s*. This surprising phenomenon which could have large significant for designing separation processes was never observed before. We developed a new method to measure directly the velocity and the direction of each droplet in a system with a large number of droplets.

We carefully investigated this phenomenon in detailed and found that this is not due to thermo-capillary motion as one can reverse the direction from the hotter into the colder region with a small change in the concentration of the solvents while maintaining costant temperature gradient. When hexadecane was the dispersed phase we proved that the motion was always in the direction of the increasing temperature. However, when we increase the acetone concentration we caused a phase inversion, the acetone becomes the continuous phase and the droplets moved to the colder side. We also cecked that there was no flow instabilities due to the small gradient and density. We used, here, the droplet itself as a tracer by taking pictures across the crossection, all droplets moved in the same direction.

The results would not only be of great theoretical significance but also have very important practical applications, some of which would be to create and control flows in a gravity free environment.

So far in our experimental work, after quenching a low-viscosity partially miscible liquid mixture *15℃* below its miscibility curve, we found that the typical size of single-phase domains grows with a growth rate $dr/dt = 100mm/s$, which is much larger than that for shallow quenches. In addition, we measured the typical velocity of *10 mm* phase-separating liquid droplets as $v = 0.2\text{-}0.7mm/s$, which is a fewer of magnitude larger than their speed due to either gravity or molecular diffusivity.

In this experimental work we intended to study the limitations of the results obtained. In fact, we expected that coalescence could be eventually retarded increasing the amount of surfactants and thickeners, thereby increasing the viscosity of the mixtures, or when we quench the mixture in its metastable region. Therefore we determined the thresholds

of the surfactant concentration and of the mixture viscosity and composition beyond which surfactants start to slow down significantly the separation process, just as they do in the absence of phase transition.

From a practical viewpoint, one of the most interesting features of spinodal decomposition in the convective range is that emulsion-promoting compounds have almost no effects on the phase separation rate. In fact, phase separation seems to occur at a rate that is independent of their presence. In our previous work we only tasted few emulsifiers and coalescence retardants, as the solute had to be transparent. However, as we die d t he s olution t o im prove v isualization, we no ted t hat t here w as no dif ference between dies that form slowly coalescing emulsions when the two phases are agitated and they have no impact on coalescing rate. In this work we investigated whether the presence of stronger and more concentrated emulsifiers has an impact on the phase separation rate. We also studied the effect of emulsifiers when the mixture was quenched into its metastable region, where convection and diffusion are comparable. As some of these emulsion stabilizers produce non-transparent systems, we had limit ourselves to observing only the time needed to complete the separation. When surface-active compounds w ere dis solved in a l iquid m ixture, c oalescence t ended t o be r etarded b y surfactants. This phenomenon, however, has been studied extensively only for systems at local equilibrium, where the composition of the dispersed and continuous phases are constant and equal to their equilibrium values. On the other hand, with the exception of our work, there are no published data on the influence of surface-active solutes on the coalescence rate of the droplets that form in deeply quenched, liquid mixtures as they phase-separate.

In all past experimental work, we studied the phase separation process of deeply quenched, low-viscosity liquid mixtures. However, although most solvents have low viscosity, studying the behavior of mixtures with higher viscosity is of great technical importance for two reasons: first, there is an interest in extracting solutes from high viscosity liquids, like lubricating oils and, second, solvent thickeners are often present within the systems to be extracted, which greatly increase the viscosity and tend to slow down the coalescence process and phase separation. It was therefore of great importance to study the impact pf surface-active compounds on the phase separation of high-viscosity liquid mixtures, determining when they start to have an impact on coalescence. To do that, we repeated the visual observations performed previously by either using high-viscosity fluids, or by adding thickeners to our low-viscosity solvent mixtures. Eventually we reached a transition point where the separation process ceases to be convection-driven and start to be diffusion-controlled, as it happens in polymer blends and alloys.

In our past research we studied the behavior of critical and mildly off-critical liquid mixtures undergoing phase separation, and found that the process is driven by convection. Since in many applications we were interested in the behavior of mixtures quenched in the vicinity of their metastable region, in this work we intended to study what happened when we repeated our experiments using strongly off-critical mixtures. Compared to the previous set of experiments, in which we increased the viscous resistance o f t he l iquid m ixture, he re w e de creased it s c onvective f lux, in b oth c ases reducing the fluidity parameter of the separation process. White studied phase separation of off-critical polymer melts and Wiltius found that the typical size of the isolated phase

separating drops grow like $t^{1/3}$. This result was confirmed in our measurements where, analyzing the few scattered drops that were suspended in the mixture at the end of phase separation (these drops constitute the so-called secondary emulsion), we found that their mean radius R grows in time as t^g, where the exponent $g = 0.3 \pm 0.04$. Clearly, by considering off-critical fluid mixtures, we determined at which point phase separation ceases to be convection-driven and start to be diffusion-controlled.

Figures

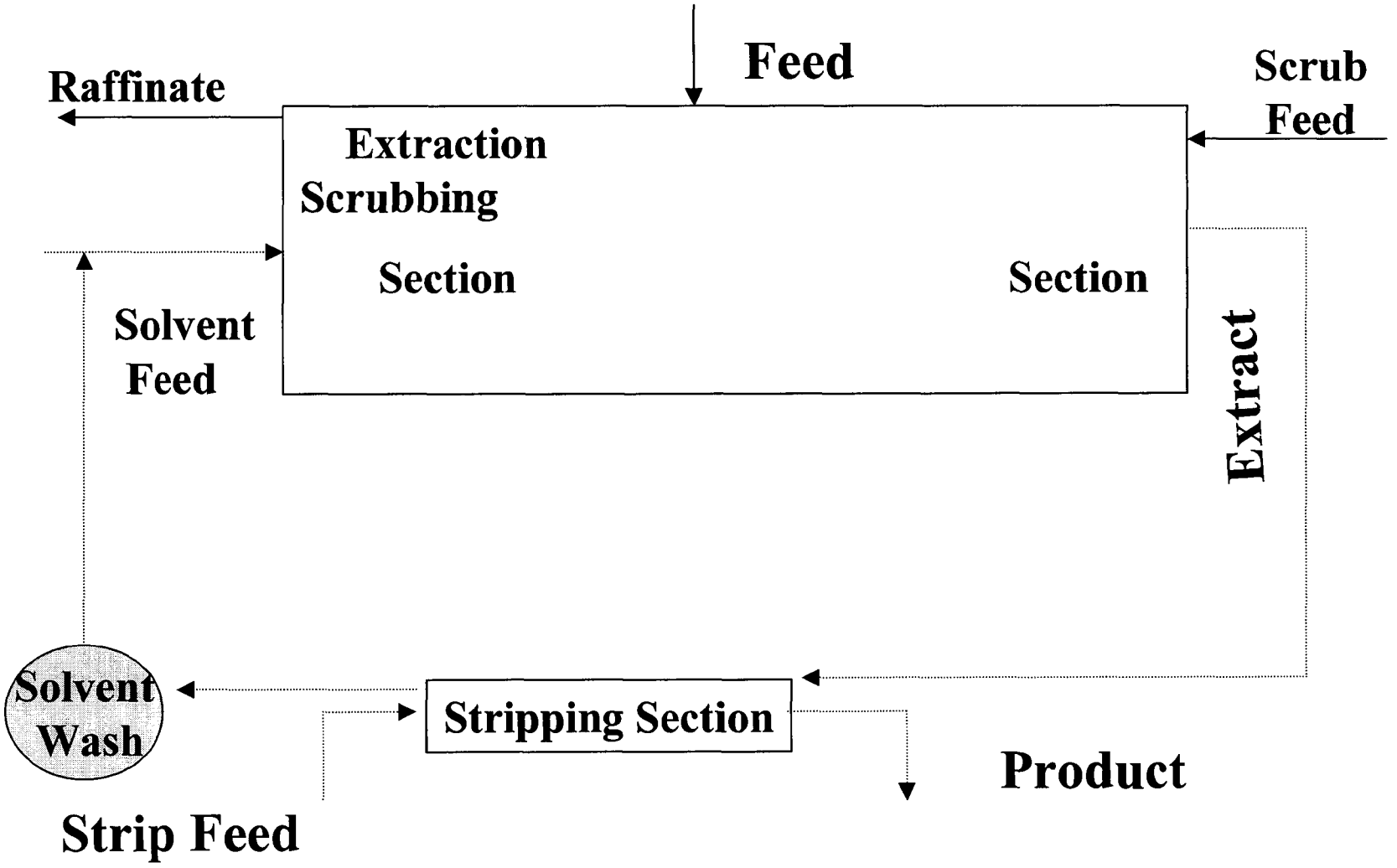

Figure 2.1 Typical Solvent Extraction Process.

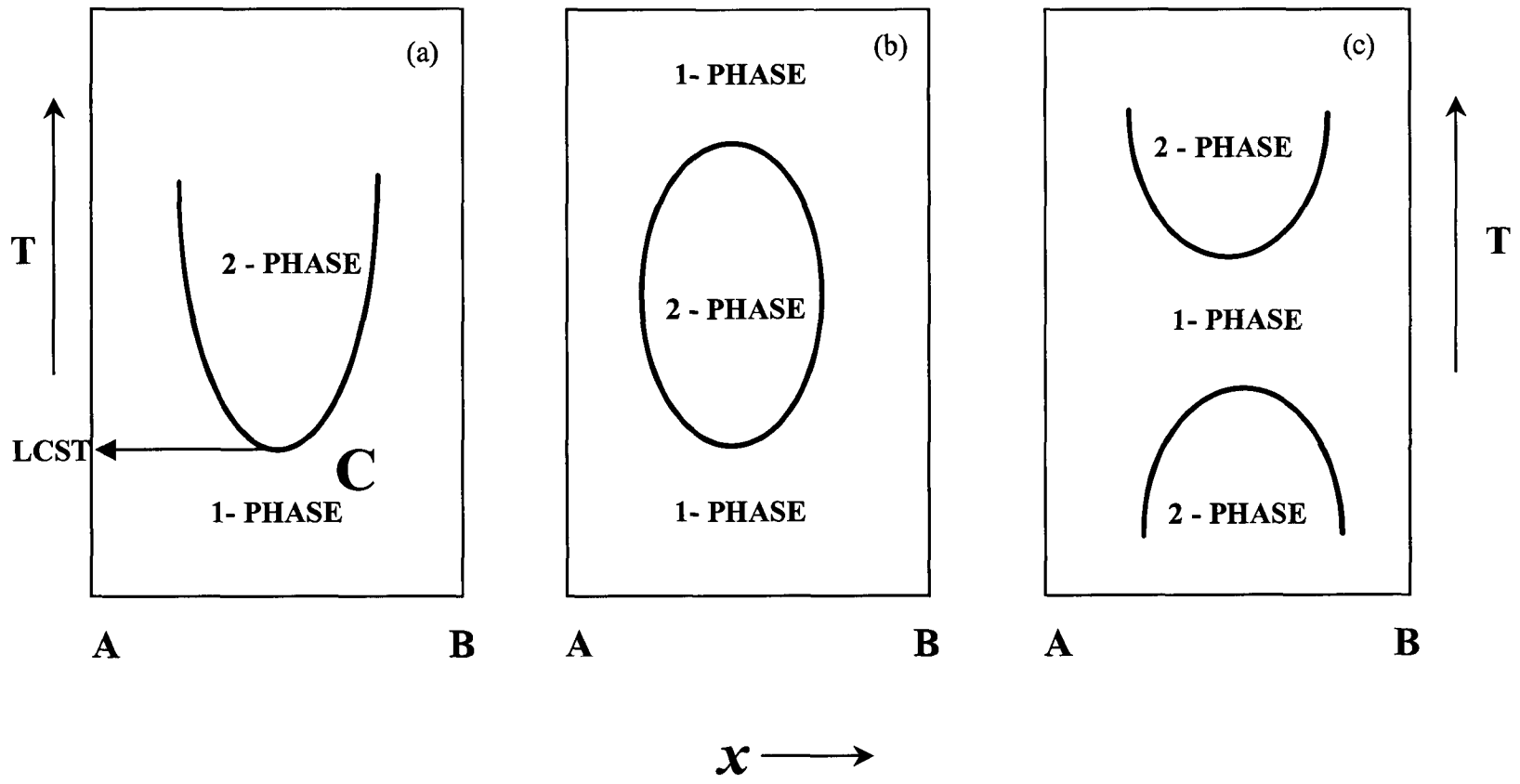

Figure 2.2: T-*x* diagram of a binary system with (a) LCST, (b) and (c) both upper and lower critical solution temperature.

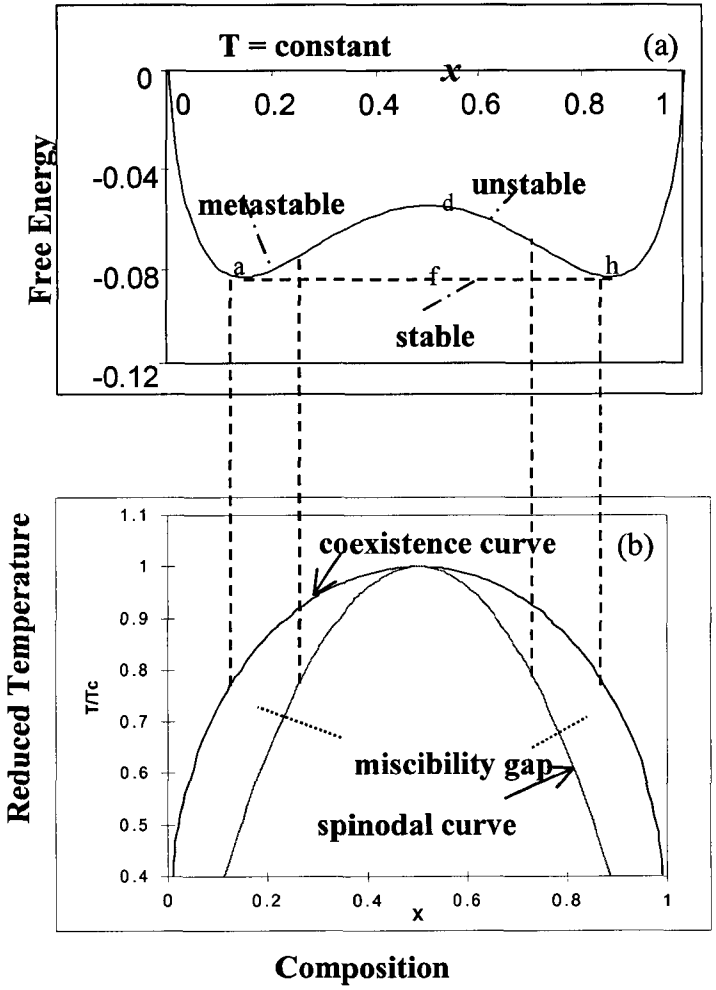

Figure 2.3: (a) Gibbs energy of binary mixtures as a function of composition, and (b) coexistence curve and spinodal curve of binary mixture.

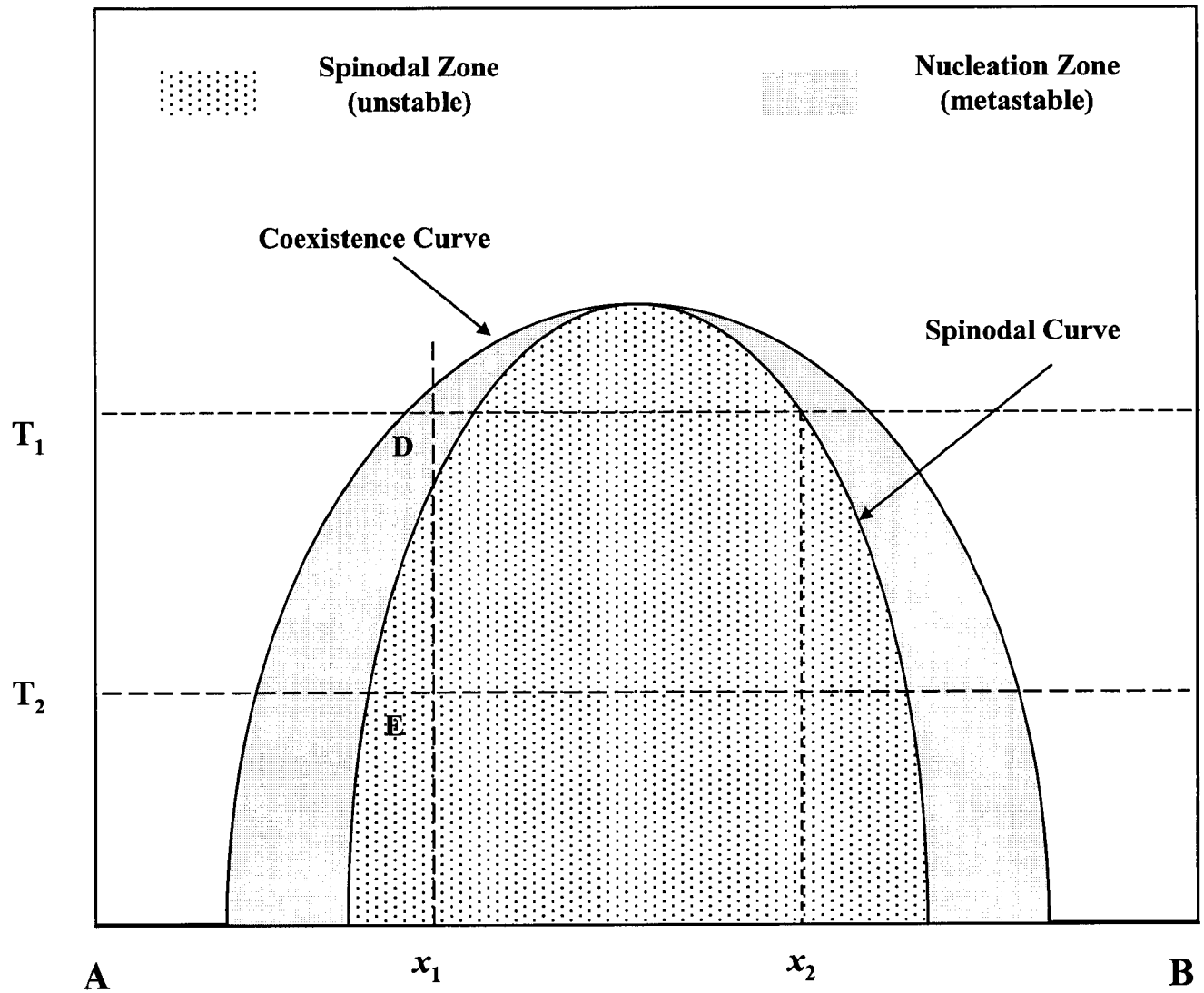

Figure 2.4: Nucleation and Spinodal regions.

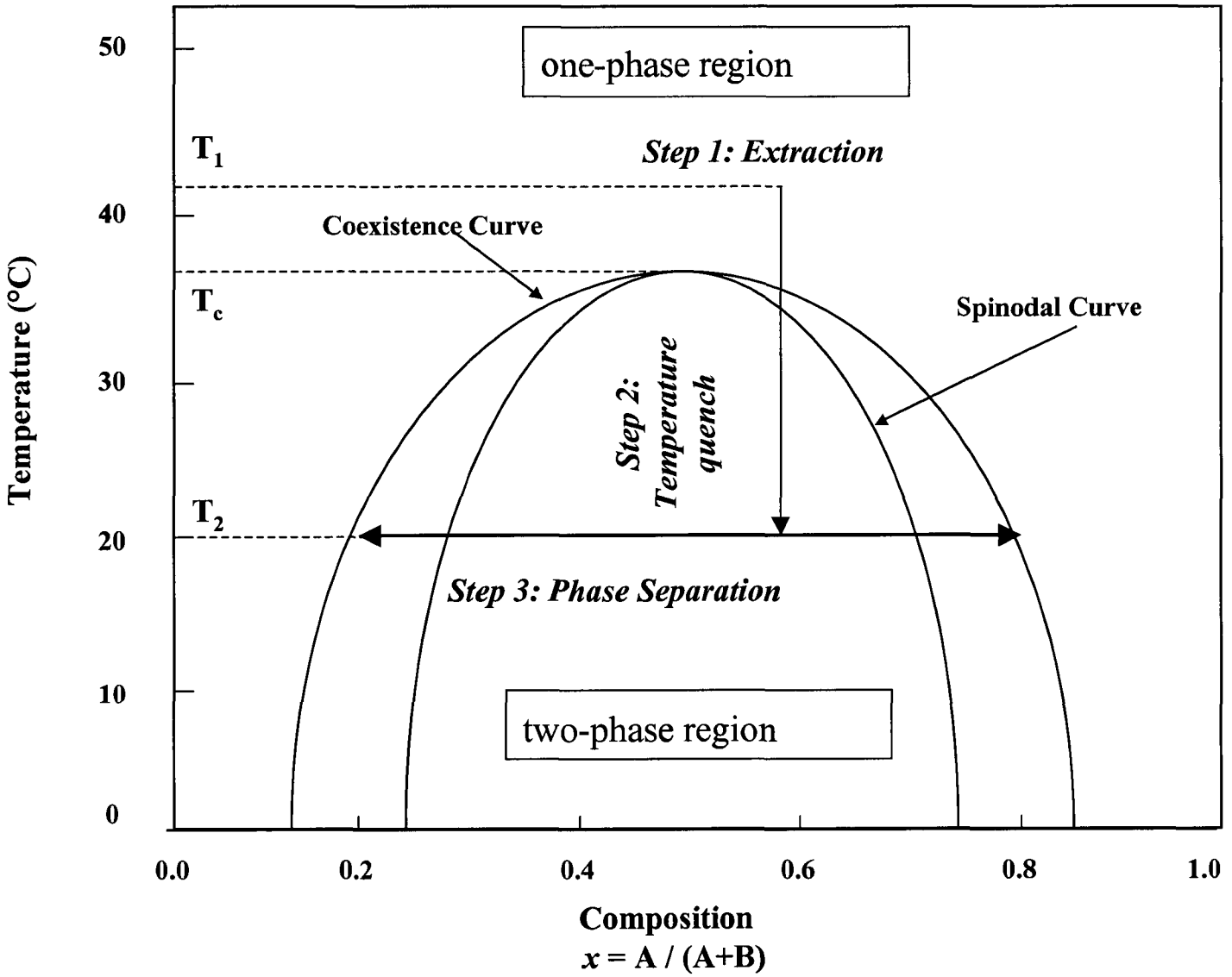

Figure 3.1: PTE process using Temperature-Induced Phase Separation (TIPS).

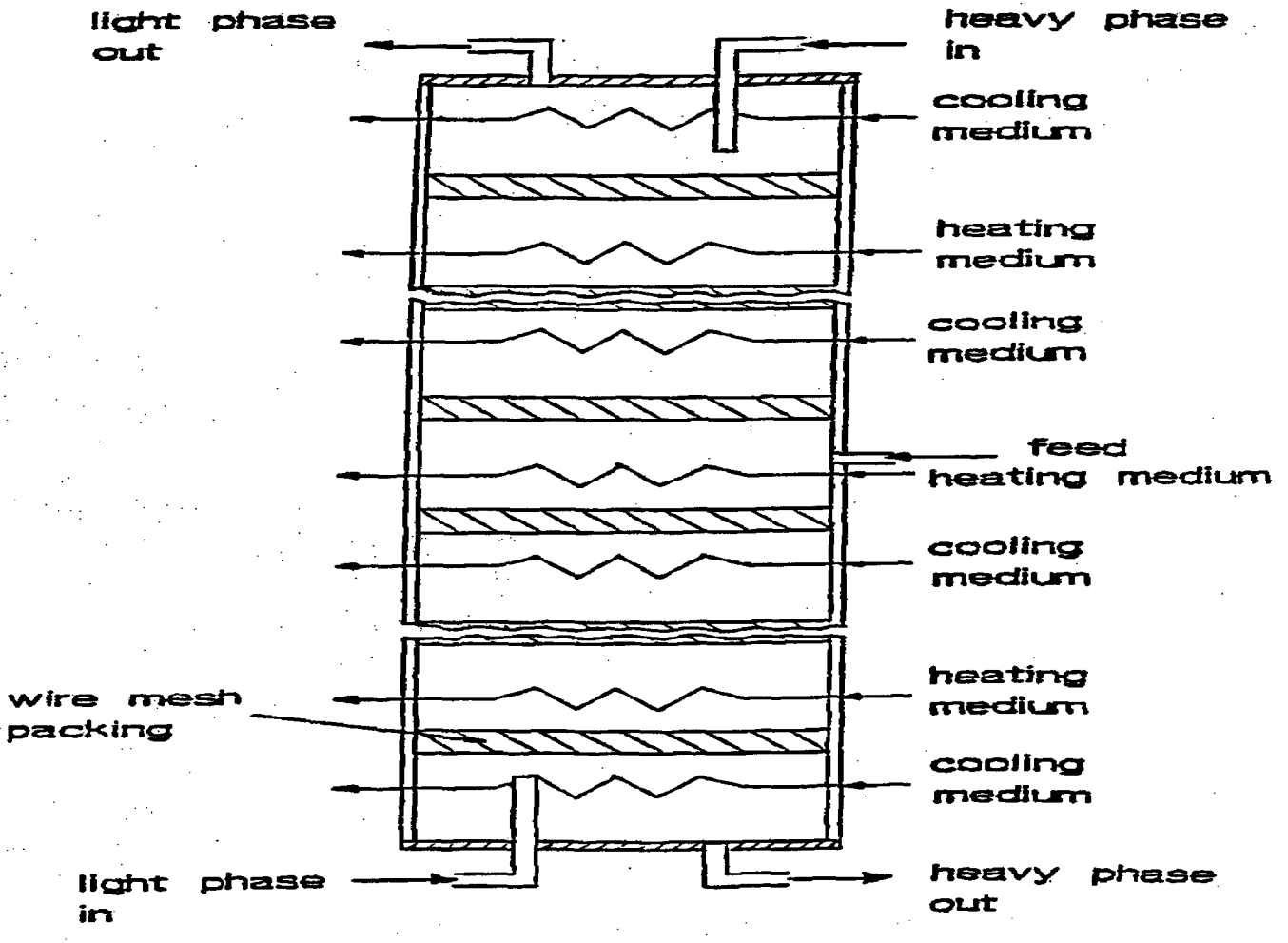

Figure 3.2: Schematic diagram of PTE Column (Ullman, Ludmer, and Shinnar, 1997).

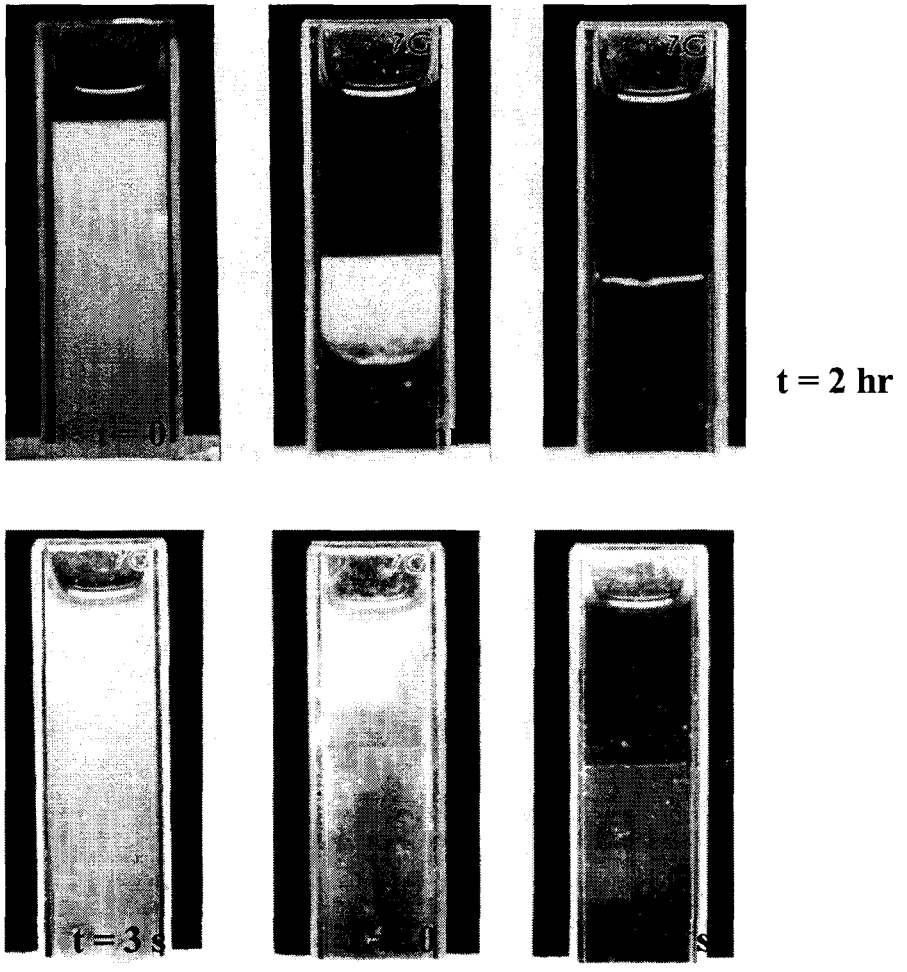

Figure 3.3: Phase separation of a water-ACN-MIBK mixture using LLE (top) and TIPS (bottom) in presence of 2 ppm of crystal violet dye.

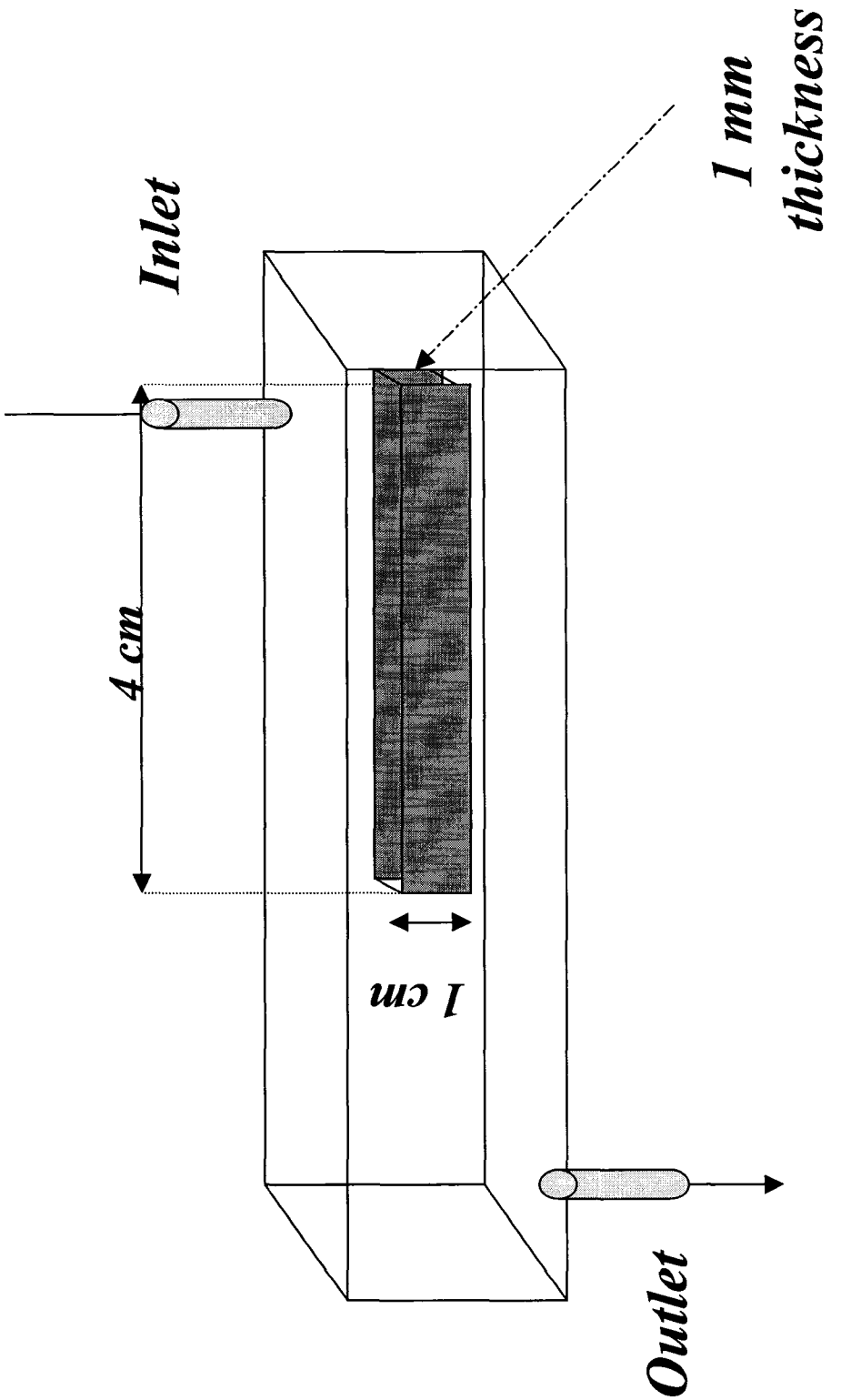

Figure 4.1: Sketch of the temperature-regulated sample Cell.

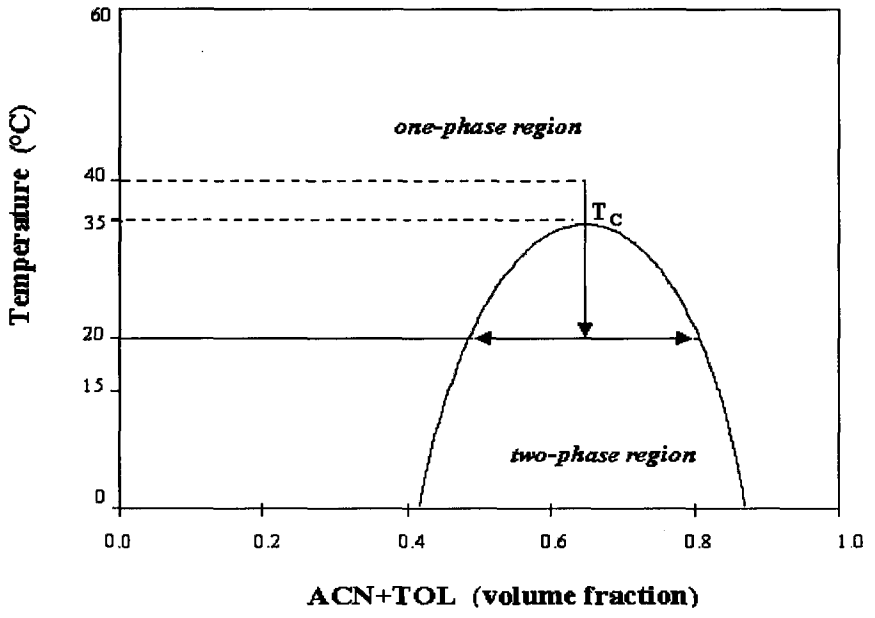

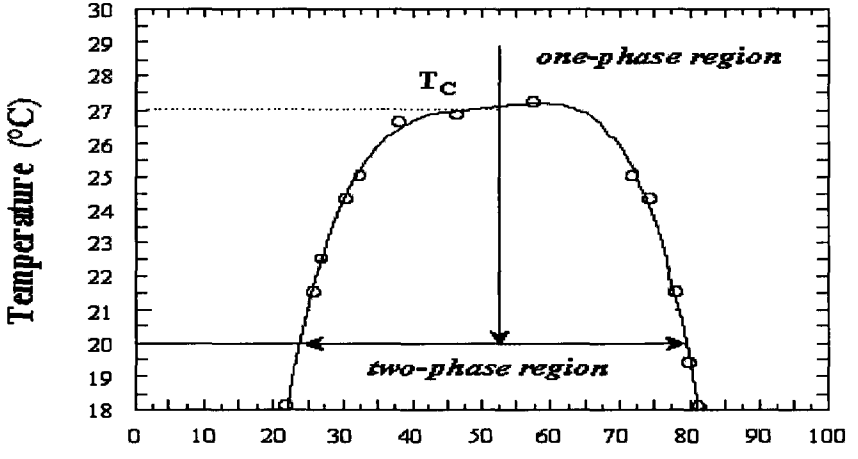

Figure 4.2:Phase Diagram of System I (Acetonitrile, Water, Toluene) and System II (Acetone, Hexadecane)

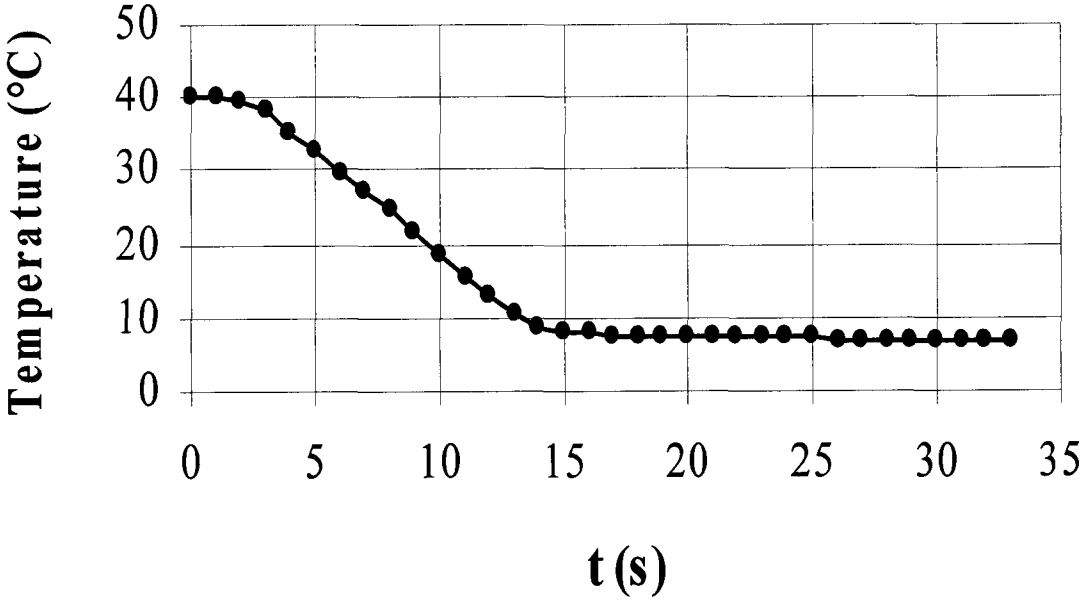

Figure 4.3: Temperature drop of the solvent mixture. Time is measured from the beginning of quench.

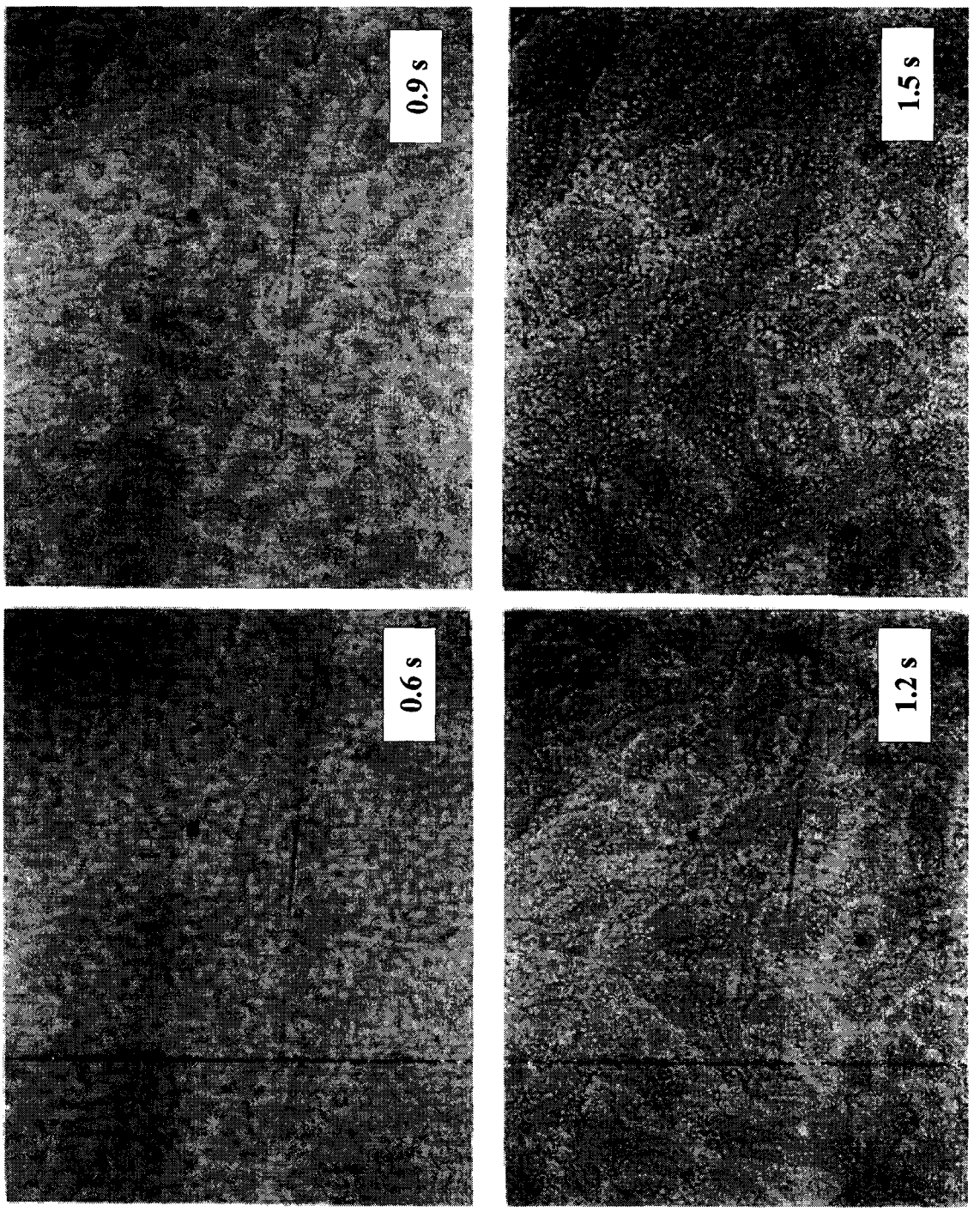

Figure 4.4: Phase separation of a water-ACN-toluene mixture (System I) using a 300μm field of view

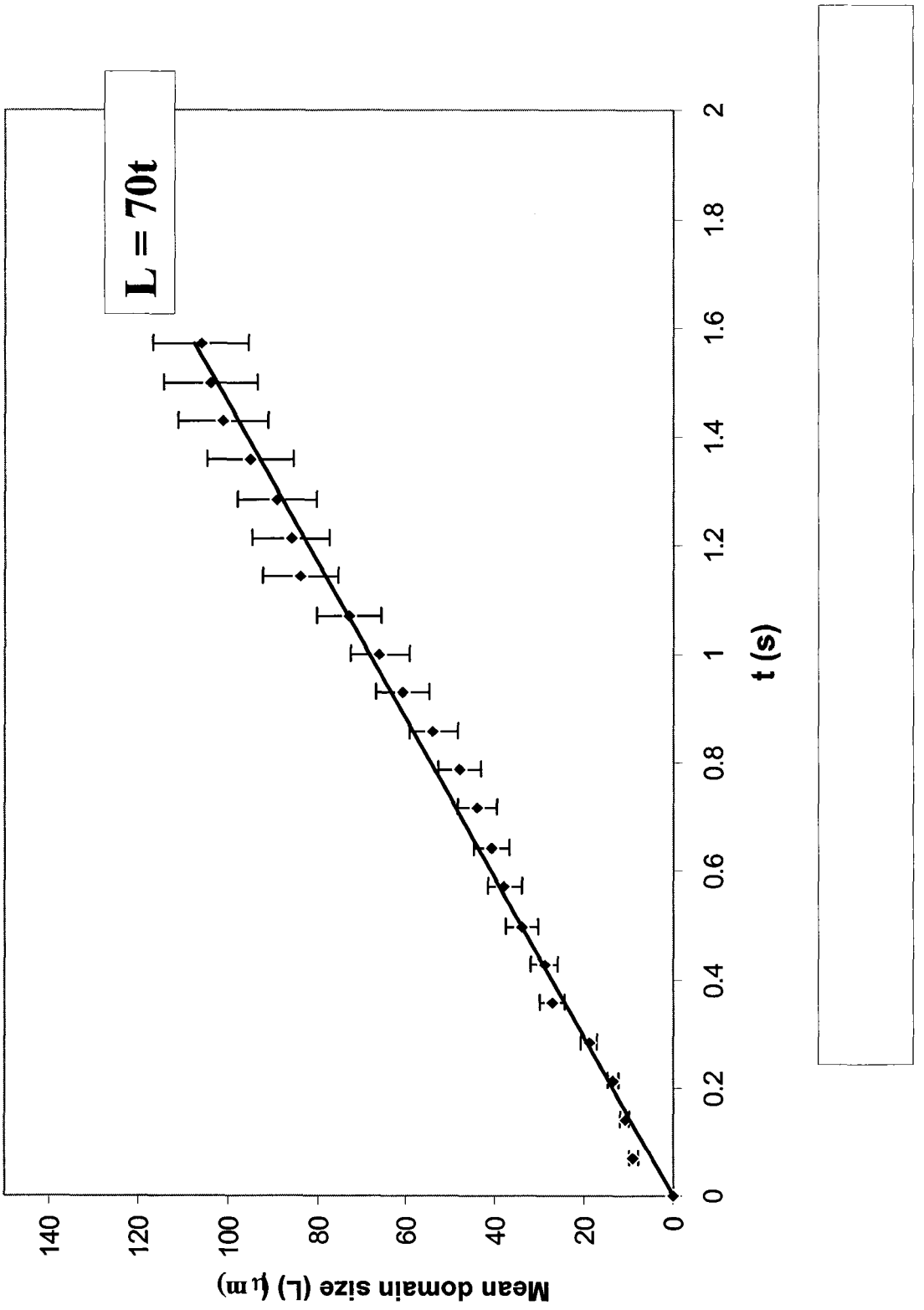

Figure 4.5: Domain growth during Critical Quench for System I

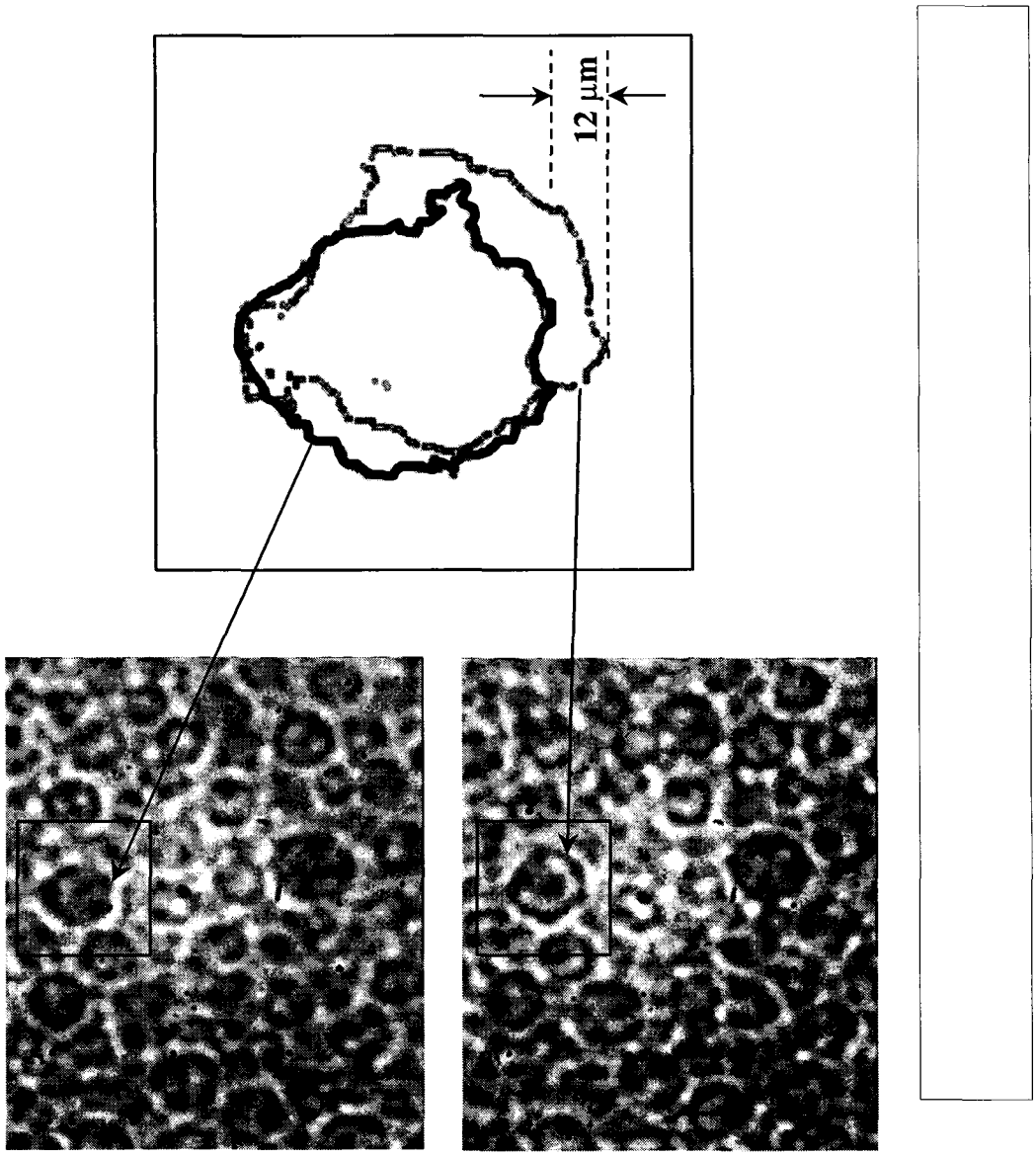

Figure 4.6: Movement of a Single Drop. The Pictures are taken 0.07s apart

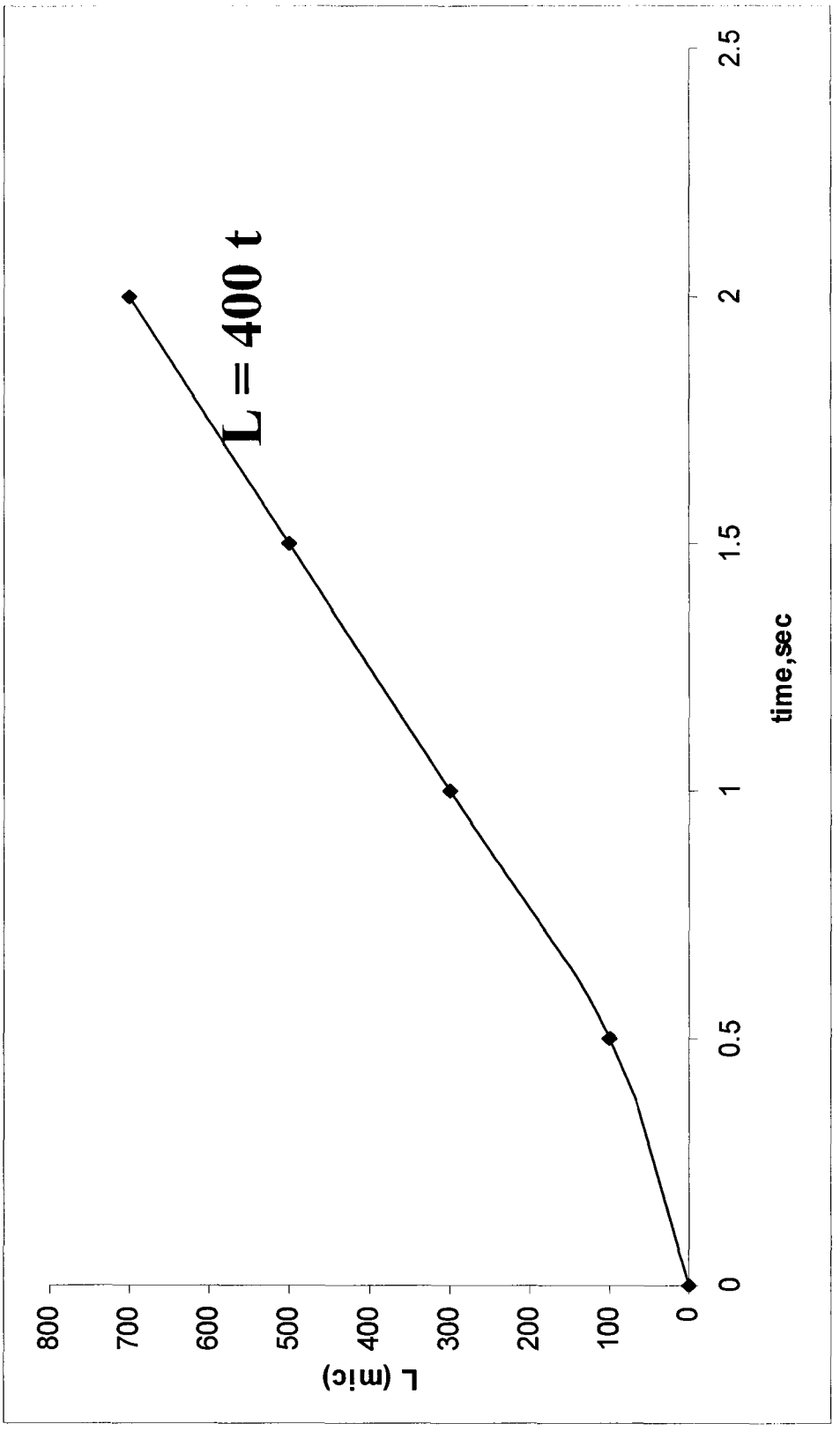

Figure 4.7: Domain Growth in System II

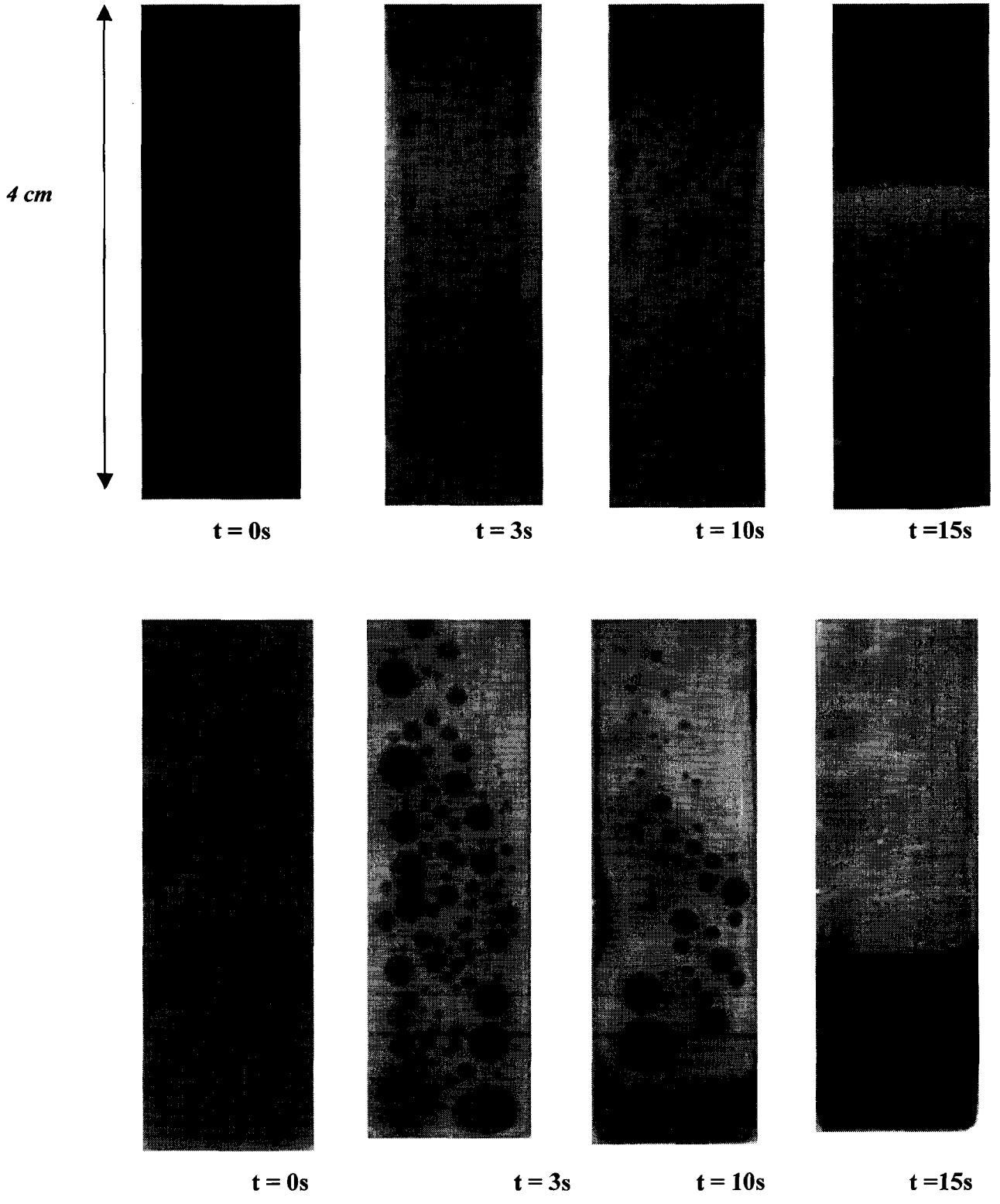

Figure 4.8: Phase Separation in Systems I and II in Vertical Cell

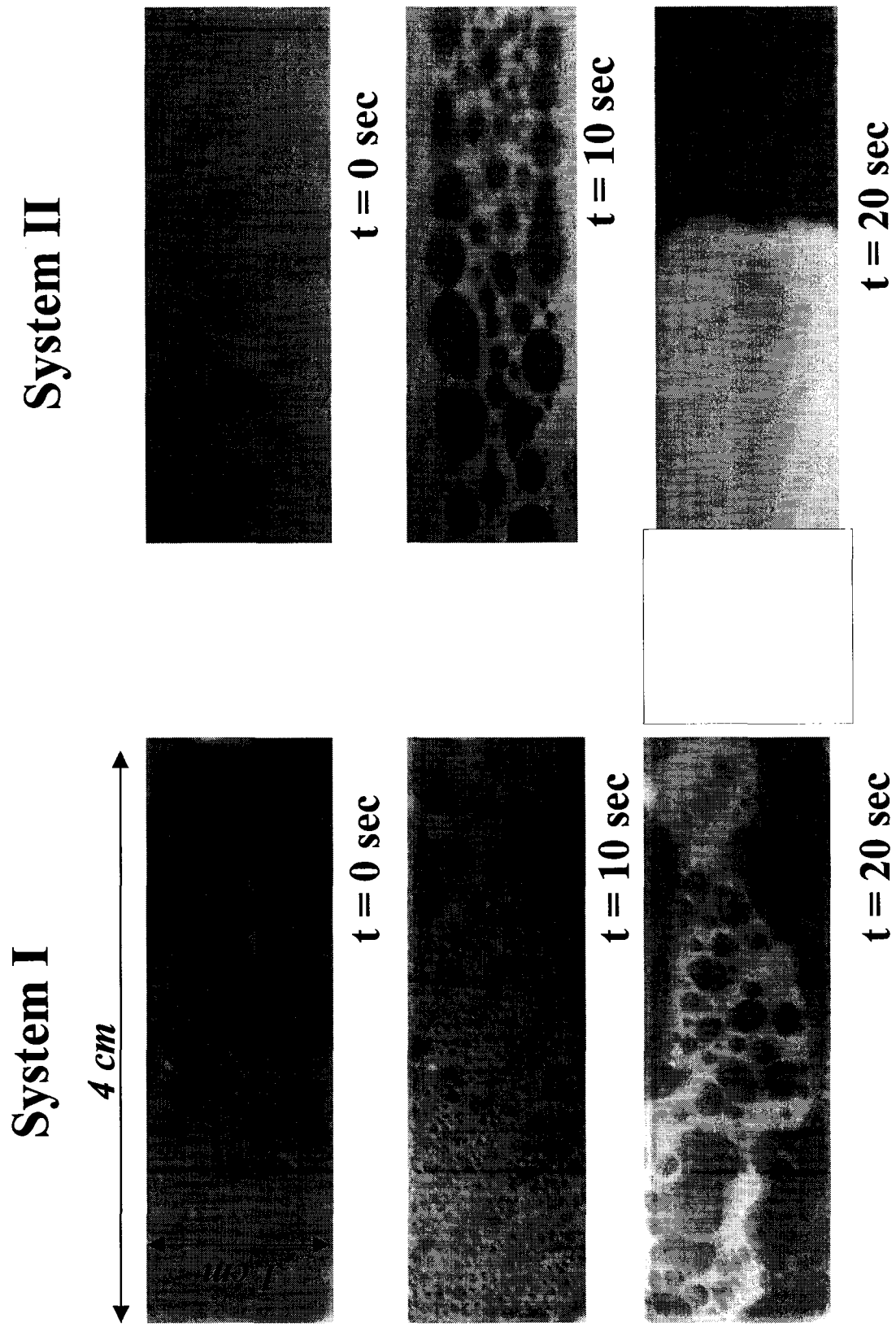

Figure 4.9: Phase separation in System I and II, when the cell is kept horizontal. Cooling temperature is 2°C

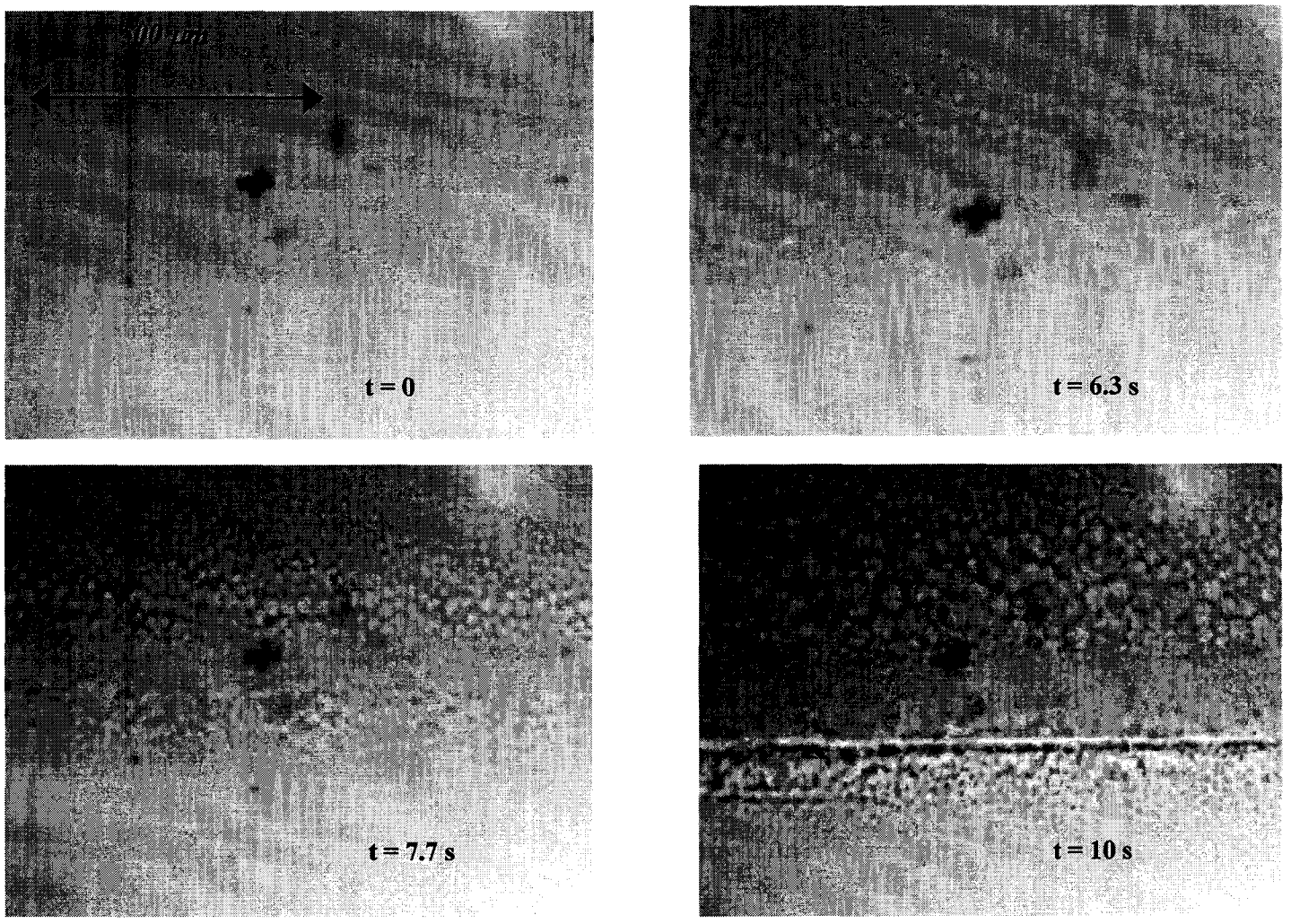

Figure 4.10: Phase separation in a critical liquid mixture (System I: Acetonitrile-Water-Toluene) with an initial concentration gradient using a *1.5 mm* field of view. Time is measured from the moment when $T = T_c$.

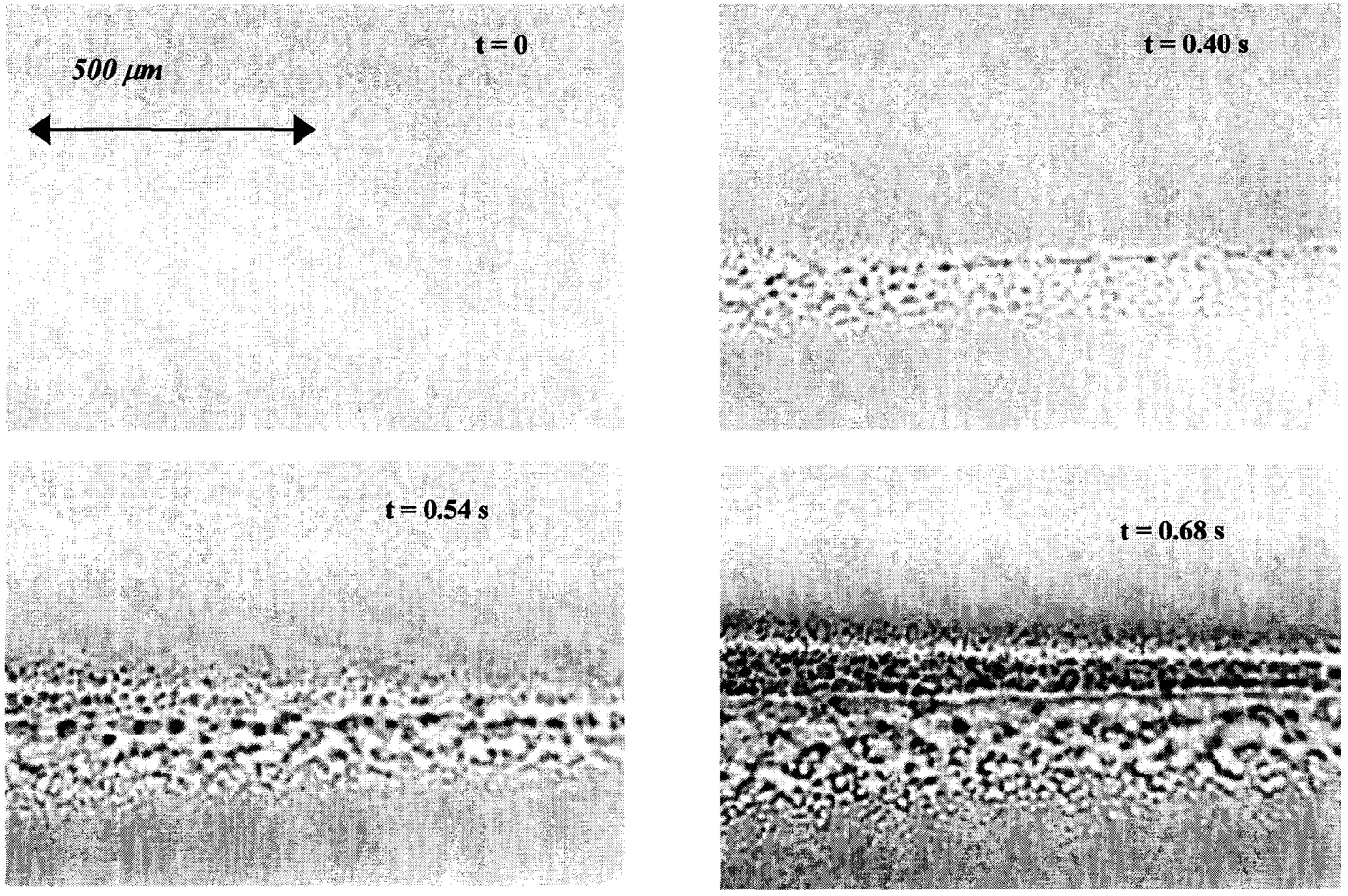

Figure 4.11: Phase separation in a critical liquid mixture (System II: 2-Propanone-Hexadecane) with an initial concentration gradient using a *1.5 mm* field of view. Time is measured from the moment when $T = T_c$.

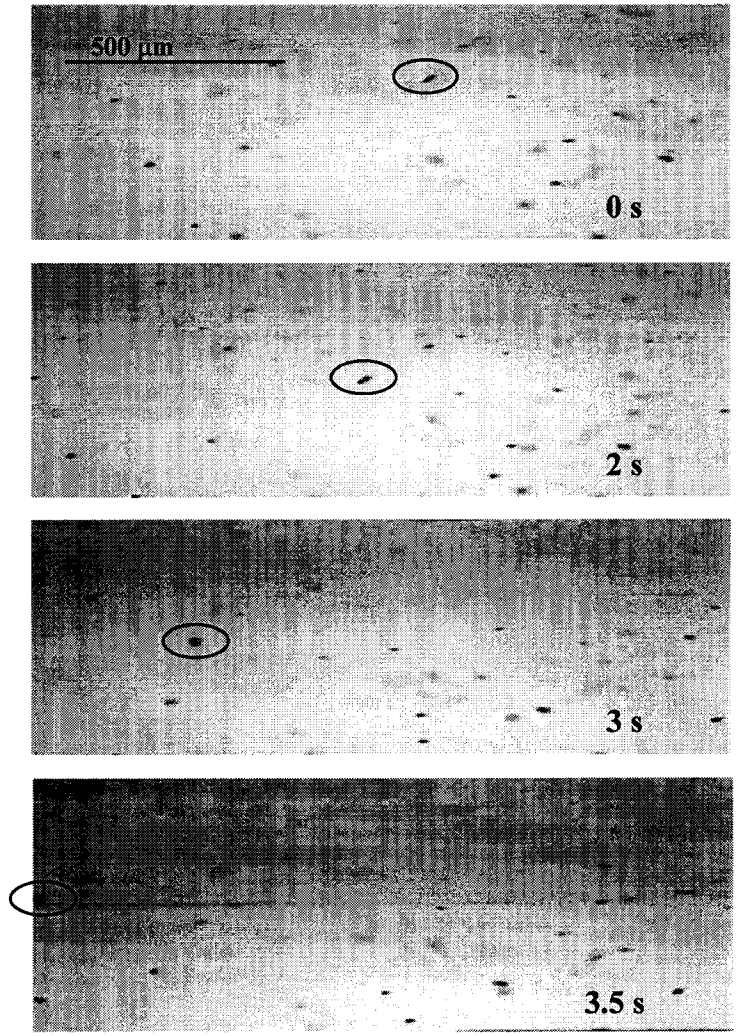

Figure 4.12: Phase separation of system I with suspended glass particles, following the trajectory of the circled particle. Time is measured from the moment when $T = T_c$.

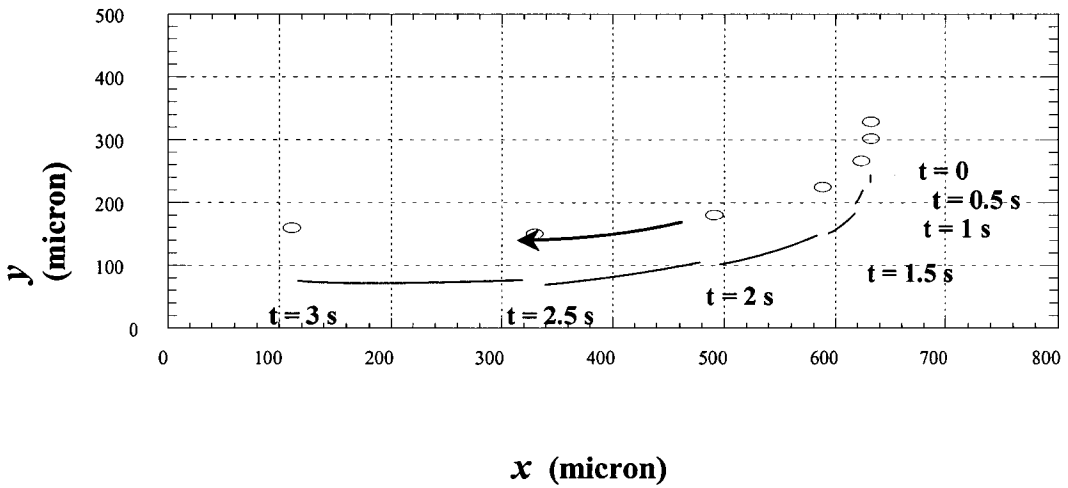

Figure 4.13: Trajectory of a glass particle suspended within the diffusion layer of system I during phase separation. Time is measured from the moment when $T = T_c$.

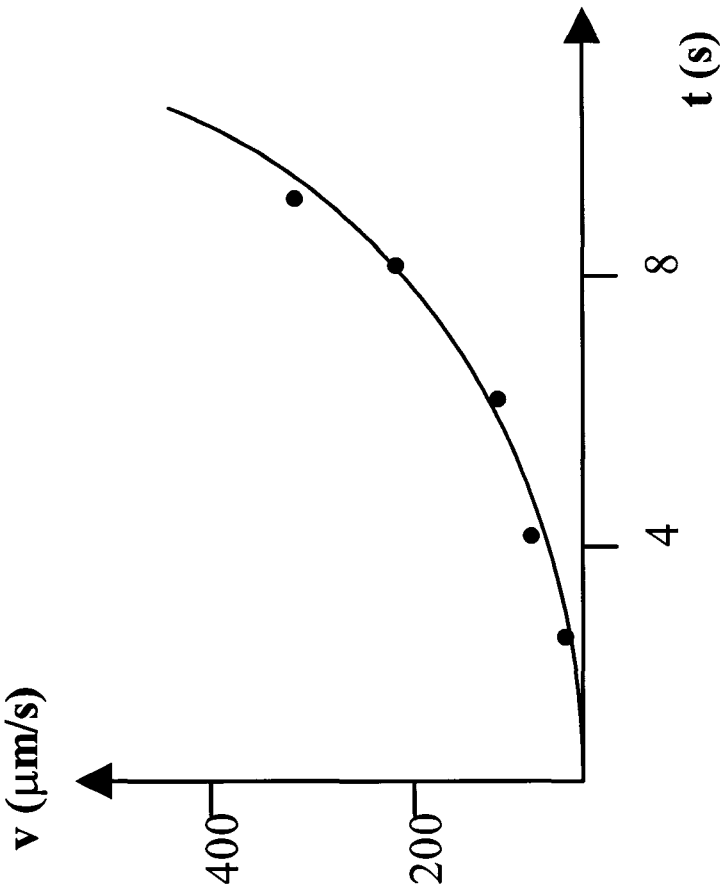

Figure 4.14: Average velocity of glass particles during phase transition in system I. Time is measured from the moment when $T = T_c$.

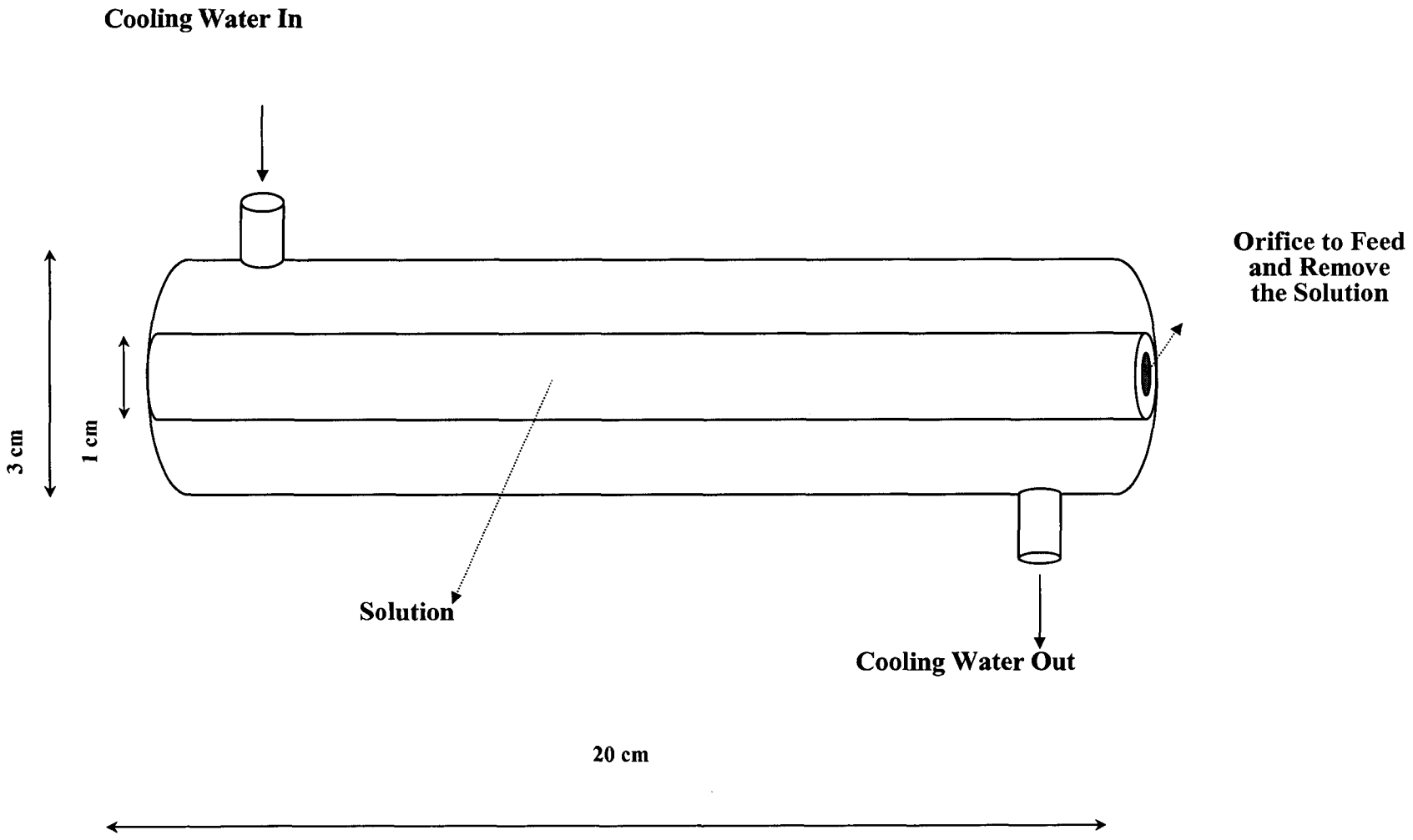

Figure 5.1: Sketch of the Condenser Tube.

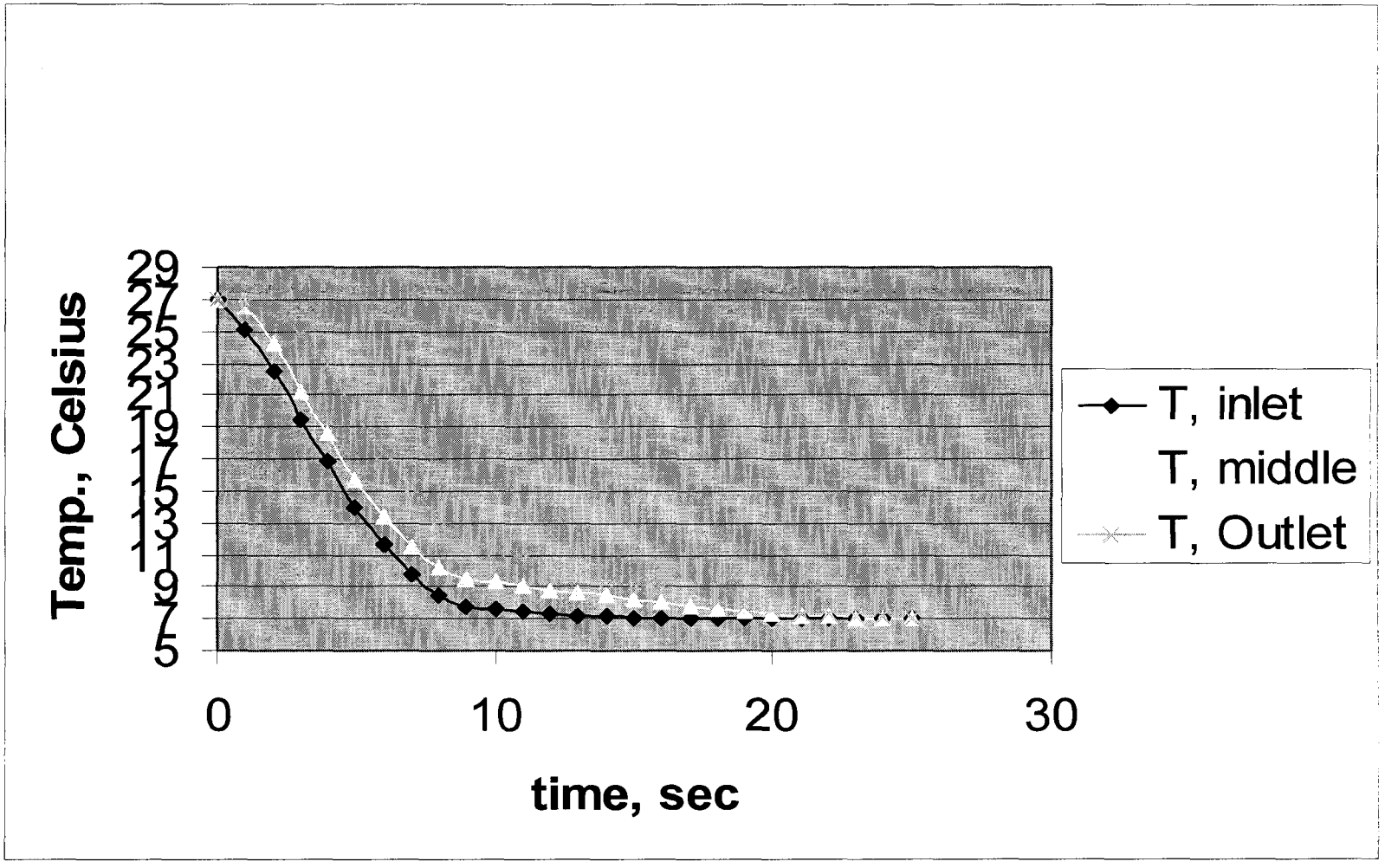

Figure 5.2: Temperature Drop in the Condenser Tube.

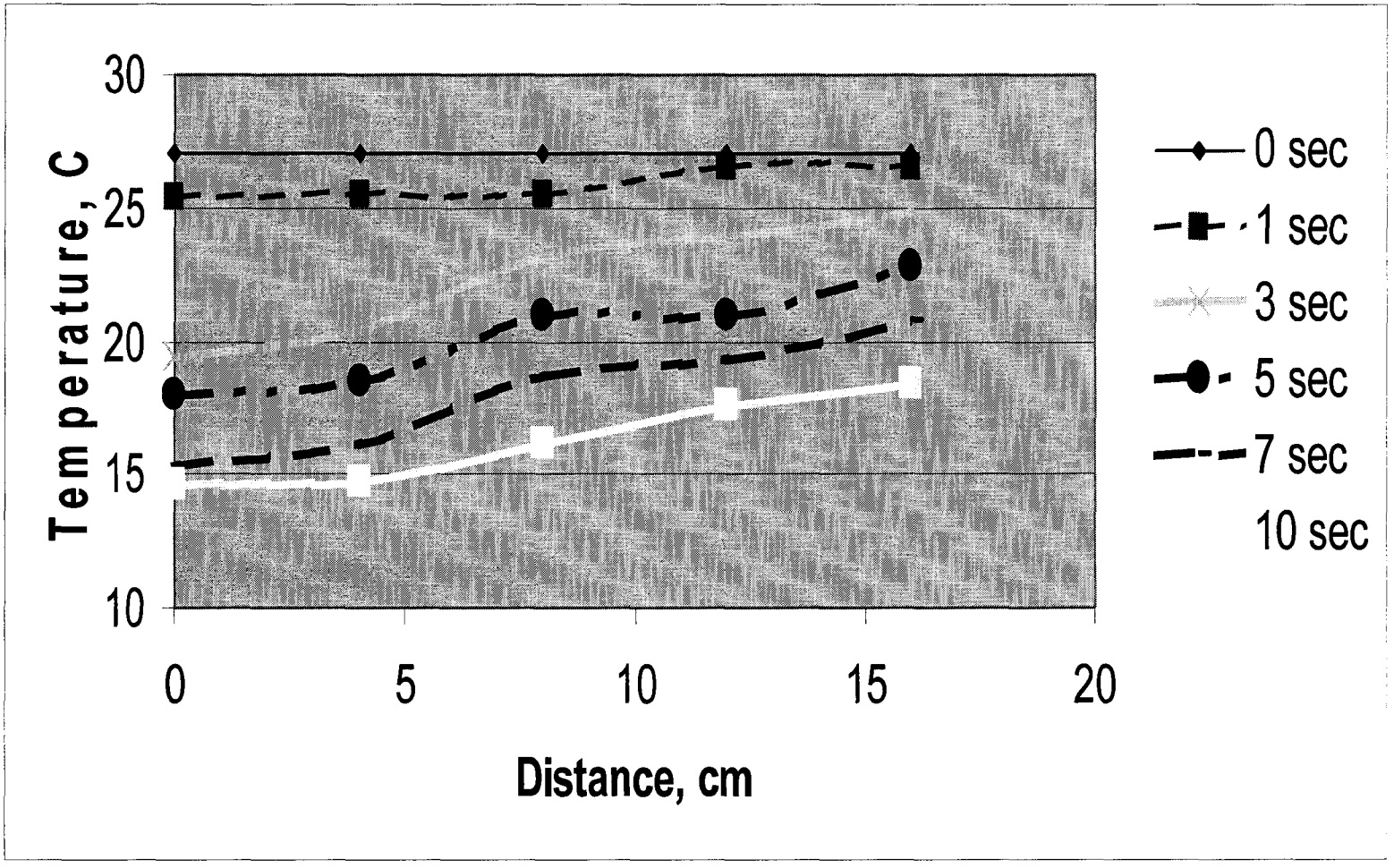

Figure 5.3: Temperature Gradient along the axial direction of the condenser tube

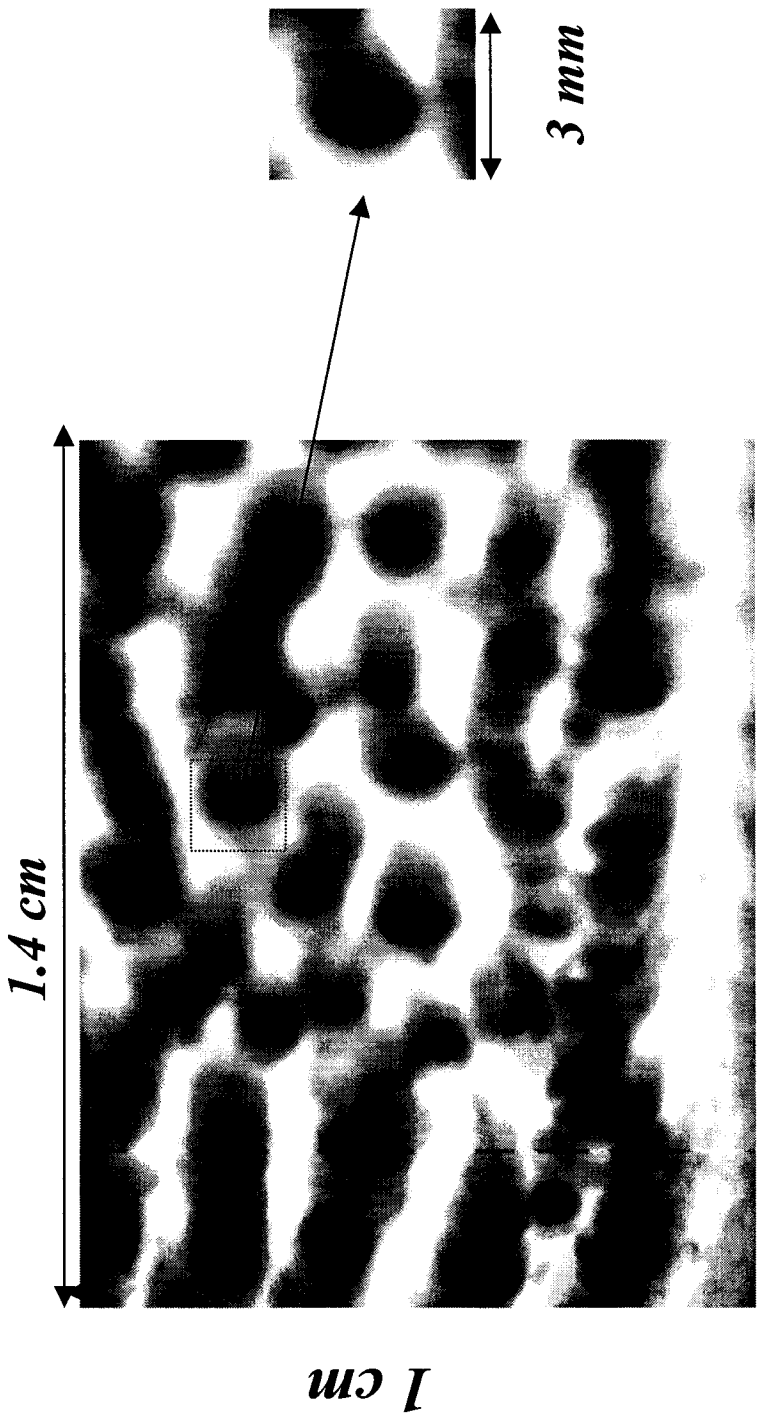

Figure 5.4: Picture taken by Digital Camera Spot (Model 3.2.1)

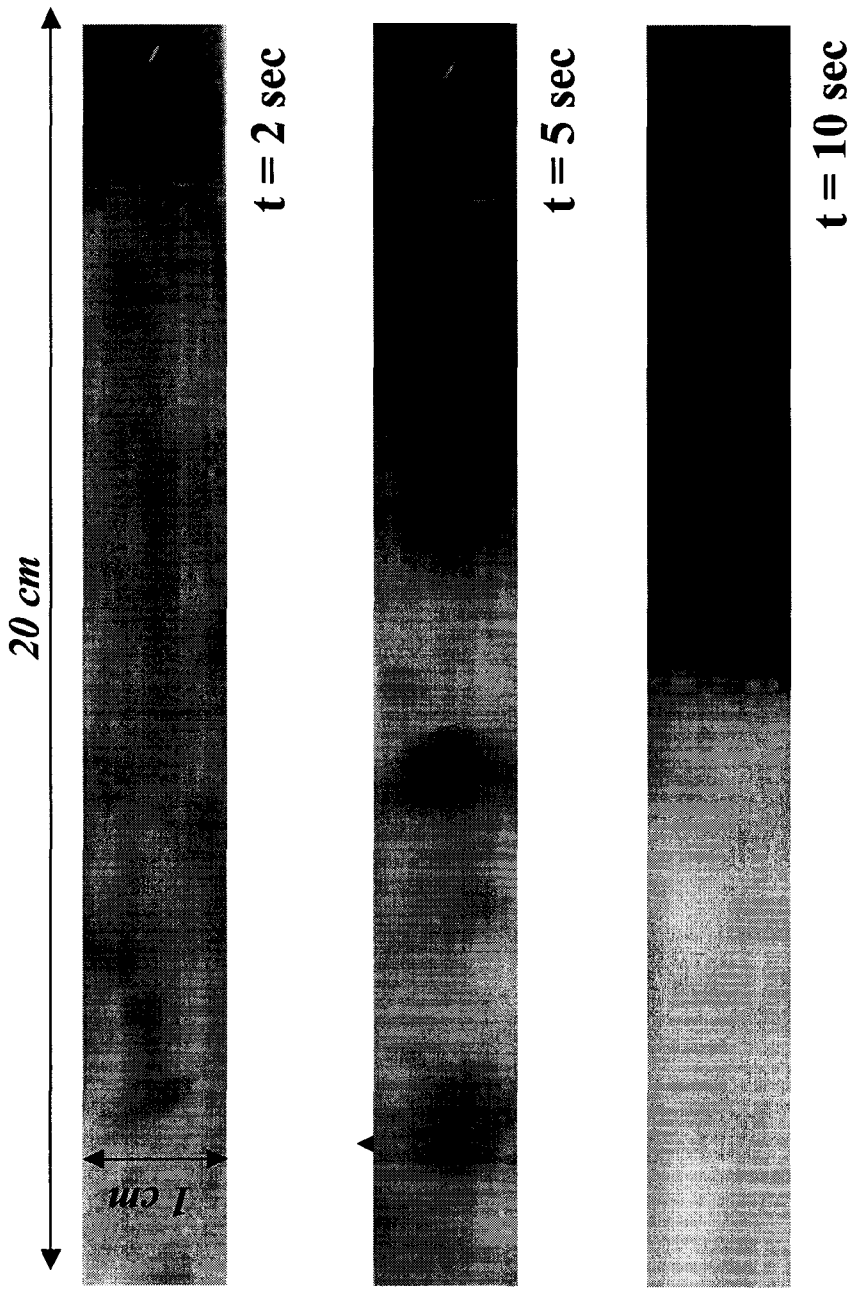

Figure 5.5: Morphology of Acetone 50%, Hexadecane 50% System within the Horizontal Condenser.

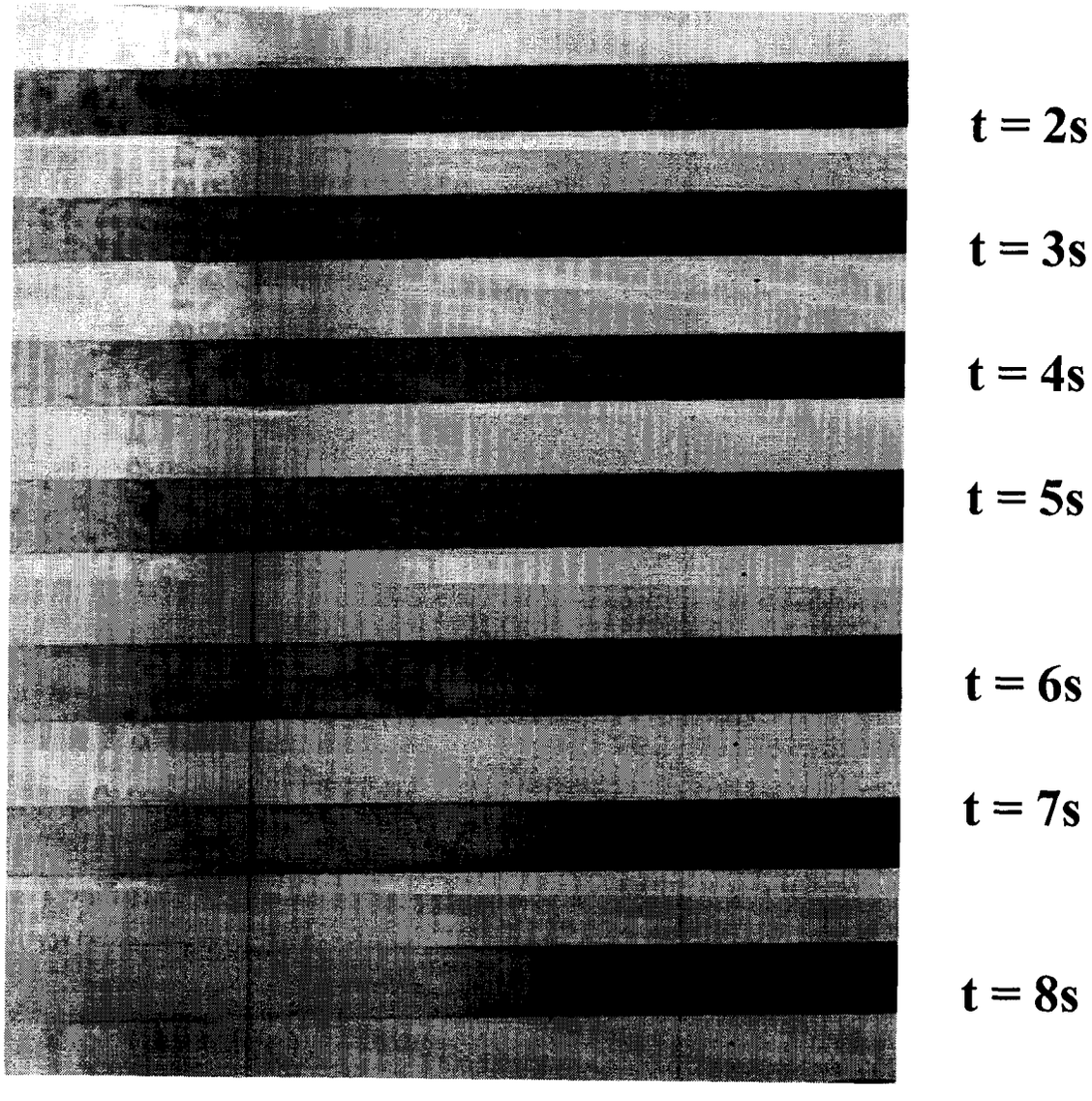

Figure 5.6:Movement of the interface for 50%Acetone and 50%Hexadecane System.

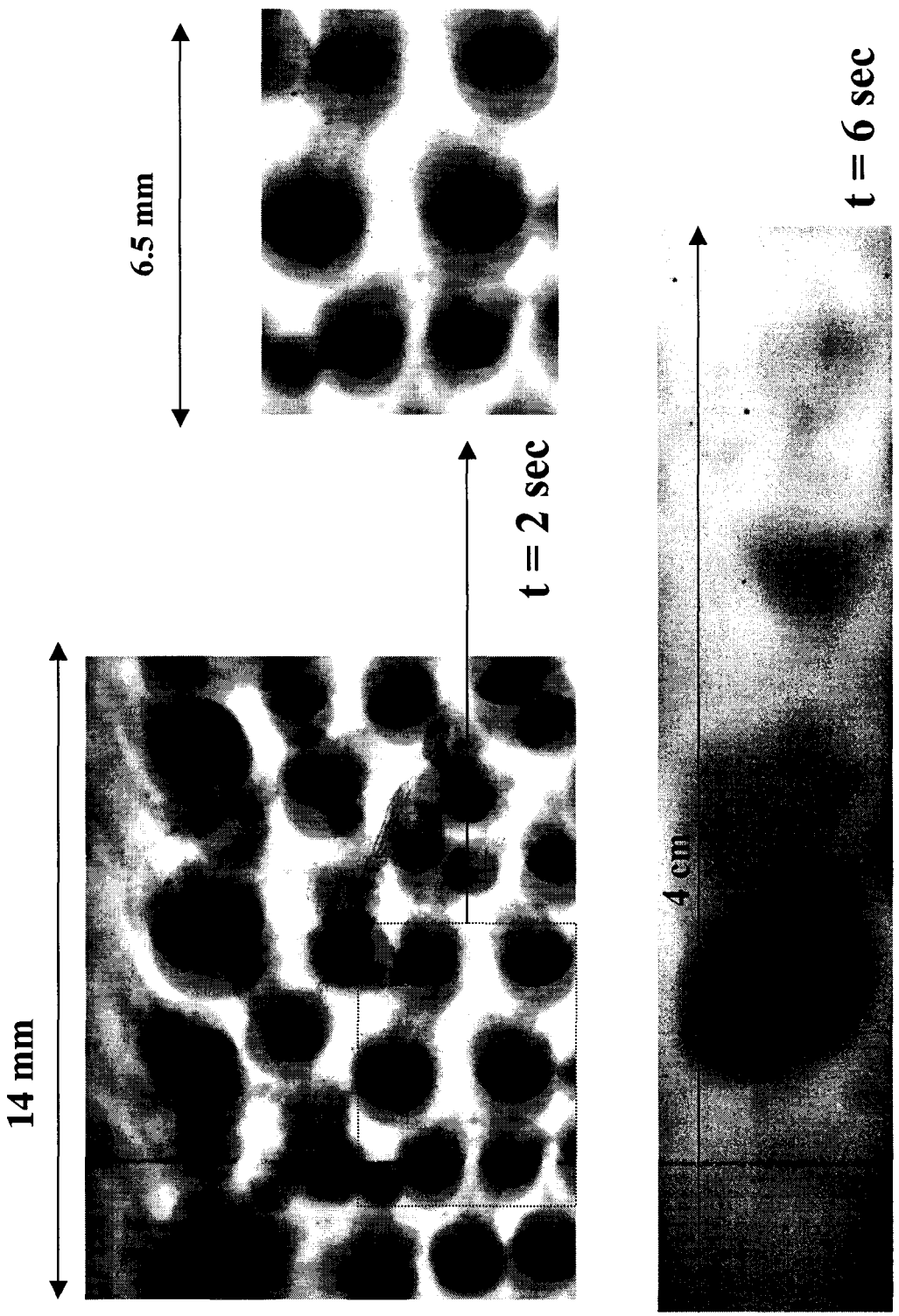

Figure 5.7: Motion of droplets of Acetone 50%, Hexadecane 50% System.

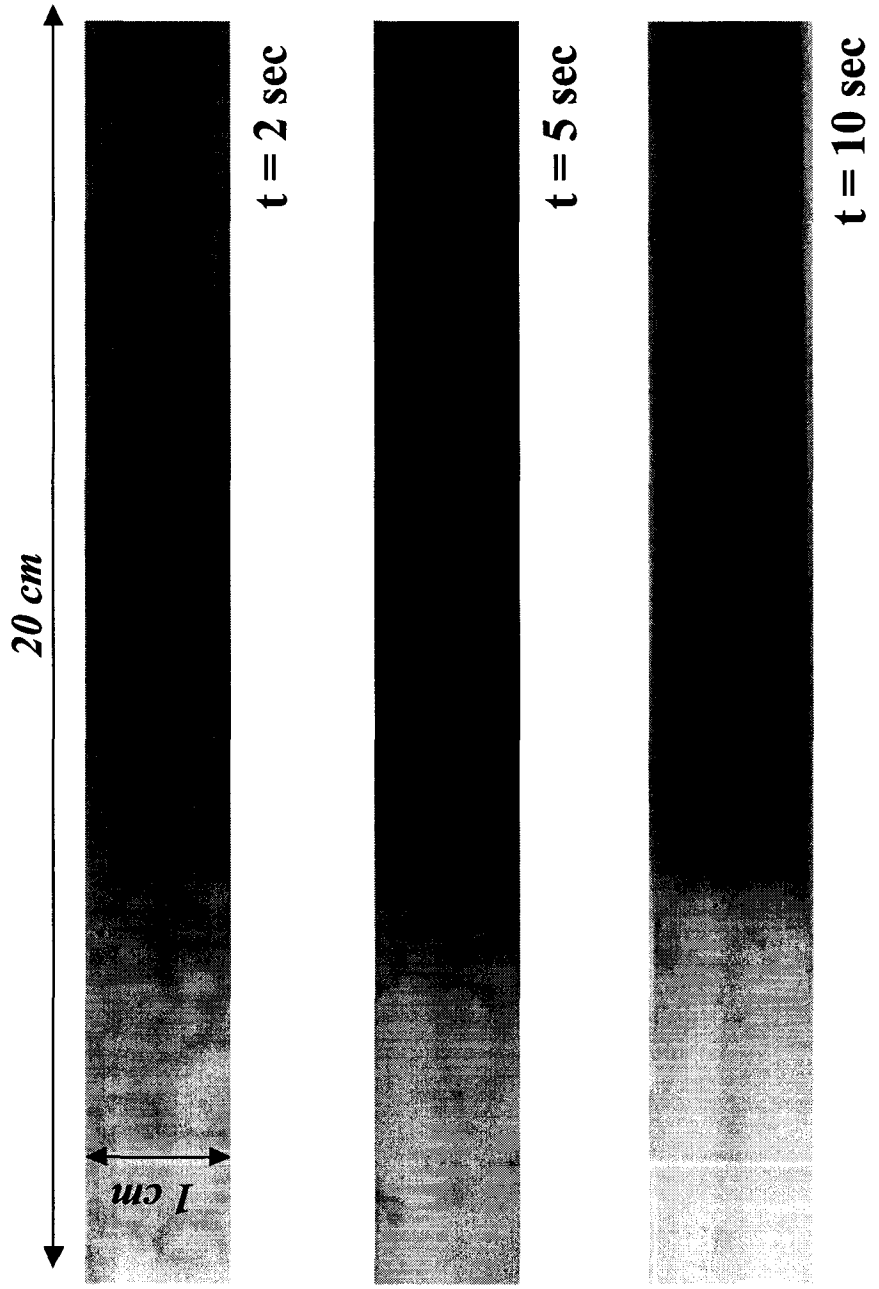

Figure 5.8: Morphology of Acetone 70%, Hexadecane 30% System within the Horizontal Condenser.

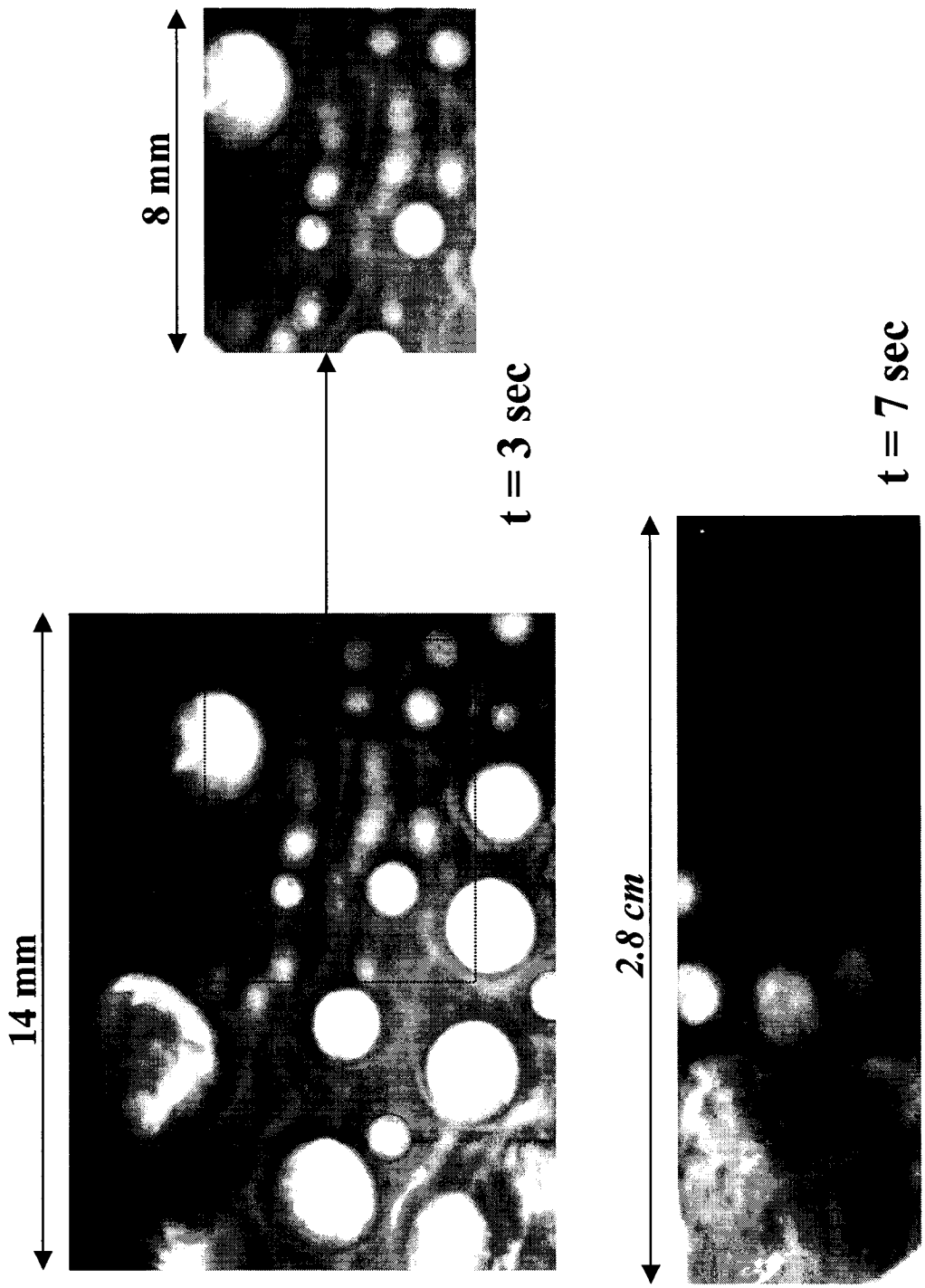

Figure 5.9: Motion of droplets of Acetone 70%,Hexadecane 30% System.

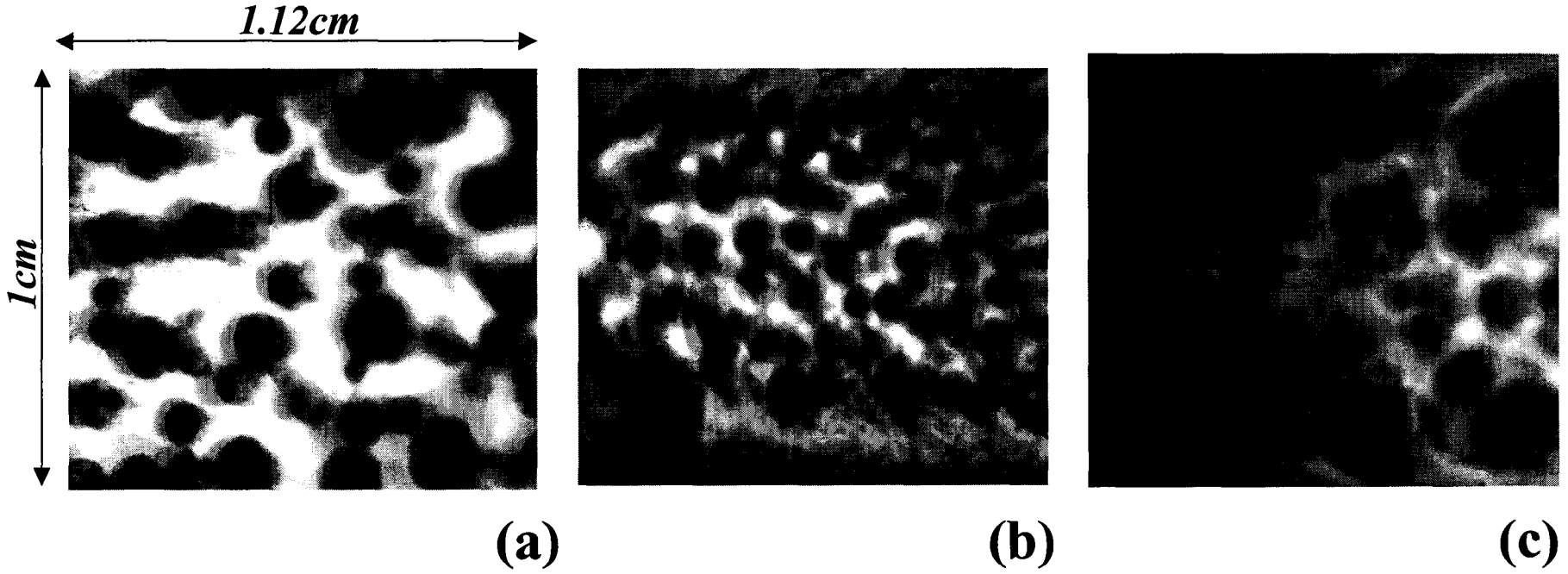

Figure 5.10: Velocity measurement after 2 seconds of cooling for 50%Acetone and 50%Hexadecane System.
(a) Droplets at inlet side of the tube.
(b) Droplets in the middle of the tube.
(c) Droplets at the outer side of the tube.

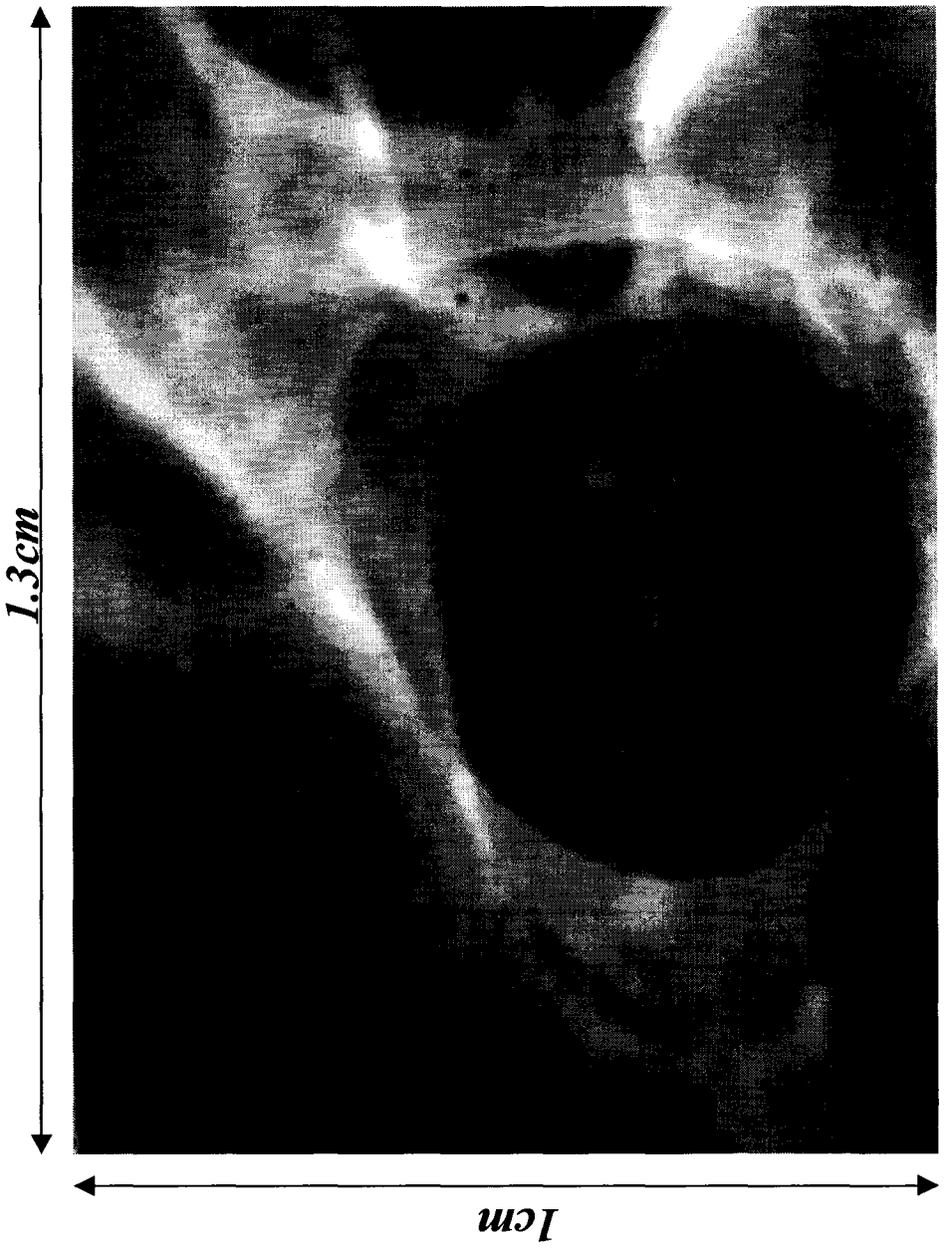

Figure 5.11: Velocity of a droplet of 5mm size.

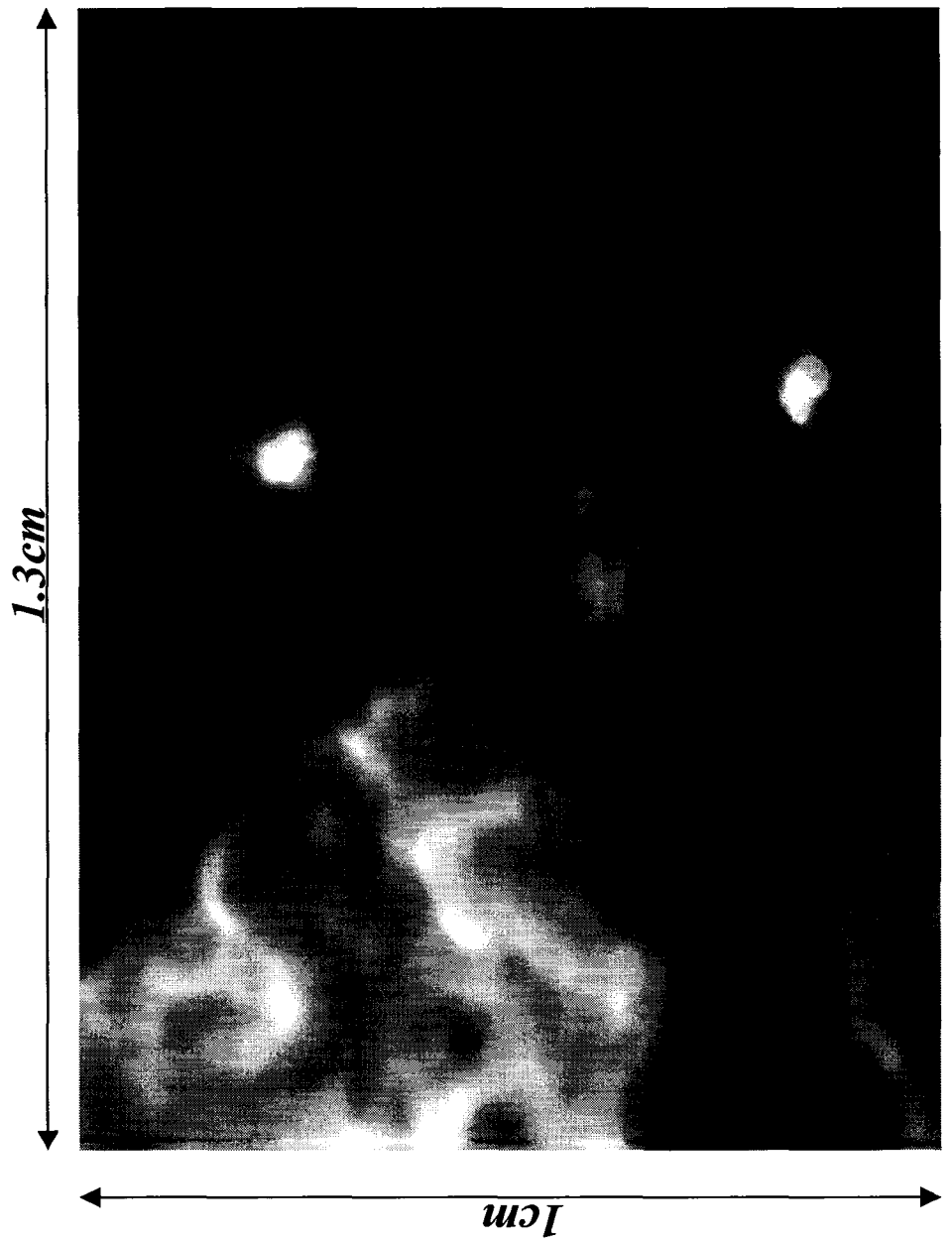

Figure 5.12: Velocity of a hexadecane droplet.

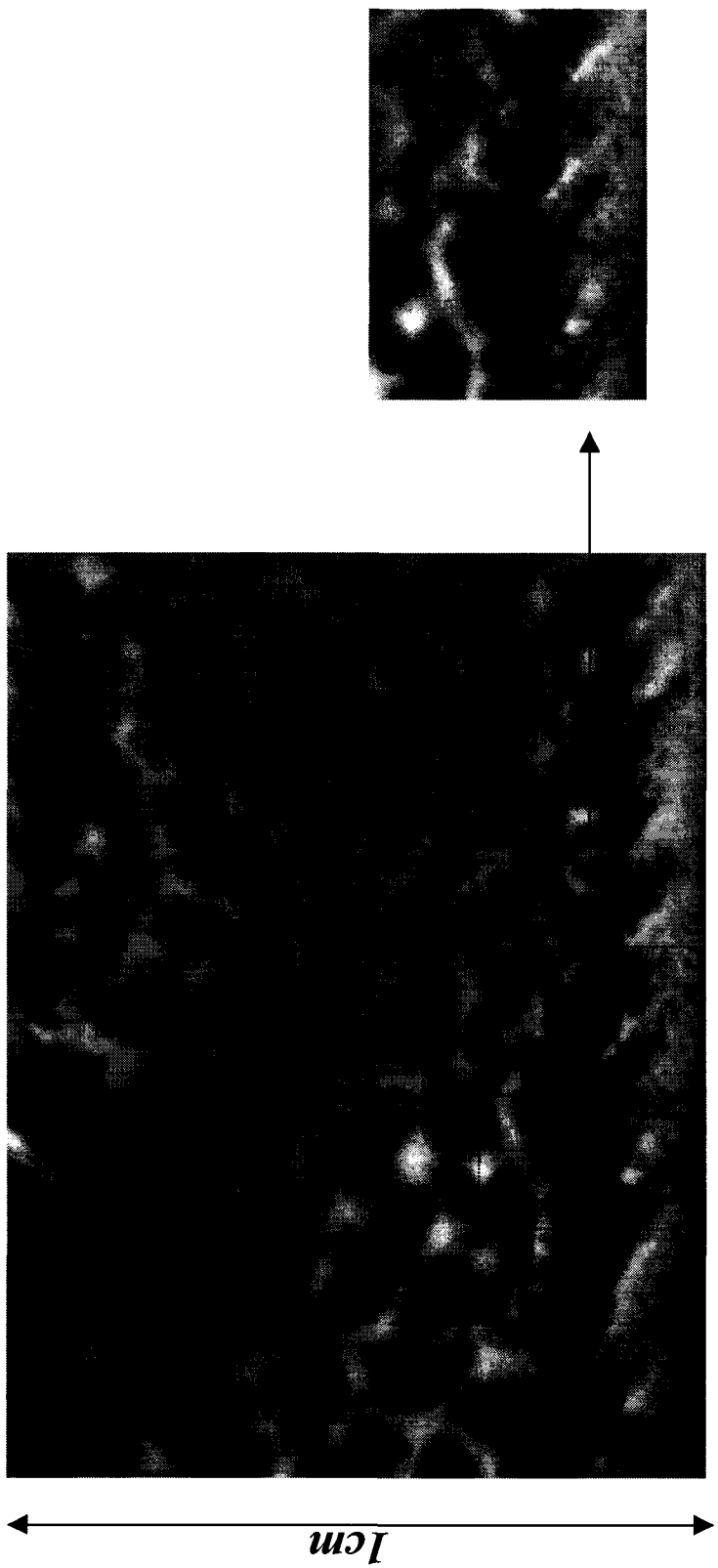

Figure 5.13: Movement near the wall of the tube (no back flow).

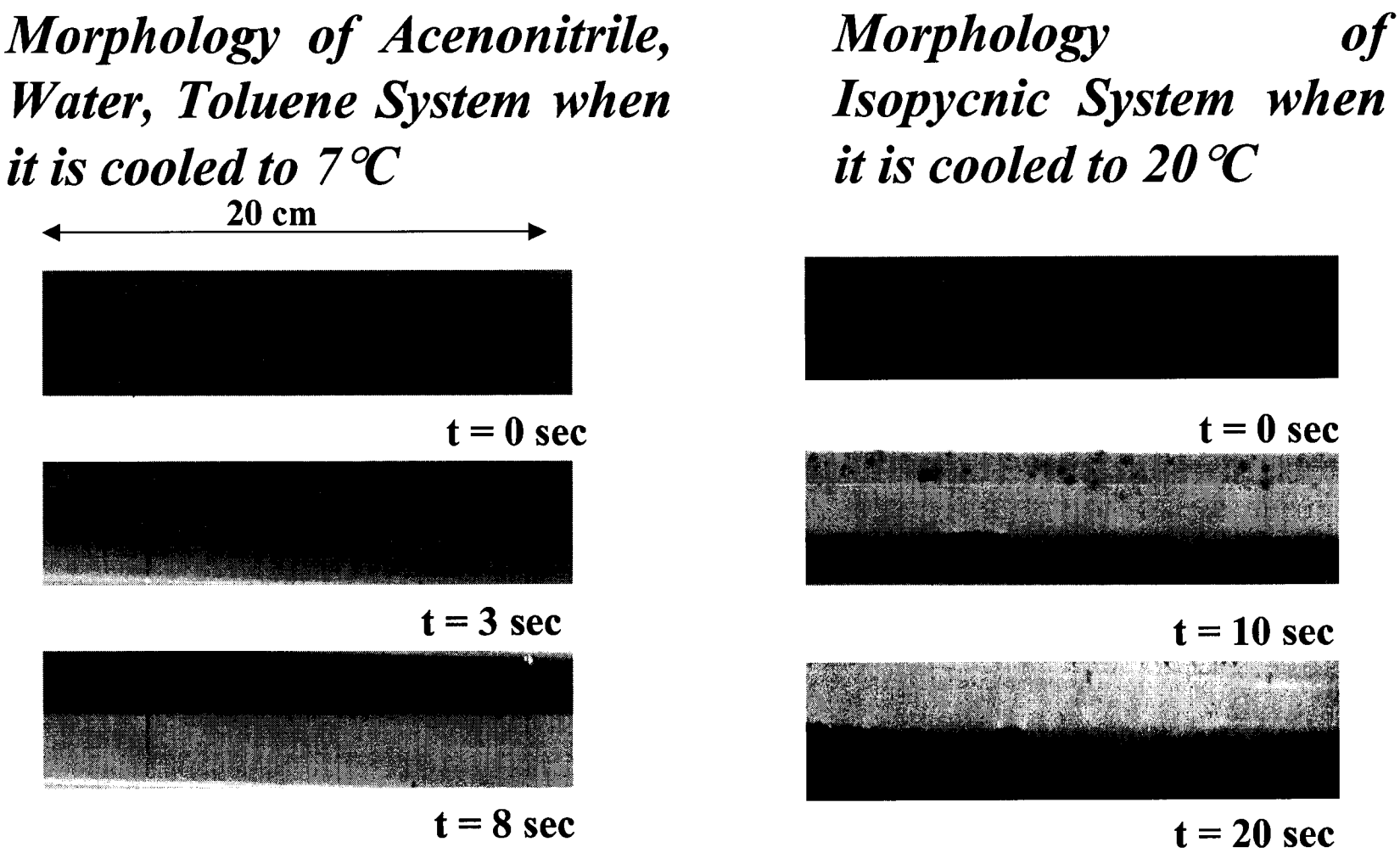

Figure 5.14: Phase Separation in Different Conditions.

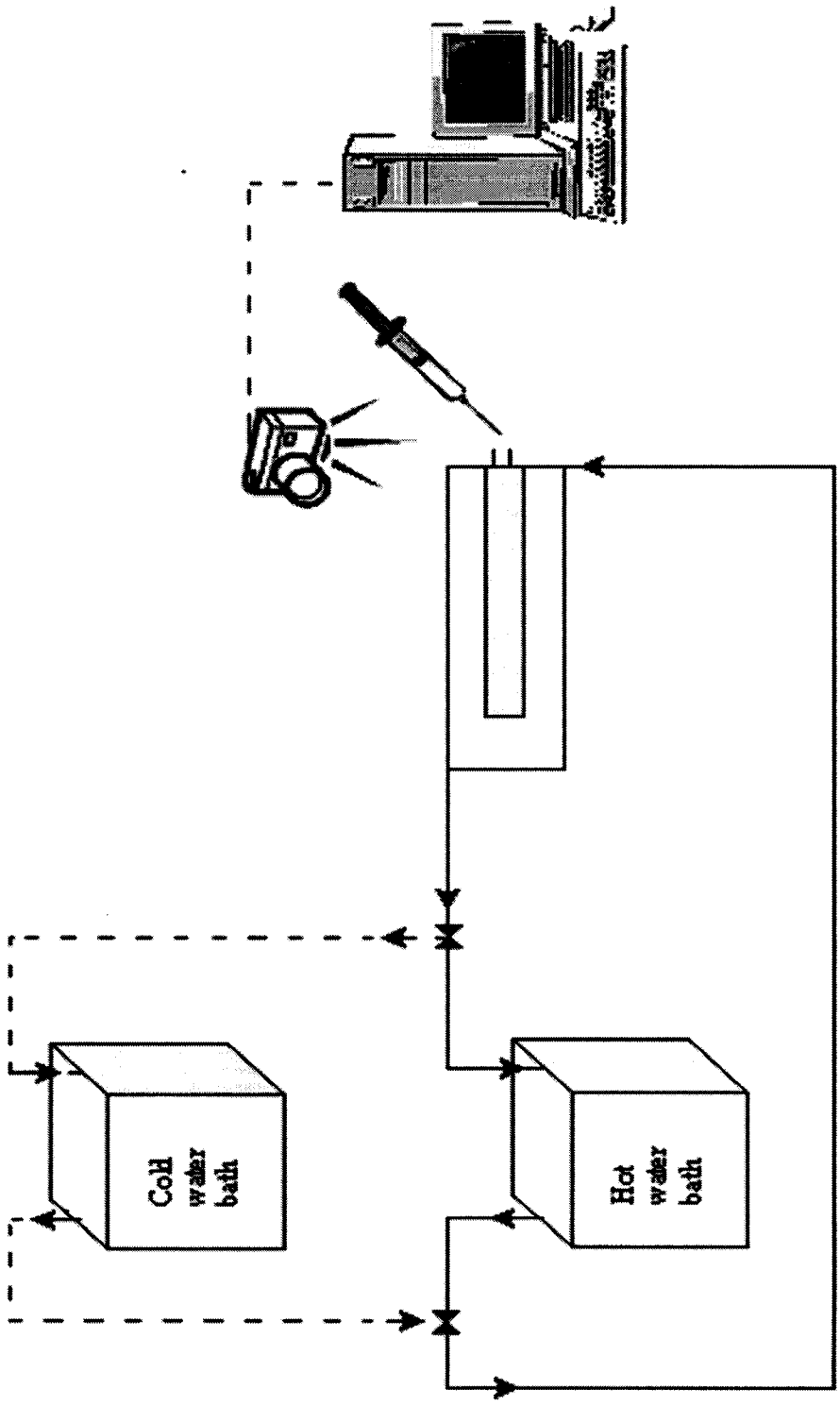

Figure 6.1: Experimental Setup

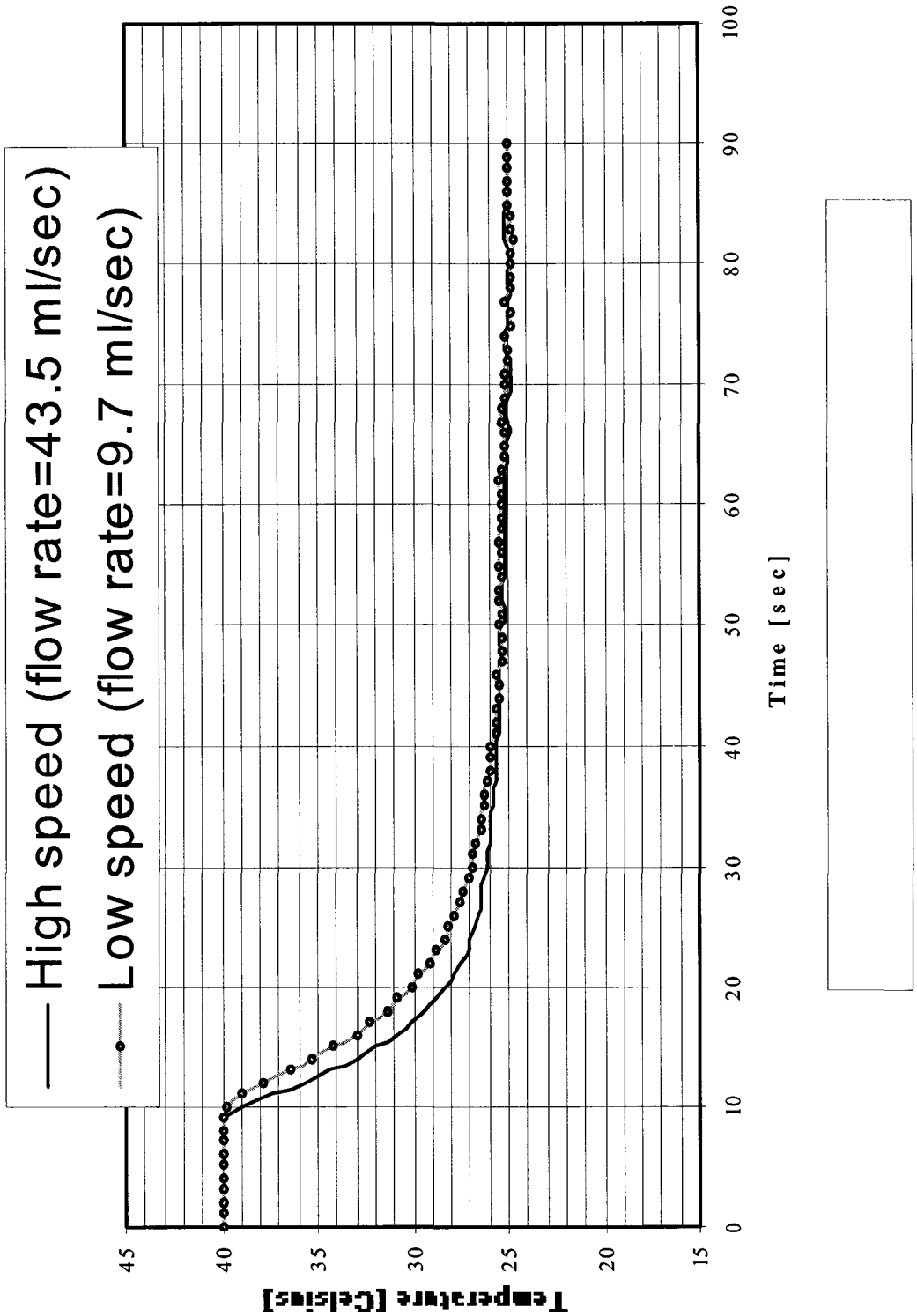

Figure 6.2: Temperature Drop in the Cell.

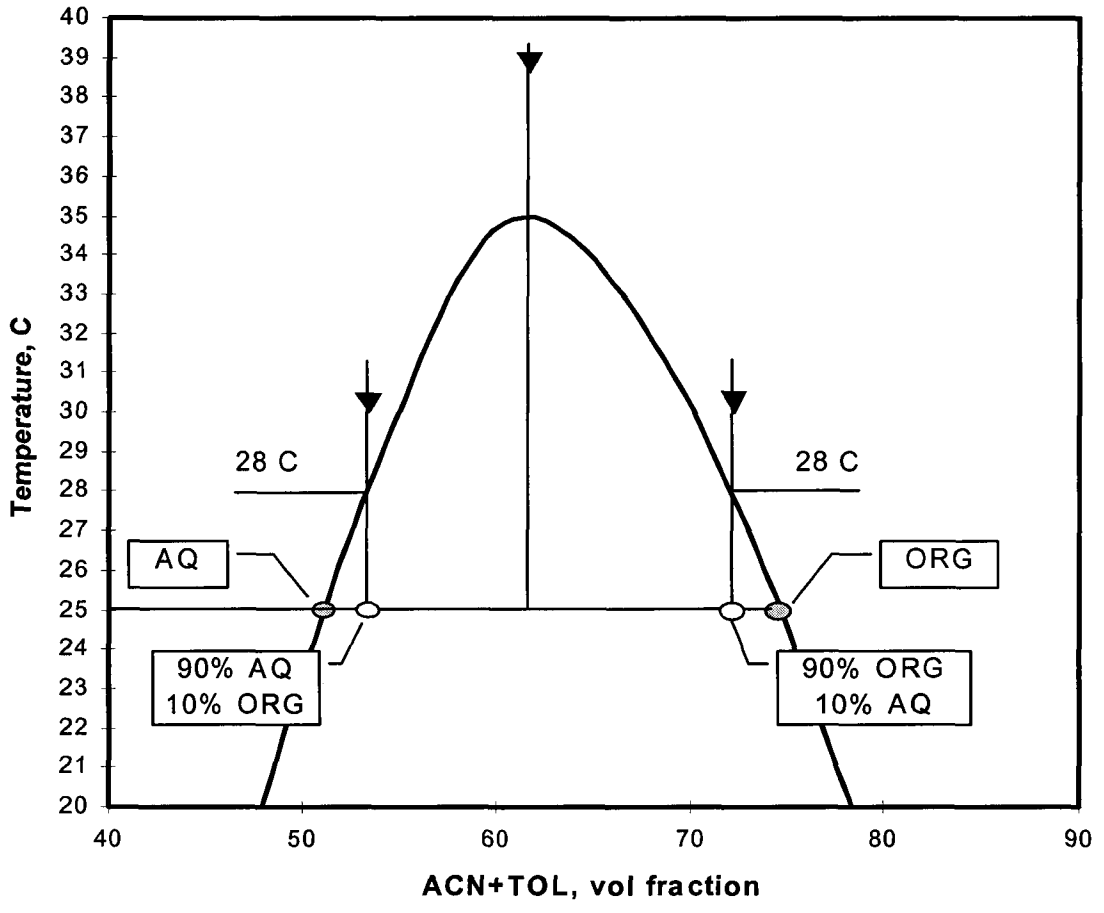

AQ = acquous phase
ORG = organic phase

Figure 6.3: Experimental Procedures.

Off- critical composition: 10% AQ, 90% ORG

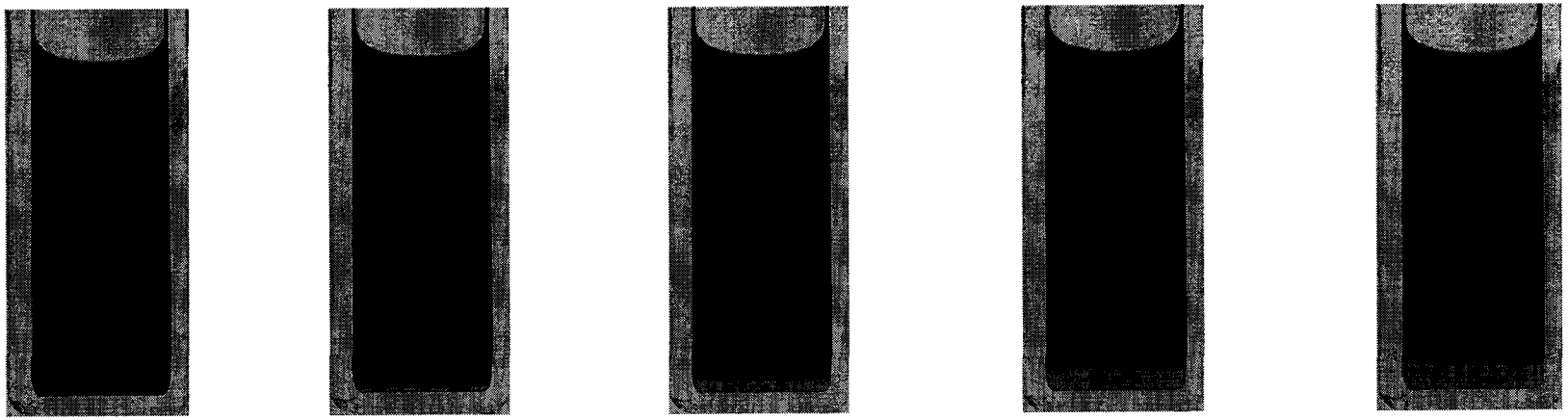

t=0sec, T=28C t=1sec t=3sec t=10sec t=16sec, T=25C

Critical composition: Acetonitrile 58%, Water 38%, Toluene 4%.

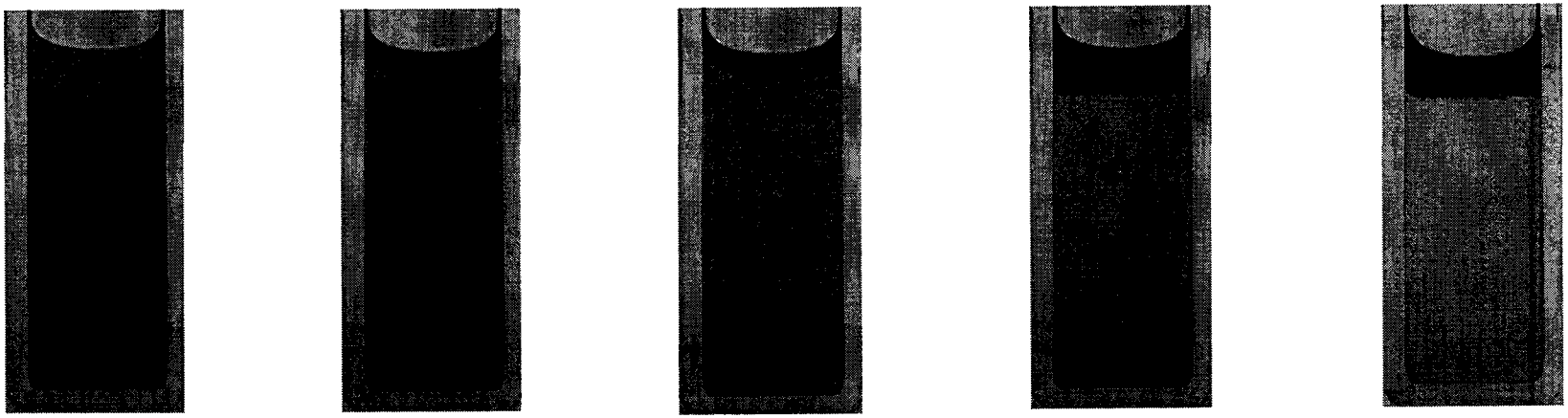

t=0sec, T=28C t=1sec t=3sec t=10sec t=20sec, T=25C

Figure 6.4: Morphology in Cell during fast cooling with no surfactant.

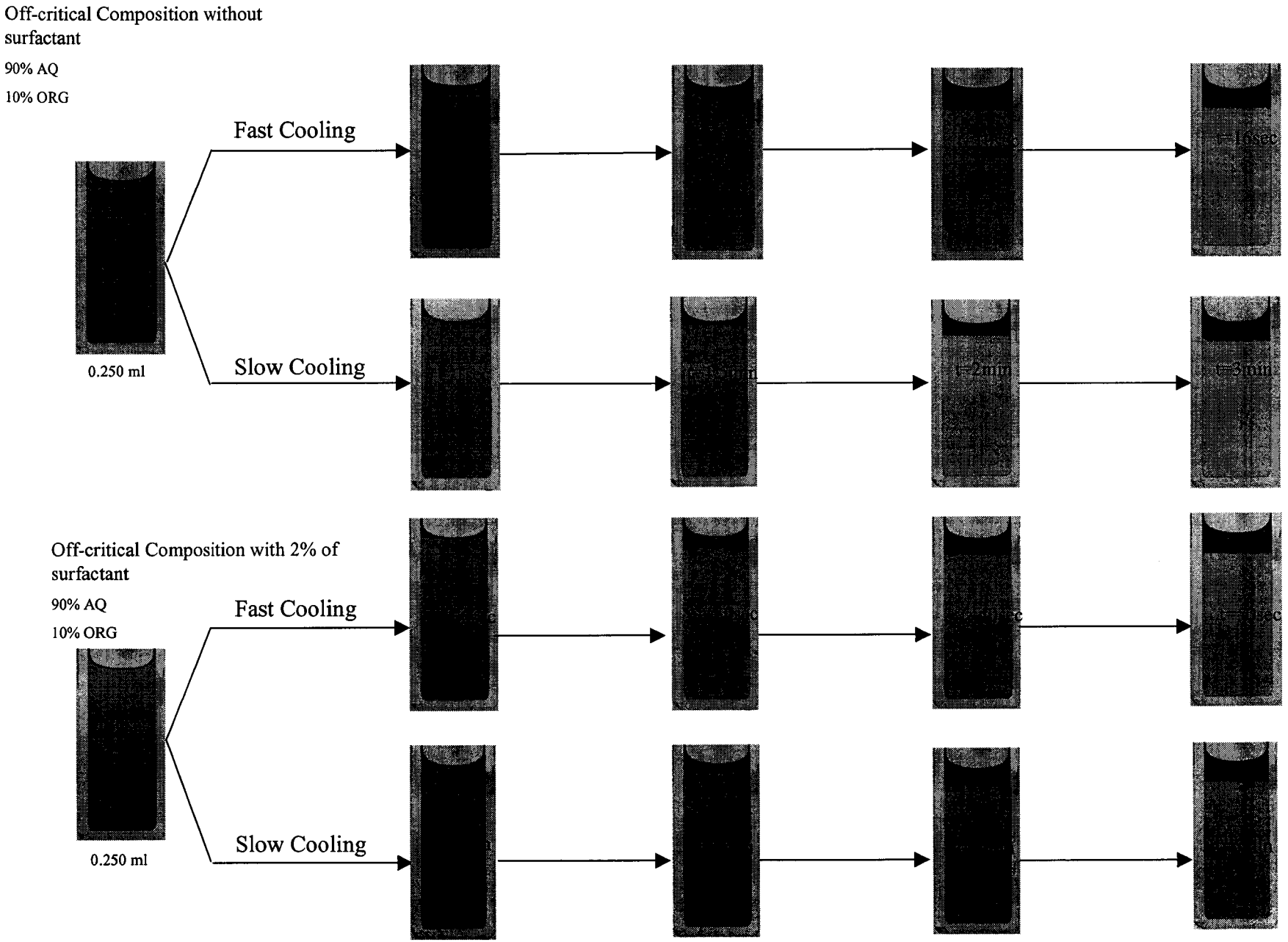

Figure 6.5: Phase Separation of Off-Critical Mixtures in Presence of Surfactants.

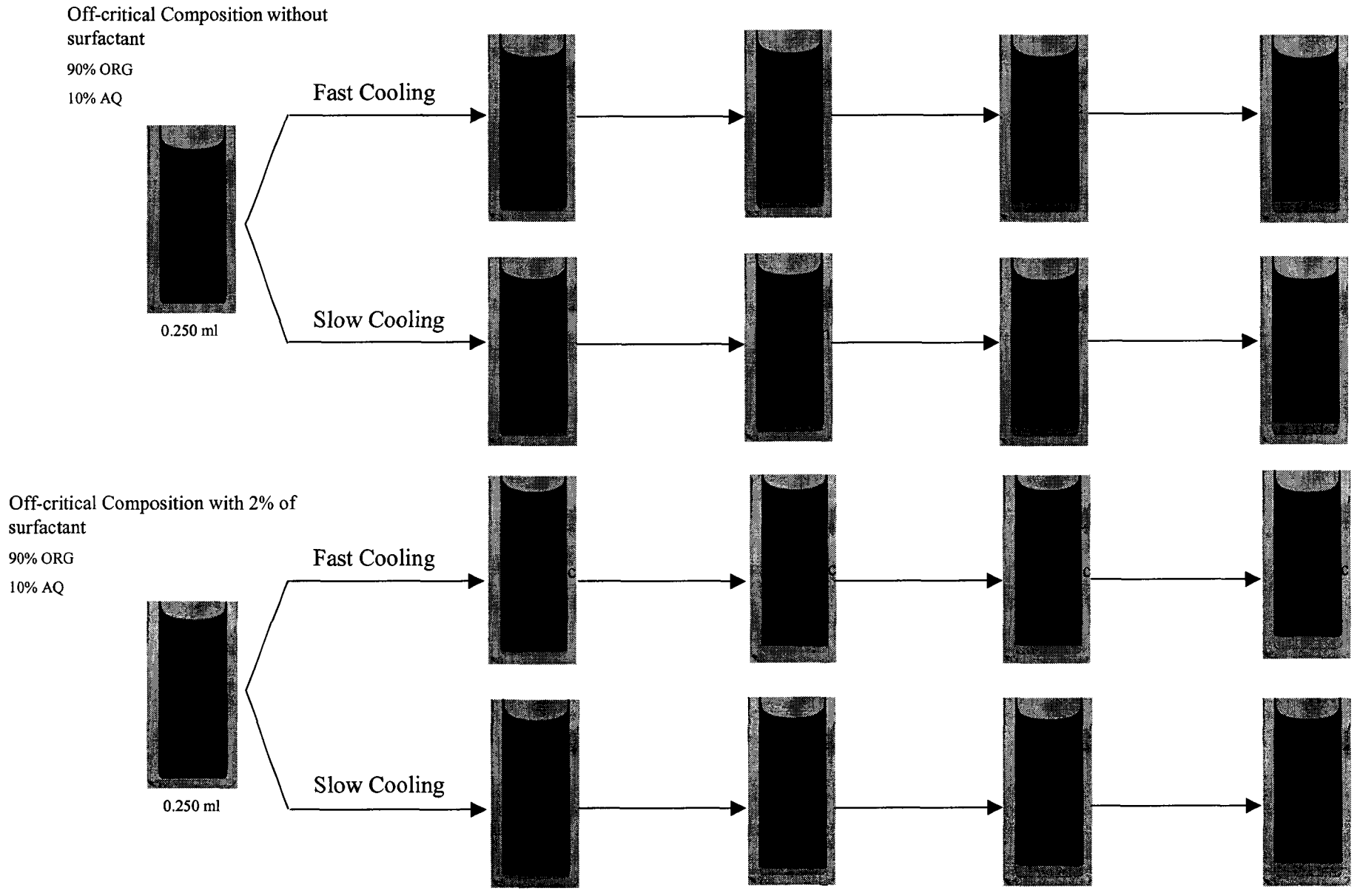

Figure 6.6: Phase Separation of Off-Critical Mixtures in Presence of Surfactants.

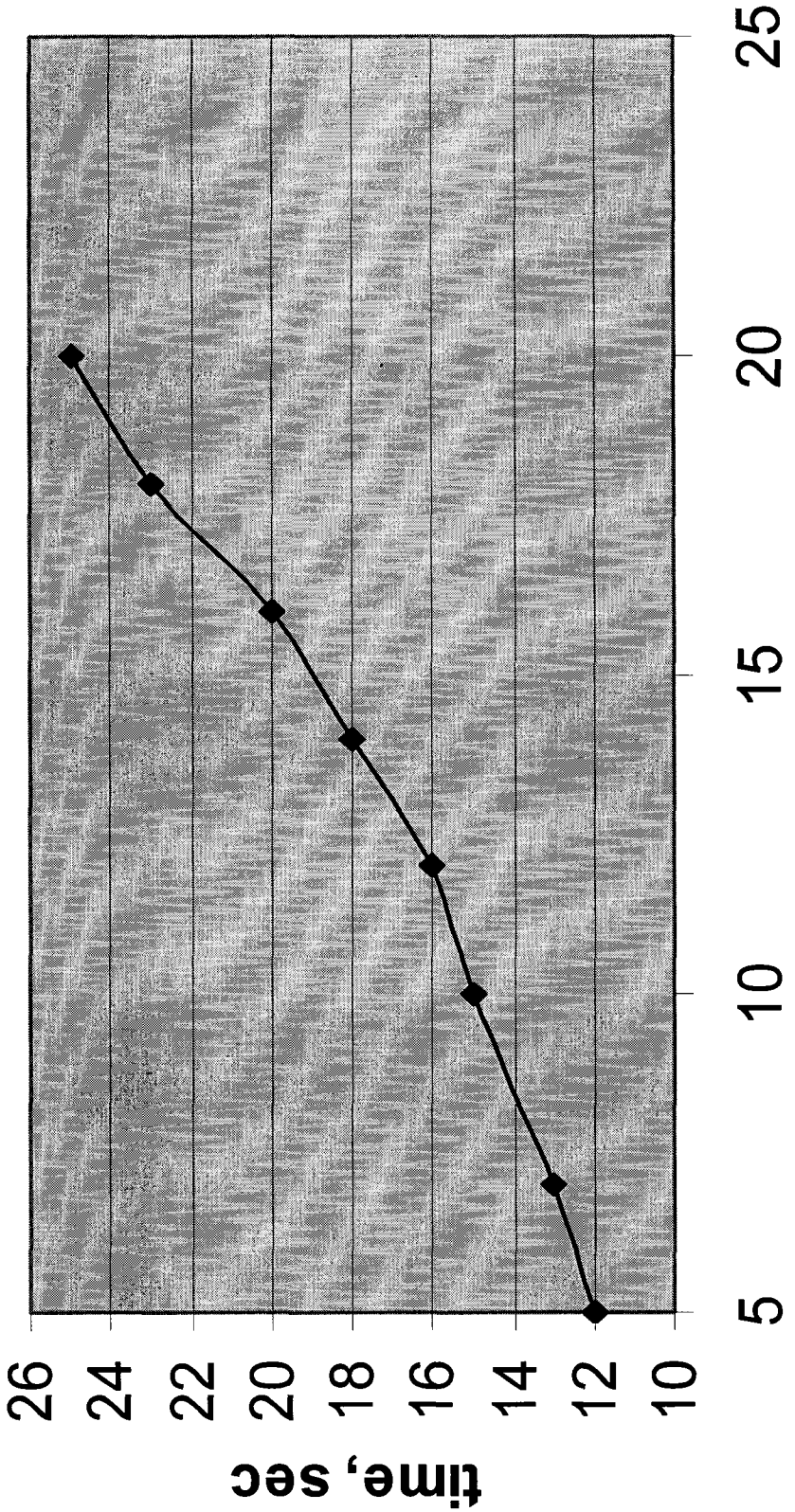

Figure 6.7: Influence of Cooled Temperature on Phase Separation for Critical Mixtures.

90% ORG, 10% AQ Acetonitrile-Water-Toluene, off-critical composition Tcr=35C, Th=40C Tc=2C with no Surfactant.

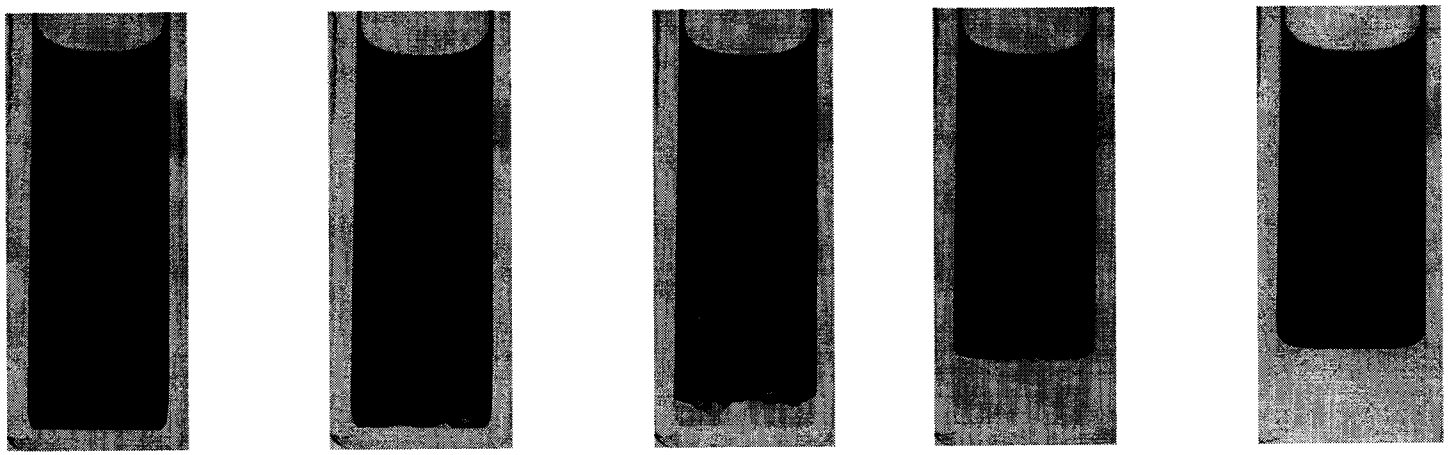

t=0sec, T=28C | t=1sec | t=4sec | t=10sec | t=14sec, T=2C

90% ORG, 10% AQ Acetonitrile-Water-Toluene, off-critical composition with 5% Surfactant (IGEPAL CO-730)

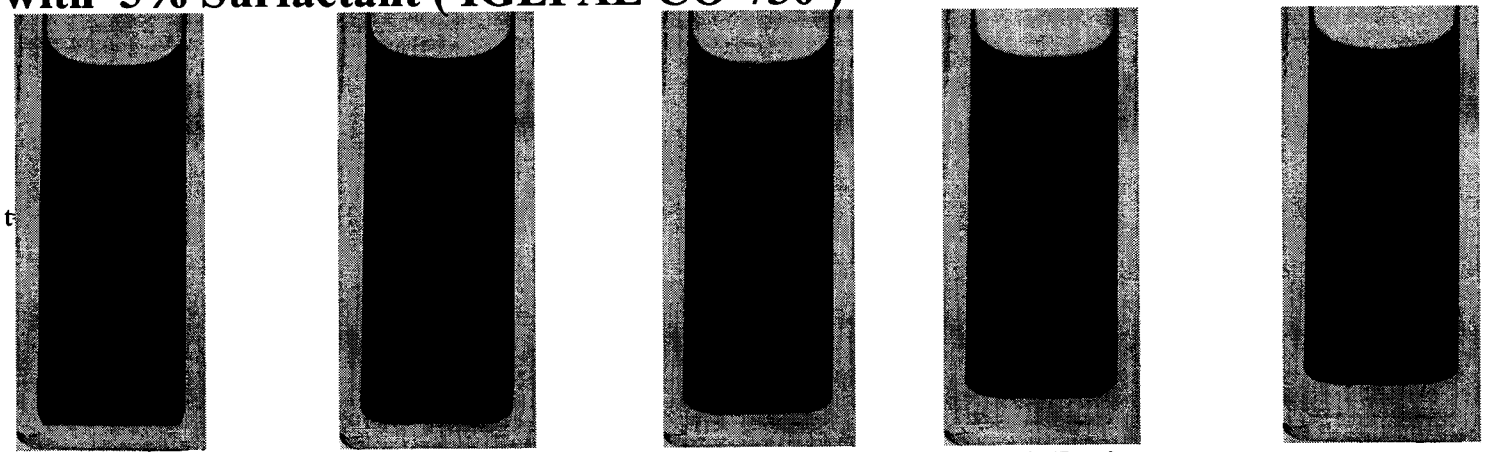

t=0sec, T=28C | t=30sec | t=1min | t=1.5min | t=2min, T=2C

Figure 6.8: Influence of Cooling temperature on Phase Separation.

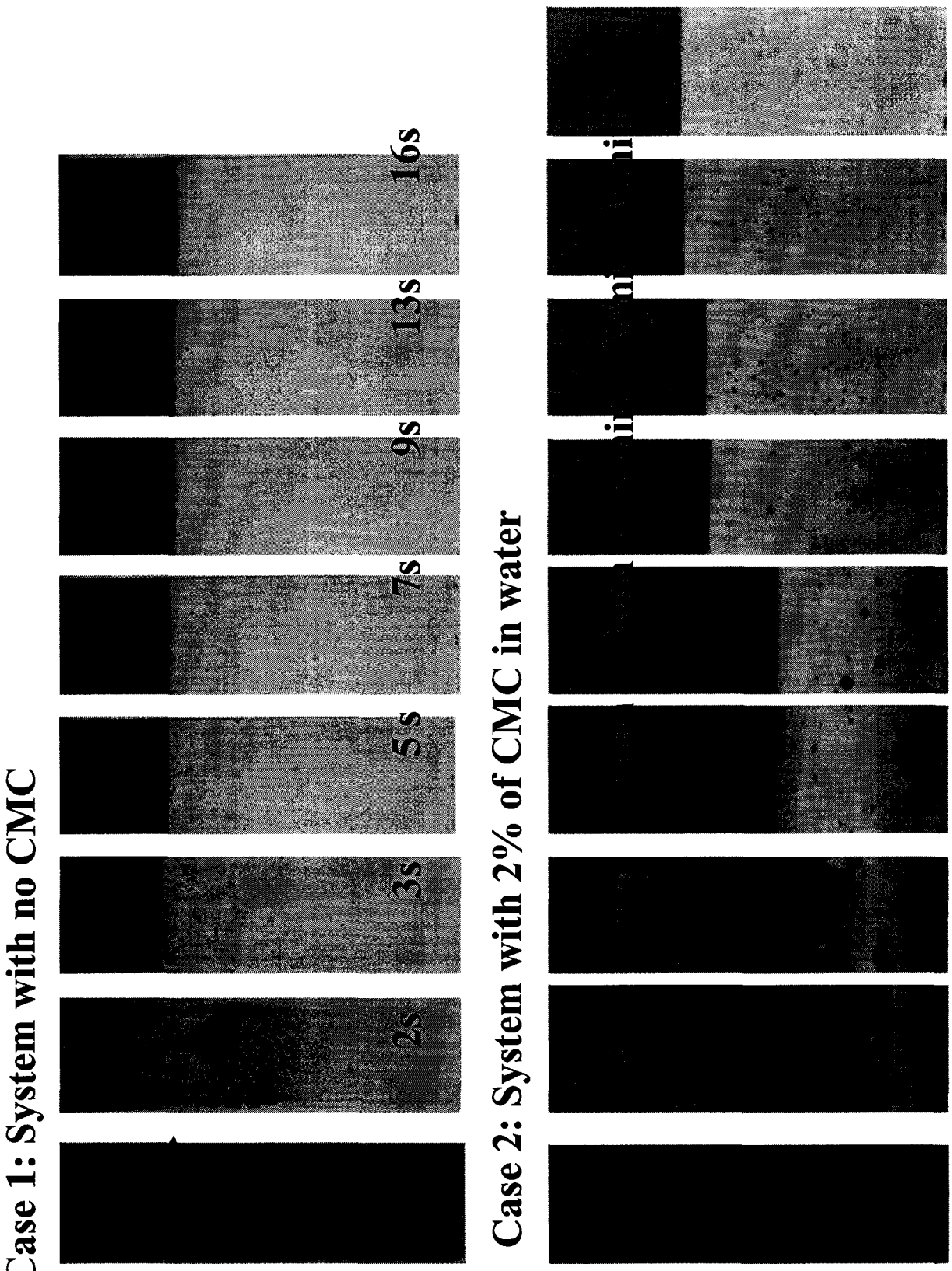

Figure 6.9 : Influence of viscosity on Phase Separation.

References

[1] Akell, R.B., and King, C.J., *"New Developments in Liquid-Liquid Extractors: Selected papers from ISEC 83"*, AIChE Symposium Series (1984).

[2] Alegret, S., *"Development in Solvent Extraction"*, John Wiley &Sons, (1988).

[3] Anderson, D.A. and Lau, E.F., Chem. Eng. Progr. 51,507, (1955).

[4] Anderson, S.O.S, and Reinart, H., *"Recovery of Metals from Liquid Effluents"*in Handbook of Solvent Extraction, p. 751.

[5] Baniel, A. and Blumberg, R., Israeli Patent 23,760 (1968).

[6] Bayewitz, M., Shinnar, R., Yerushalmi, S., J. of Atoms. Sci., Vol. 31, No. 6, 1974

[7] Bencher, P., Editor, *"Encyclopedia of Emulsion Technology"*, Vol. I, Marcel Dekker (1983).

[8] Beysens, D., P. Guenoun, R. Gastaud, F. Perrot *"Spinodal decomposition patterns in an isodensity critical binary fluid: direct-visualization and light-scattering analyses,' Phy. Rev. A* **36**, 4876 (1987).

[9] Bikerman, J.J., *"Surface Chemistry"*, Academic, New York, (1958).

[10] Blumberg, R., *"Liquid-Liquid Extraction"*, Academic Press (1988).

[11] Brown, C.G and Sanderson, B.R., US Patent 4,058,588 Nov. (1977).

[12] J.W. Cahn and J.E. Hilliard, `Free energy of a nonuniform system. III. Nucleation in a two-component incompressible fluid,' *J. Chem. Phys.* **31**, 688 (1959).

[13] Charles, G.E, Mason, S.G., J. Colloid Sci. 15, 105,235 (1960).

[14] F. Califano and R. Mauri, "Drop Size Evolution during the Phase Separation of Liquid Mixtures," *Ind. Eng. Chem. Res.* **43**, 349-353 (2004).

[15] F. Califano, R. Mauri and R. Shinnar, "Large-scale and rapid motion of drops forming during the phase separation of liquid mixtures," *Phys. Fluids* (submitted).

[16] Y.C. Chou and W.I. Goldburg, W.I., `Phase separation and coalescence in critically quenched isobutyric-acid-water and 2-6-lutidine-water mixtures,' *Phys.Rev. A* **20**, 2105 (1979) and references therein.

[17] Cohn, R.H., and Jacob, D.T., *"Acetone Impurity Effects on Binary Fluid Mixture Methanol-Cyclohexane"*, J. Chem. Phys., 80, 856, (1984).

[18] Cote, G. and Bauer, D., Hydrometallury 5, 149, (1980).

[19] Cumming, P. Wiltzius, F.S. Bates and J.H. Rosedale, `Light-scattering experiments on phase-separation dynamics in binary fluid mixtures,' *Phys. Rev. A*, **45**, 885 (1992) and references therein.

[20] DeBenedetti, P.G., *"Metastable Liquid Concepts and Principles"* Princeton University Press, Princeton, NJ, 1996.

[21] P. Diamond, J. Harvey, J. Katz, D. Nelson. "Drag reduction by polymer additieves".

[22] Domb, C., and Green, M.S., *"Phase Transition and Critical Phenomena"*, Academic Press, (1972).

[23] Epstein, J.A, Feist, E.M., Marcus, Y., and Zomra, J., Hydrometallurgy 6, 269, (1981).

[24] Francis, A.W., *"Liquid Liquid Equilibriums"*, Wiley-Interscience, 1963.

[25] Frankel, J. *"Kinetic Theory of Liquids"*, Dover, New York, 1946.

[26] Goldin, M., Pfeffer, R., Yerushalmi, J. and Shinnar, R., *J. of Fluidmechanics* 38, 689, 1989.

[27] Guenoun, P., Gastaud, R., Perrot, F., D. Phys. Rev., 4876, (1987).

[28] Gunton, J.D, Miguel, M.S., Sahni, P.H., *"Phase Transition and Critical Phenomena"*, Academic Press, London, 1983.

[29] R. Gupta, R. Mauri and R. Shinnar, `Liquid-liquid extraction using the composition induced phase separation process,' *Ind. Eng. Chem. Res.* **35**, 2360 (1996).

[30] R. Gupta, R. Mauri and R. Shinnar, *`Phase separation of liquid mixtures in the presence of surfactants,' Ind. Eng. Chem. Res.* **38**, 2418 (1999).

[31] Hales, B.j., Bertrand, G.L., and Hapler, L.G., J. Phys. Chem., 70, 3970, (1966).

[32] Hanson, C., (ed.) *"Recent Advance in Liquid-Liquid Extraction"*, Pergamon Press, 1971.

[33] Harland, S., *"Counter-Current Extraction"*, Pergamon Press, New York, (1963).

[34] Heller, W., and Pugh, T.L., Chem. Phys. 22, 1778, (1954).

[35] Hohenberg, P .C, H alperin, B .I, " *Theory of Dynamic Critical Phenomena*", R ev. Mod. Phys., 1977.

[36] Hsien-Wen, H., "*Techniques of Chemistry*", Weissberger, A., Editor, Chap. VI, Wiley Interscience Publication, (1980).

[37] D. J asnow a nd J . Viñ als, ` Coarse-grained de scription o f t hermo-capillary flow,' *Phys. Fluids*, **8**, 660 (1996).

[38] Kawasaki, K. in *"Phase Transition and Critical Phenomena"* Vol. 5A, Academic Press, 1976.

[39] E.M. Lifshitz and L.P. Pitaevskii, *Physical Kinetics*, (Ch. 12). Pergamon Press, New York (1984).

[40] Lo, T.C., Baird, M.H.I, *"Handbook of Solvent Extraction"*, Wiley-Interscience,1983.

[41] Lupis, C.H.P., "*Chemical Thermodynamics of Materials"*, Elsevier, 1983.

[42] R. Mauri, R. Shinnar and G. Triantafyllou, `Spinodal decomposition in binary mixtures,' *Phys. Rev. E* **53**, 2613 (1996).

[43] Muhl, P., Gloe, K., Fischer, C., Ziegenbalg, G., and Hoffman, H., Hydrometallurgy 5, 161, (1980).

[44] Randall, J.M., Schultz, W.G., and Morgan, A.I, Confructa 16, 1971.

[45] Ritcey, G.M., *"Solvent Extraction Principles and Applications to Process Metallurgy"*. Parts I and II, Elsevier, 1979.

[46] Rogers, D.W., *"Cloud-Point Analysis of Microliter Samples Determination of Water in Six Common Solvents"*, Talanta, 1969.

[47] Rowlison, J.S., "*Liquid-Liquid Mixtures*", 2nd edition, Plenum, New York, (1969).

[48] Schepper, A.D., Hydrometallurgy 4, 285, (1978).

[49] G. Santonicola, R. Mauri and R. Shinnar, `Phase separation of initially non-homogeneous liquid mixtures,' *Ind. Eng. Chem. Res.* **40**, 2004 (2001).

[50] Schweiter, P.A., editor-in-Chief, *"Handbook of Separation Techniques for Chemical* Engineers", McGraw-Hill, (1970).

[51] Sekine, T. and Hasegawa, Y. *"Solvent Extraction Chemistry"*, Dekker, New York, (1977).

[52] *R.* Shinnar and R. Mauri, *The Concentration Induced Phase Separation ({CIPS}) Process*, U.S. Patent, No. 8,274,546 (1996).

[53] Shinnar, R., J. of Fluid Mechan. 10 part 2, 1961.

[54] Siggia, `Late stages of spinodal decomposition in binary mixtures,' *Phys. Rev. A* **20**, 595 (1979).

[55] Stround, S.W., and Ransley, H.M.P, British Patent 760,351, 1956.

[56] Snyder, R.B, and Eckert, C.A., J. Chem. Engin. Data, 18,282, (1973).

[57] Tadros, T.F, and Vincent, B., *"Emulsion Stability"* in Encyclopedia of Emulsion Technology, Vol. 1, Becher P., ed., Mercel Dekker, New York, (1983).

[58] H. Tanaka, `Coarsening mechanisms of droplet spinodal decomposition in binary fluid mixtures,' *J. Chem. Phys.* 105, 10099 (1996).

[59] H. Tanaka and T. Araki, `Spontaneous double phase separation induced by rapid hydrodynamic coarsening in two-dimensional fluid mixtures,' *Phys. Rev. Lett.* **81**, 389 (1998).

[60] Treybal, R.E., *"Liquid Extraction"*, Sec. Ed., McGrwa-Hill, 1963.

[61] Treybal, R.E., *"Mass Transfer Operations"*, McGraw-hill, 1980.

[62] Tveekrem, J.L., and Jacob, D.T., *"Impurity Effects in Near-Critical Binary-Fluid Mixtures"*, Phys. Rev., 27, 2773, (1983).

[63] Ullmann, Z. Ludmer and R. Shinnar, `Novel continuous multistage extraction column based on phase transition of critical-solution mixtures,' *Chem. Engng. Sci.* **52**, 567 (1997).

[64] Ullmann, Z. Ludmer and R. Shinnar, `Phase transition extraction using solvent mixtures with a critical point of miscibility,' *A.I.Ch.E. J.* **41**, 489 (1995).

[65] O.T. Valls and J.E. Farrell, `Spinodal decomposition in a three-dimensional fluid model,' *Phys. Rev. E* **47**, R36 (1993), and references therein.@

[66] Van der Waals, J. The thermodynamic Theory of Capillarity Under the Hypotesis of a Continuous Variation of density. Z. Phys. Chem, 1979.

[67] N. Vladimirova, A. Malagoli and R. Mauri, `Two-dimensional model of phase segregation in liquid binary mixtures,' *Phys. Rev. E* **60**, 6968 (1999).

[68] N. Vladimirova, A. Malagoli and R. Mauri, `Diffusion-driven phase separation of deeply quenched mixtures,' *Phys. Rev. E* **58**, 7691 (1998).

[69] N. Vladimirova, A. Malagoli and R. Mauri, `Two-dimensional model of phase segregation in liquid binary mixtures with an initial concentration gradient,' *Chem. Engng. Sci.* **55**, 6109 (2000).

[70] J.D. Van der Waals, `The thermodynamic theory of capillarity under the hypothesis of a continuous variation of density,' English translation by J.S. Rowlinson, in *J. Stat. Phys.* **20**, 200 (1979).

[71] N.C. Wong and C. Knobler, `Light-scattering studies of phase separation in isobutyric acid + water mixtures: hydrodynamic effects,' *Phys. Rev. A* **24**, 3205 (1981) and references therein.

[72] W.R. White and P. Wiltzius, `Real space measurement of structure in phase separating binary fluid mixtures,' *Phys. Rev. Lett.* **75**, 3012 (1995).